EFFICIENT FREQUENCY MODULATION SYSTEMS

by B.R. DAVIS, B.E. (Hons.), B.Sc.

Electrical Engineering Department,

University of Adelaide,

March 1968.

A thesis submitted for the degree of Doctor of Philosophy.

AVAILABILITY OF THESIS FOR LOAN AND PHOTOCOPYING.

I hereby consent to my thesis, "Efficient Frequency Modulation Systems", being available for loan and photocopying.

3rd January, 1969. B. R. DAVIS.

INDEX

SUMMARY.

This thesis considers some aspects of frequency modulation systems using frequency compressive feedback. The most common of these is the frequency modulation with feedback (FMFB) system and the ensuing investigation will be principally related to this system.

The first chapter contains a brief outline of the historical development of frequency compressive systems.

In the second chapter, a theoretical and experimental investigation into the threshold of FMFB under unmodulated conditions is conducted. It is shown that feedback causes a threshold which is due to the non-linear response of the IF tuned circuits to phase (or frequency) modulation. It is also shown that this threshold can be adequately described in terms of impulse phenomena.

The third chapter considers modulation dependent effects in the threshold of FMFB. It is shown that several independent effects related to the IF filter and frequency detector raise the FMFB threshold under modulated conditions, and their minimisation requires much more careful design than is immediately obvious.

Chapter four contains an evaluation of the possibility of applying FMFB to a time multiplex telemetry system. It is shown that under typical conditions the advantages are likely to be marginal.

In the final chapter, a preliminary consideration of systems related to FMFB is presented. In particular the dynamic filter system and the phase locked frequency divider are shown to have similar properties to FMFB, although there are some aspects which are peculiar to each device.

This thesis contains no material which has been accepted for the award of any other degree or diploma in any University, and, to the best of my knowledge, contains no material previously published or written by another person, except where due reference is made in the text of the thesis.

B.R. Davis

March 1968.

LIST OF SYMBOLS AND ABBREVIATIONS.

arg	argument of a complex number
A	loop gain
B	bandwidth (H_z)
CNR	carrier to noise ratio
f	frequency (H_z)
f_a	audio bandwidth (H_z)
f_d	peak frequency deviation (H_z)
F	feedback factor
FM	frequency modulation
FMFB	frequency modulation with feedback
G(f)	power spectral density ($-\infty \leqslant f \leqslant \infty$)
h(t)	filter impulse response
H(S)	filter transfer function
IF	intermediate frequency
m	radius of gyration (rad/sec), modulation index
mod	modulus of a complex number
n(t)	noise
p	probability density function
pdf	probability density function
psd	power spectral density
P	total probability
r(t)	amplitude
Re	real part of
RF	radio frequency

S	laplace variable, bandwidth parameter
SNR	signal to noise ratio
t	time
VCO	voltage controlled oscillator
W	IF output phasor
x(t)	inphase noise component
y(t)	quadrature noise component
Z(t)	IF input phasor, z(t) noise phasor x(t) + jy(t)
α	phase, frequency constant
β	communication efficiency
γ	phase
Δ	IF semi 3db bandwidth (rad/sec)
ε	error
λ	frequency offset (rad/sec)
ρ	carrier to noise ratio
ϕ	local oscillator phase
θ	IF phase
τ	time
ω	frequency (rad/sec)
<>	ensemble average
||	modulus
Ω	normalised frequency
η	noise power spectral density

CHAPTER I: INTRODUCTION.

In 1937 Armstrong [1] first demonstrated the practicability of frequency modulation and showed the necessity of using an amplitude limiter if the best performance (in terms of noise rejection) was to be obtained.

J.G. Chaffee [2] in 1939 proposed the use of negative feedback in an FM receiver to achieve essentially the same result as the amplitude limiter. His aim was to show that the use of feedback in a system without a limiter produced comparable results to the use of an amplitude limiter.

In 1944, Beers [21] described a frequency compression receiver employing frequency division. He found it necessary to supplement his system with frequency feedback in order to handle the frequency deviation desired.

In the late 1950's interest in frequency modulation with feedback (FMFB) was revived , as it seemed that the use of feedback in a system with an amplitude limiter could improve upon the performance of ordinary FM receivers. The limitation with ordinary FM was that to obtain a high output signal to noise ratio (SNR), a large deviation ratio was necessary, and the wider bandwidth necessary to pass these signals resulted in more noise in the RF and IF sections of the receiver. It was shown that if the carrier to noise ratio (CNR) prior to detection fell below 10-12 db, then a threshold phenomenon occurred, the salient feature being a rapid rise in output noise.

The fact that FMFB reduces the deviation ratio of the signal

indicated that an IF amplifier of smaller bandwidth than before could be used. Due to the reduction in the IF noise an extension of the acceptable operating range to smaller carrier powers should be expected, or alternatively, for the same carrier level a much wider deviation signal could be transmitted resulting in a higher output SNR. Improvements were obtained, although indefinite improvement could not be achieved by increasing the feedback factor.

In 1962, Enloe [3] showed that the use of feedback could only improve the performance of an FM system by a limited amount. This he attributed to a feedback threshold which occurred at higher carrier levels as the feedback was increased.

In the succeeding chapters it is intended to present results of some recent investigations into the nature and properties of FMFB threshold. The implications, as far as optimisation in different circumstances is concerned, are discussed.

FMFB is in fact only one member of a class of FM detection systems employing feedback. Other systems in this class and their relation to FMFB are discussed in a later chapter.

CHAPTER 2: FMFB THRESHOLD UNDER UNMODULATED CONDITIONS.

2.1 Discriminator threshold.

This occurs in an FM system when the small noise approximation to the output SNR breaks down. This effect has been analysed extensively (e.g. Stumpers [4]) and has been shown to depend on the predetection CNR and the deviation ratio of the FM signal. Such analyses gave important results, but did not shed much light on the mechanism of threshold.

The approach of Rice [5] , who describes the onset of threshold as a superposition of two processes, has done much to improve the understanding of FM threshold. The two processes are the linear model giving rise to noise with a quadratic power spectrum, and an impulsive process giving rise to noise with a uniform power spectrum. The impulses result from phase jumps in the signal caused by the carrier plus noise phasor encircling the origin.

2.2 Feedback threshold.

In an FMFB system, Enloe [3] considered that there were two thresholds, one the ordinary discriminator threshold and the other a feedback threshold. He showed that in systems where the feedback threshold was predominant, this occurred at a mean square local oscillator phase deviation of about 0.1 rad^2.

He attributed this threshold to an interaction of the incoming in phase noise components with the local oscillator phase modulation. The figure of 0.1 rad^2 was obtained from measurements on several FMFB systems and the figure was reasonably consistent.

It was apparent, however, from observations made on the experimental model described in Appendix F, that feedback threshold was a result of impulsive noise and in fact was indistinguishable from discriminator threshold.

An analysis on the basis of impulsive noise was performed by Schilling and Billig [6] . Although superficially promising, the effect of feedback is entirely disregarded as an impulse source.

2.3 System equations.

Figure 2.1 shows the block diagram of an FMFB system along with its small noise linearised low pass equivalent circuit. The approximations are concerned with the replacement of the IF filter by a linear transfer function $H_1(S)$ and the representation of the input by its phase alone.

The differentiation of phase produced by the frequency detector is compensated by integration in the VCO. The nett effect is simply a gain term $A = K_1 K_2$.

We shall first study the system under unmodulated conditions. If the carrier is $\cos \omega_1 t$, then additive gaussian noise $n(t)$ may be resolved into inphase and quadrature components, so that the received signal may be expressed as:

$$v_1(t) = R_e \left\{ (1 + x(t) + j\, y(t)) e^{j \omega_1 t} \right\} \qquad \ldots\ldots (1)$$

where $x(t)$ and $y(t)$ are low pass gaussian random time variables i.e. we represent $n(t)$ by the phasor $z(t) = x(t) + j\, y(t)$. In order that the resolution (1) be unique, we assume there are no significant noise

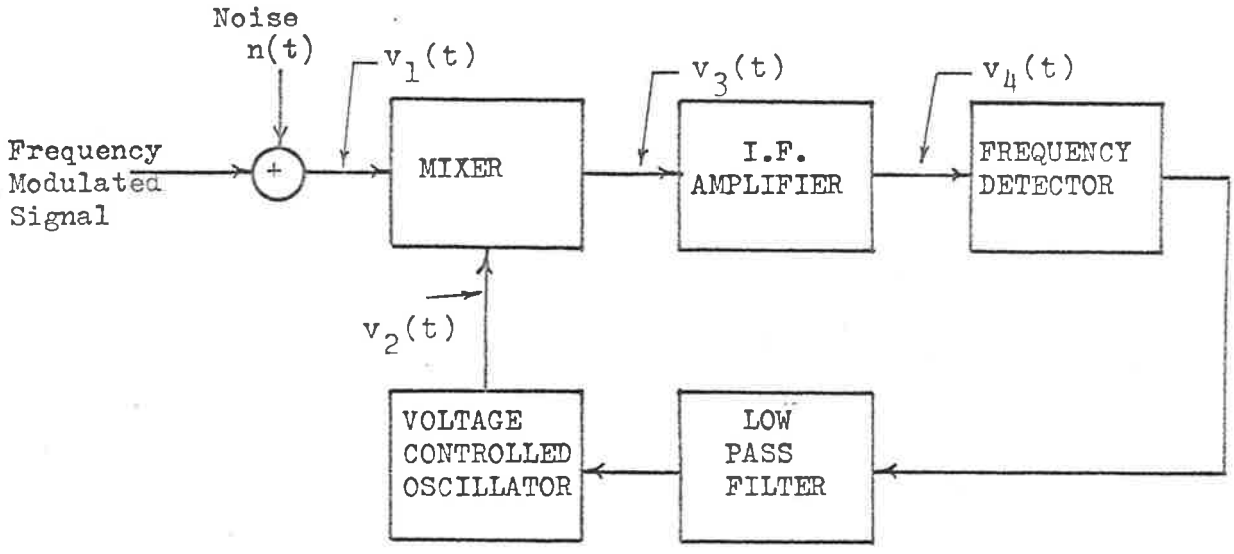

FIGURE 2.1a: BLOCK DIAGRAM OF FMFB SYSTEM.

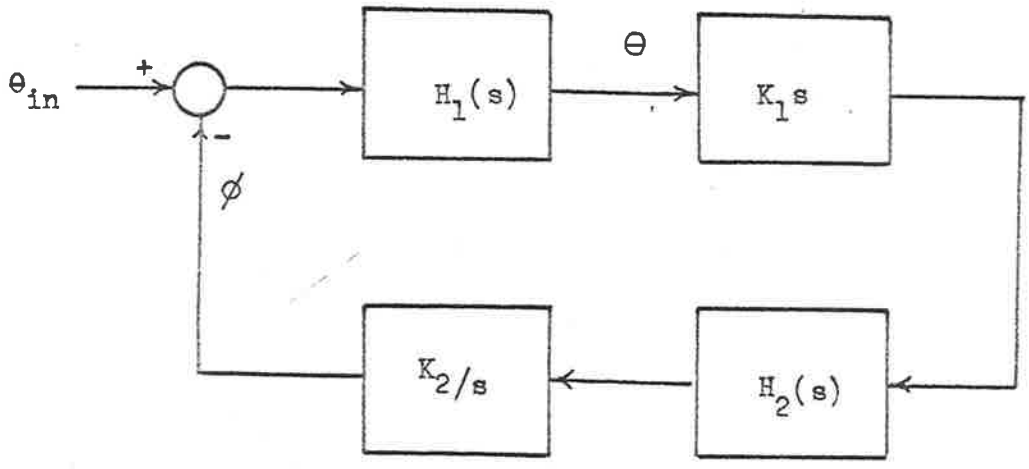

FIGURE 2.1b: LOW NOISE PHASE EQUIVALENT CIRCUIT.

components at frequencies exceeding $2\omega_1$.

On multiplication with the local oscillator signal $v_2(t) = R_e\left\{ 2\, e^{j(\omega_2 t + \phi(t))} \right\}$ and assuming the sum frequency components are removed, the IF signal is:

$$v_3(t) = R_e\left\{(1 + x(t) + j\, y(t))e^{j(\omega_3(t) - \phi(t))}\right\} \quad \ldots\ldots (2)$$

where $\omega_3 = \omega_1 - \omega_2$. If the IF filter has a transfer function H(S), then the output from the IF filter is:

$$v_4(t) = R_e\left\{ \overline{(1 + x(t) + jy(t))\, e^{-j\phi(t)}}\ \ e^{j\omega_3 t} \right\} \quad \ldots\ldots (3)$$

where the bar denotes the effect of passing the quantity under the bar through a filter of transfer function $K(S) = H(S + j\omega_3)$, i.e. we may define the bar operation by:

$$\bar{v}(t) = \int_0^\infty k(\tau)\, v(t - \tau)\, d\tau$$

where $k(t)$ is the impulse response corresponding to the transfer function $H(S + j\omega_3)$.

The instantaneous IF phase is given by:

$$\theta(t) = \arg\left\{ \overline{(1 + x(t) + jy(t))\, e^{-j\phi(t)}} \right\} \quad \ldots\ldots (4)$$

The feedback is accounted for by the fact that the VCO phase is obtained by passing $\theta(t)$ through a baseband filter $H_2(S)$ and amplifying it. i.e.

$$\phi(t) = A\, \theta^*(t) \quad \ldots\ldots (5)$$

where the asterisk denotes the effect of passing $\theta(t)$ through a filter of transfer function $H_2(S)$. i.e.

$$\theta^*(t) = \int_0^\infty h_2(\tau)\ \theta(t - \tau)\, d\tau$$

where $h_2(t)$ is the impulse response of the filter of transfer function $H_2(S)$.

The simultaneous solution of equations (4) and (5) describes the unmodulated behaviour of FMFB. The effect of modulation is considered in Chapter 3.

2.4 Power series approximations.

If $K(S) = H(S + j\omega_3) = K_r(S) + j\,K_i(S)$ where $K_r(S)$ and $K_i(S)$ are real for S real, then

$$K_r(S) = \tfrac{1}{2}\left\{ H(S + j\omega_3) + H(S - j\omega_3) \right\}$$

$$K_i(S) = \frac{1}{2j}\left\{ H(S + j\omega_3) - H(S - j\omega_3) \right\}$$

$K(S)$ is the transfer function describing the bar operation.

If $K_i(j\omega) = 0$ for all ω in the range of significant frequency components of $x(t)$, $y(t)$ and $\phi(t)$, then $K(S)$ represents a real filter to these signals (i.e. one in which a real excitation gives a real output).

The requirement $K_i(j\omega) = 0$ is equivalent to the IF transfer function having a symmetrical amplitude response and an antisymmetrical phase response about ω_3. This condition is usually closely approximated over the IF passband in practice, provided ω_3 corresponds to the centre frequency. We may take $H(j\omega_3) = 1$ without loss of generality.

Let $Z(t) = (1 + x(t) + j\,y(t))\, e^{-j\phi(t)}$

Expanding the exponential as a power series gives:

$$Z(t) = 1 + x(t) + y(t)\phi(t) + j(y(t) - \phi(t) - x(t)\phi(t)) + O(\phi^2)$$

Hence $\bar{Z}(t) = 1+\bar{x}(t) + \overline{y(t)\phi(t)} + j(\bar{y}(t)-\bar{\phi}(t) - \overline{x(t)\phi(t)}\ ) + O(\phi^2)$

Assuming the IF filter has the symmetry properties discussed above, then all barred terms are real.

If we also assume $\bar{x}(t)$, $\bar{y}(t)$ and $\phi(t)$ are small compared with unity, then:

$$\theta(t) = (\bar{y}(t) - \bar{\phi}(t))(1 - \bar{x}(t)) - \overline{x(t)\ \phi(t)} + \varepsilon(t) \quad \ldots\ (6)$$

where $\varepsilon(t)$ contains terms of third order and higher.

If the system is above discriminator threshold, $\bar{x}(t) \ll 1$ and may be ignored in the first term on the right hand side of (6). The term $\overline{x(t)\ \phi(t)}$ is not necessarily negligible however, and this was considered by Enloe to be the non-linear term causing feedback threshold.

If the IF filter has a transfer function H(S), then it can be shown (e.g. [3]) that the transfer function to small phase variations on a carrier frequency ω_3 is given by:

$$H_1(S) = \tfrac{1}{2}\left\{ \frac{H(S + j\omega_3)}{H(j\omega_3)} + \frac{H(S - j\omega_3)}{H(-j\omega_3)} \right\} \qquad \ldots\ (7)$$

If the IF response has the symmetry properties discussed earlier, then $H(j\omega_3)$ is pure real and may be taken as unity as before. Equation (7) then reduces to:

$$H_1(S) = K(S) \qquad \ldots\ (8)$$

i.e. in this case the incremental phase transfer function is the same as that of the bar operation.

Putting $1 - \bar{x}(t) \approx 1$ in (6) and combining with (5) gives:

$$\phi(t) + A\,\bar{\phi}(\overset{*}{t}) = A\left\{ \bar{y}(\overset{*}{t}) - \overline{x(t)\ \phi(t)}^{\,*} \right\} \qquad \ldots\ (9)$$

Omission of the term $\overline{x(t)\,\phi(t)}^{*}$ in (9) yields the linear model. In this case $\phi(t)$ depends only on $y(t)$, and the transfer function connecting them is:

$$H_c(S) = \frac{A\,H_1(S)\,H_2(S)}{1 + A\,H_1(S)\,H_2(S)} \qquad \ldots\ldots (10)$$

where $H_c(S)$ is called the closed loop transfer function. If the psd of the incoming RF noise is $\eta(f)$ = constant, then $x(t)$ and $y(t)$ each has a psd of $2\eta(f)$. The psd of $\phi(t)$ is therefore:

$$G_\phi(f) = 2\,\eta(f)\,\left|\,H_c(j\omega)\,\right|^2 \qquad \ldots\ldots (11)$$

If the term $\overline{x(t)\,\phi(t)}^{*}$ is retained in (9) then we can rewrite (9) in the form:

$$\phi(t) = \hat{y}(t) - \widehat{x(t)\;\phi(t)} \qquad \ldots\ldots (12)$$

where the cap denotes the effect of filtering by $H_c(S)$ i.e.

$$\hat{y}(t) = \int_0^\infty h_c(\tau)\;\; y(t-\tau)\;d\tau$$

where $h_c(t)$ is the impulse response corresponding to the transfer function $H_c(S)$.

If the second term on the right hand side of (12) is small then we may put $\phi(t) \approx \hat{y}(t)$ in this term. Hence

$$\phi(t) \approx \hat{y}(t) - \widehat{x(t)\;\hat{y}(t)} \qquad \ldots\ldots (13)$$

Now since $x(t)$ and $y(t)$ are independent, the psd of $x(t)\;\hat{y}(t)$ is found by convolving the individual spectra. Also the cross spectrum of $\hat{y}(t)$ and $x(t)\;\hat{y}(t)$ is zero since the cross-correlation function is identically zero.

$$R_{cross}(\tau) = \langle \hat{y}(t)\, x(t+\tau)\, \hat{y}(t+\tau) \rangle$$
$$= \langle x(t+\tau) \rangle \langle \hat{y}(t)\, \hat{y}(t+\tau) \rangle$$
$$= 0 \text{ since } x(t) \text{ has zero mean.}$$

Hence we may add the psd's of $\hat{y}(t)$ and $\widehat{x(t)\,\hat{y}(t)}$ to give the psd of $\phi(t)$: viz.

$$G_{\phi}(f) = |H_c(j\omega)|^2 \left\{ G_y(f) + \int_{-\infty}^{+\infty} |H_c(j2\pi\lambda)|^2 G_y(\lambda) G_x(f-\lambda)\, d\lambda \right\}$$

where $G_x(f)$ and $G_y(f)$ are the psd's of $x(t)$ and $y(t)$ respectively. As shown previously these are both equal to $2\eta(f)$. Therefore, by using the fact that $\eta(f)$ = constant:

$$G_{\phi}(f) = 2\eta(f)\, |H_c(j\omega)|^2 \left\{ 1 + \langle \hat{y}(t)^2 \rangle \right\} \qquad \ldots\ldots (14)$$

To satisfy our approximation in (13) we need $\langle \hat{y}(t)^2 \rangle \ll 1$.

We define the closed loop bandwidth B_c as:

$$B_c = \left(\frac{F}{F-1}\right)^2 \int_{-\infty}^{+\infty} |H_c(j\omega)|^2\, df$$

and the parameter ρ_c as:

$$\rho_c = \frac{1}{4\eta(f)\, B_c}$$

where ρ_c is in fact the CNR which would exist if the RF signal were passed through a bandpass filter of bandwidth equal to B_c. Hence ρ_c is called "the CNR in the closed loop bandwidth." [3] .

Since $\langle \hat{y}^2(t) \rangle = 2\eta(f) \int_{-\infty}^{+\infty} |H_c(j\omega)|^2\, df$, we can also write:

$$\langle \hat{y}(t)^2 \rangle = \frac{(F-1)^2}{2F^2 \rho_c}$$

The linear model corresponds to the term $\{1 + \langle \hat{y}(t)^2 \rangle\}$ in (14) being unity. If we assume threshold corresponds to $\frac{1}{2}$db deviation from linearity, then the value of ρ_c at threshold is:

$$\rho_{c(th)} = 4.13 \left\{ \frac{F-1}{F} \right\}^2 \qquad \ldots\ldots (15)$$

This agrees with the experimental result obtained by Enloe, except that his result was $4.8 \left\{\frac{F-1}{F}\right\}^2$. Equation (15) indicates a mean square local oscillator phase deviation calculated from (14) of $\langle \phi^2(t) \rangle = 0.136$ rad^2. [c.f. Enloe 0.103 rad^2 $\pm$ 14%, although it was not clear whether this was measured directly or calculated from other parameters using the linear equivalent circuit. Also Enloe's threshold criterion was an impulse rate of 1 per second. This corresponds to $\frac{1}{2}$db increase in output noise if ρ_{IF} = 13db in his system. His system had a 3KH$_z$ baseband bandwidth and a 6KH$_z$ 3db bandwidth single pole IF filter.]

The value of $\langle \hat{y}^2(t) \rangle$ at threshold as defined by equation (15) is 0.121. This is also the value of $\langle \phi(t)^2 \rangle$ calculated from the linear model.

A digital simulation of the system represented by equation (9) gave close agreement with equation (14) . This is shown in Figure 2.2 (0db input noise corresponds to $\eta(f) = 1/6$ volt^2/H$_z$ for the model of Appendix E. This also corresponds to $\rho_c = \frac{1}{2}(F-1)^2/F^2$. Further details of digital simulations are found in Appendix G).

The approximation (14) predicts no change in the shape of the output

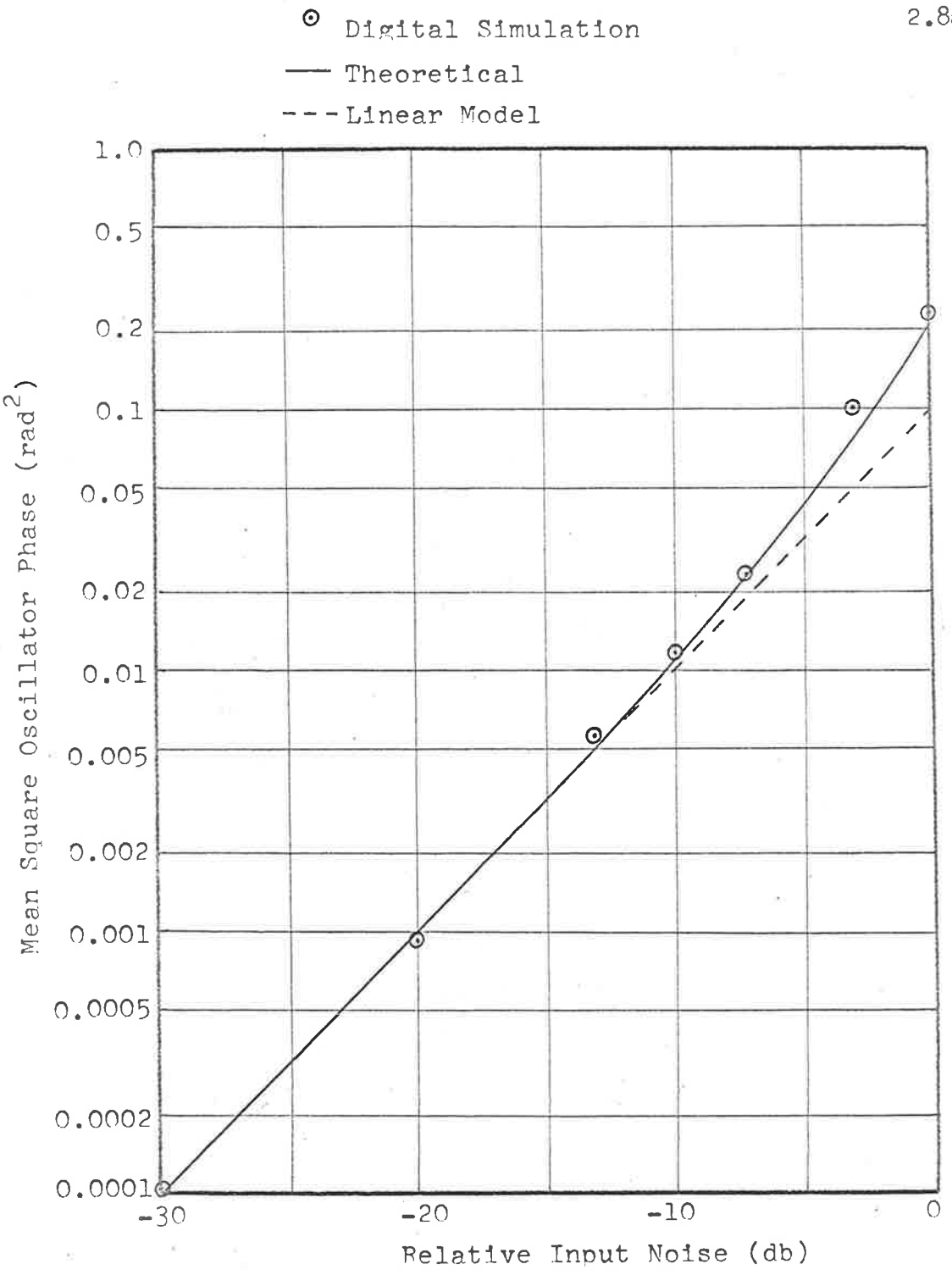

FIGURE 2.2: THRESHOLD IN FMFB- POWER SERIES MODEL I.

spectrum.

The apparent agreement between this model and the experimental results of Enloe is rather deceptive, since the region of deviation from linearity is also the region where the approximations made become increasingly inaccurate.

This fact was emphasised when equation (6) with all second order terms retained was used in a digital simulation. The results are shown in Figure 2.3. This indicated little change from linearity, which is inconsistent with experimental evidence. It seems, therefore, that power series approximations do not lead to satisfactory models for explaining threshold behaviour.

However the results obtained are useful in that they indicate the critical parameters involved in the occurrence of threshold. In particular, it is noted that the mean square value of $\phi(t)$ is significant, in that if this is small enough, the system is above threshold (provided the system is also above discriminator threshold).

A simulation of the exact relations in equations(4) and (5) and practical experiments indicated that the occurrence of feedback threshold is not a smooth rise in output noise. Rather, it is impulsive in nature, similar to discriminator threshold in normal FM.

Figure 2.4 shows the results of the digital simulation. For input noise levels exceeding -10db, the mean square value of ϕ does not converge. This was due to jumps in the mean value of ϕ, each jump corresponding to an impulse of noise in the output.

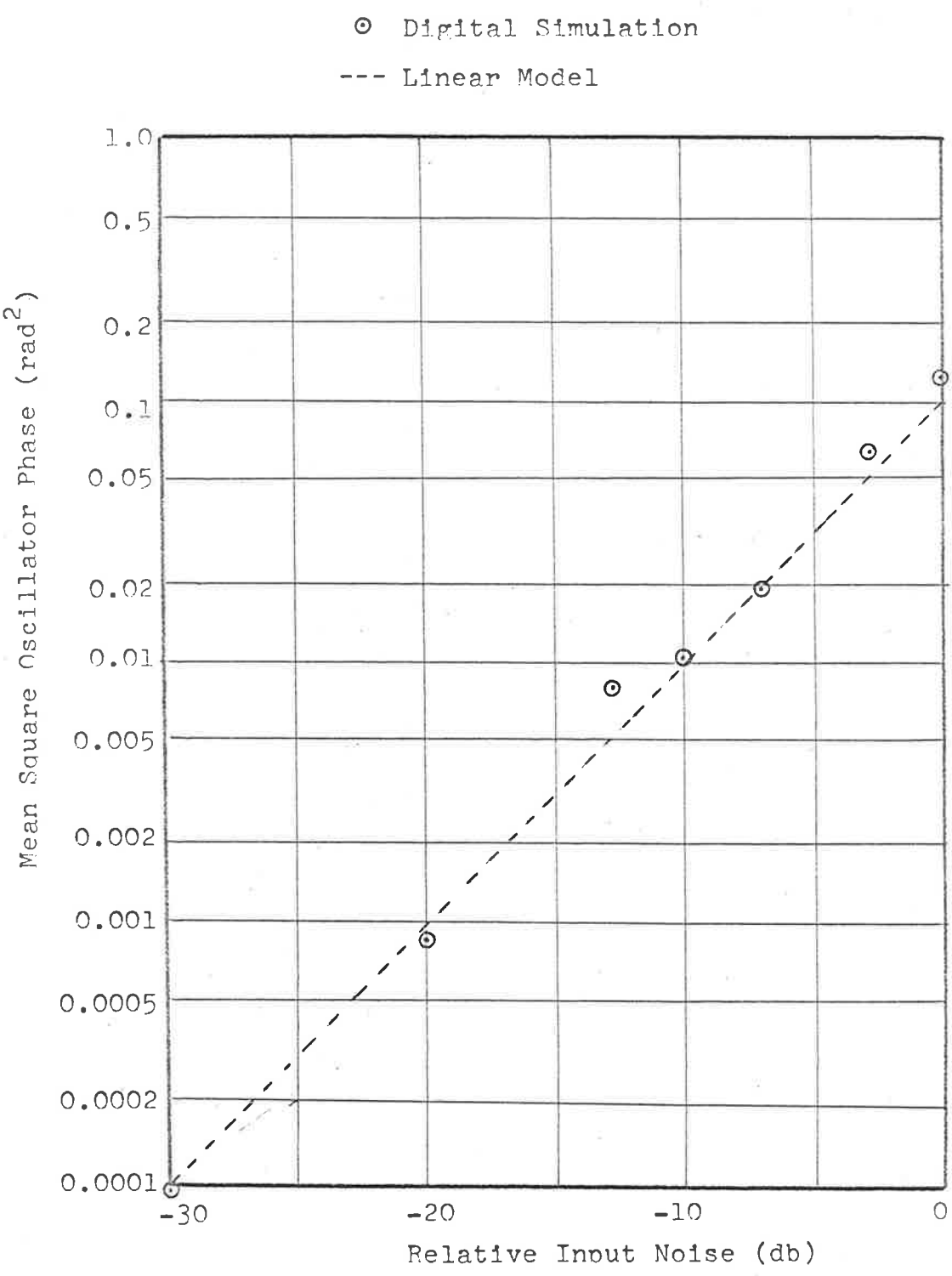

FIgure 2.3: THRESHOLD IN FMFB - POWER SERIES MODEL II.

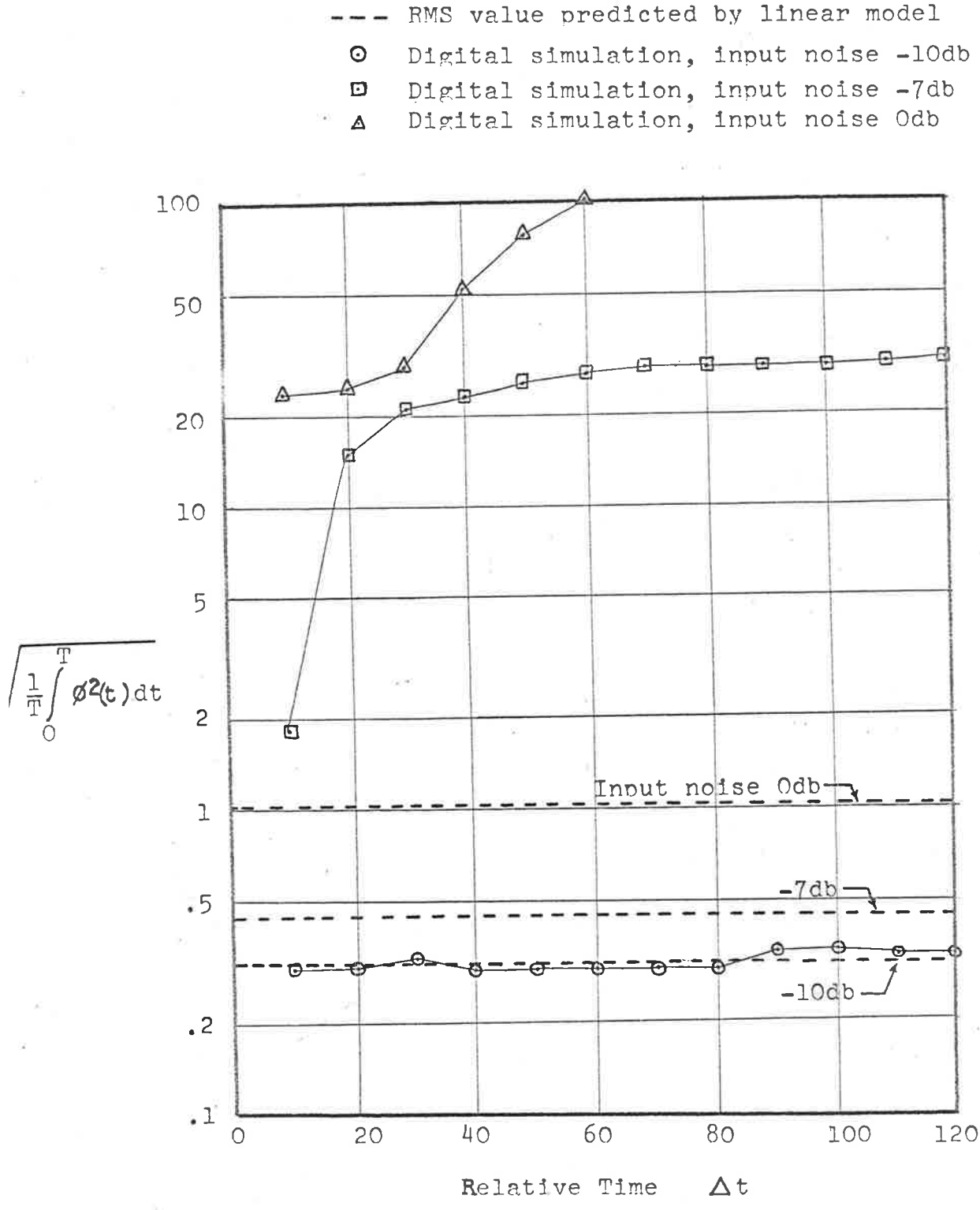

FIGURE 2.4: THRESHOLD IN FMFB - EXACT MODEL.

2.5 Impulse approximations.

2.5.1 Impulse mechanisms.

Using the approach of Rice [5] and regarding the threshold as the result of two separate processes, the linear process and the impulsive process, the number of jumps in the mean value of ϕ was counted. This was obtained from a digital simulation of the exact equations (4) and (5).

The results are shown in Figure 2.5 (simulation 1). Approximately equal numbers of positive and negative jumps occurred, the magnitude of the jumps being $2\pi(F-1)/F$.

The theoretical treatment of this approximation requires a prediction of the impulse rate in terms of system parameters. For ordinary discriminator threshold, Rice was able to predict the impulse rate by multiplying together the zero crossing rate for the quadrature noise component and the probability of the signal (carrier + noise) phasor lying in the second or third quadrants. The cause of the impulse in this case is an encirclement of the origin by the signal phasor, corresponding to a phase jump of $\pm 2\pi$ radians, and the frequency detector gives an output corresponding to the time derivative of phase (i.e. an impulse).

In feedback threshold, however, impulses occur even when there would normally be no encirclement in the absence of feedback. To study the behaviour of the system, it is convenient to consider a low frequency model in which phase is the variable. The frequency detector, baseband filter and voltage controlled oscillator represent linear

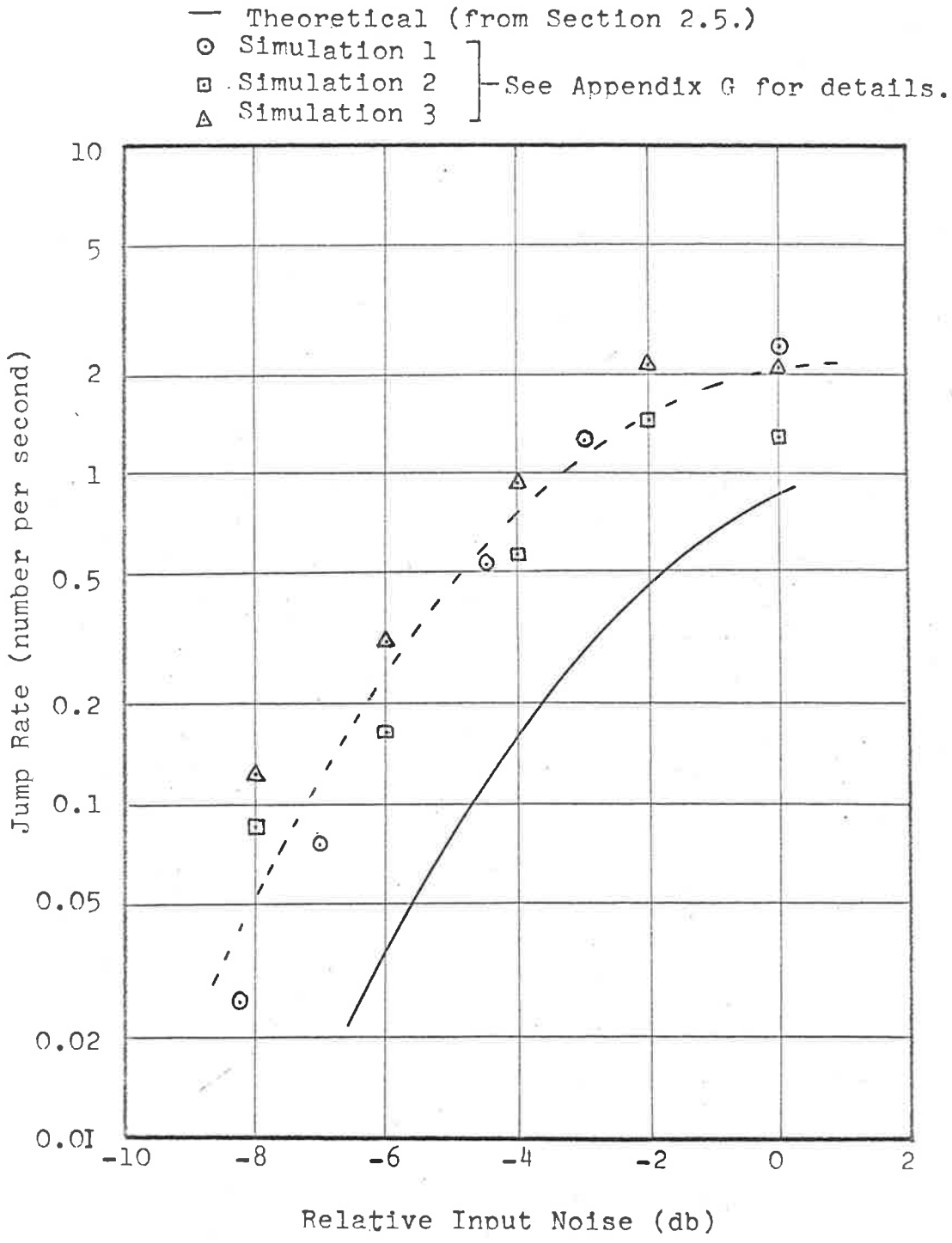

FIGURE 2.5: IMPULSE RATES IN FMFB.

operations on the phase, being differentiation, low pass filtering and integration respectively. Since integration and differentiation are complementary, it is convenient to ignore them completely in the analysis of the system, except to remember the output is finally the time derivative of the phase.

The mixer is a linear phase differencing device if the sum frequency components can be neglected. The IF filter, although linear to the cartesian components of the signal phasor, is not linear to phase itself.

If the input to the IF channel is of the form

$$v_i(t) = R_e \left\{ Z(t) \quad e^{j\omega_3 t} \right\} \qquad \ldots\ldots (16)$$

where $Z(t)$ is the phasor representation of $v_i(t)$, then the output is of the form:

$$v_o(t) = R_e \left\{ W(t) \quad e^{j\omega_3 t} \right\} \qquad \ldots\ldots (17)$$

If the IF filter transfer function is $H(S)$, the transfer function linking $Z(t)$ to $W(t)$ is $H(S+j\omega_3)$. A high Q LC resonant circuit closely approximates the symmetry requirements mentioned previously and hence $K(S) = H(S+j\omega_3)$ corresponds to a real filter. The differential equation corresponding to $K(S)$ is:

$$\frac{1}{\Delta} \frac{dW(t)}{dt} + W(t) = Z(t) \qquad \ldots\ldots (18)$$

where Δ is the semi 3db bandwidth of the IF filter in radians/sec. This is shown in Appendix B, which also considers the case where the Q is

not necessarily high and the filter resonant frequency is different from the carrier frequency.

The differential equation (18) has a particularly simple geometrical interpretation. At any instant the response phasor W(t) moves towards Z(t) with a velocity proportional to the separation distance. If Z(t) is constant, the path of W(t) is a straight line.

Equation (18) may be converted into an equation in the IF phase $\theta(t)$, with excitations x(t), y(t) and $\phi(t)$. For FMFB the vector Z is given by:

$$Z(t) = (1 + z(t))e^{-j\phi(t)} \qquad \ldots\ldots (19)$$

where $z(t) = x(t) + jy(t)$ is the noise phasor.
On putting $W(t) = r(t)\, e^{j\theta(t)}$ and eliminating r(t) from equation (18), the phase equation is:

$$\left\{ y(\ddot{\theta} - \Delta\dot{\theta}) - \dot{\theta}\dot{y} + (2\dot{\theta}^2 + \dot{\theta}\dot{\phi})(1 + x) \right\} \cos(\theta + \phi)$$
$$- \left\{ (1+x)(\ddot{\theta} - \Delta\dot{\theta}) + \dot{\theta}\dot{x} - (2\dot{\theta}^2 + \dot{\theta}\dot{\phi})y \right\} \sin(\theta + \phi) = 0 \quad \ldots(20)$$

It is evident that although linear in Z(t) and W(t), the system is not linear in $\theta(t)$, particularly when Z(t) and W(t) are markedly different. The general effect for large differences in the arguments of Z(t) and W(t) is that the response is initially more sluggish than predicted by the linear model.

Figure 2.6 shows the response if the phasor W is displaced angularly by an amount θ_i from its rest position $Z(t) = 1+j0 =$

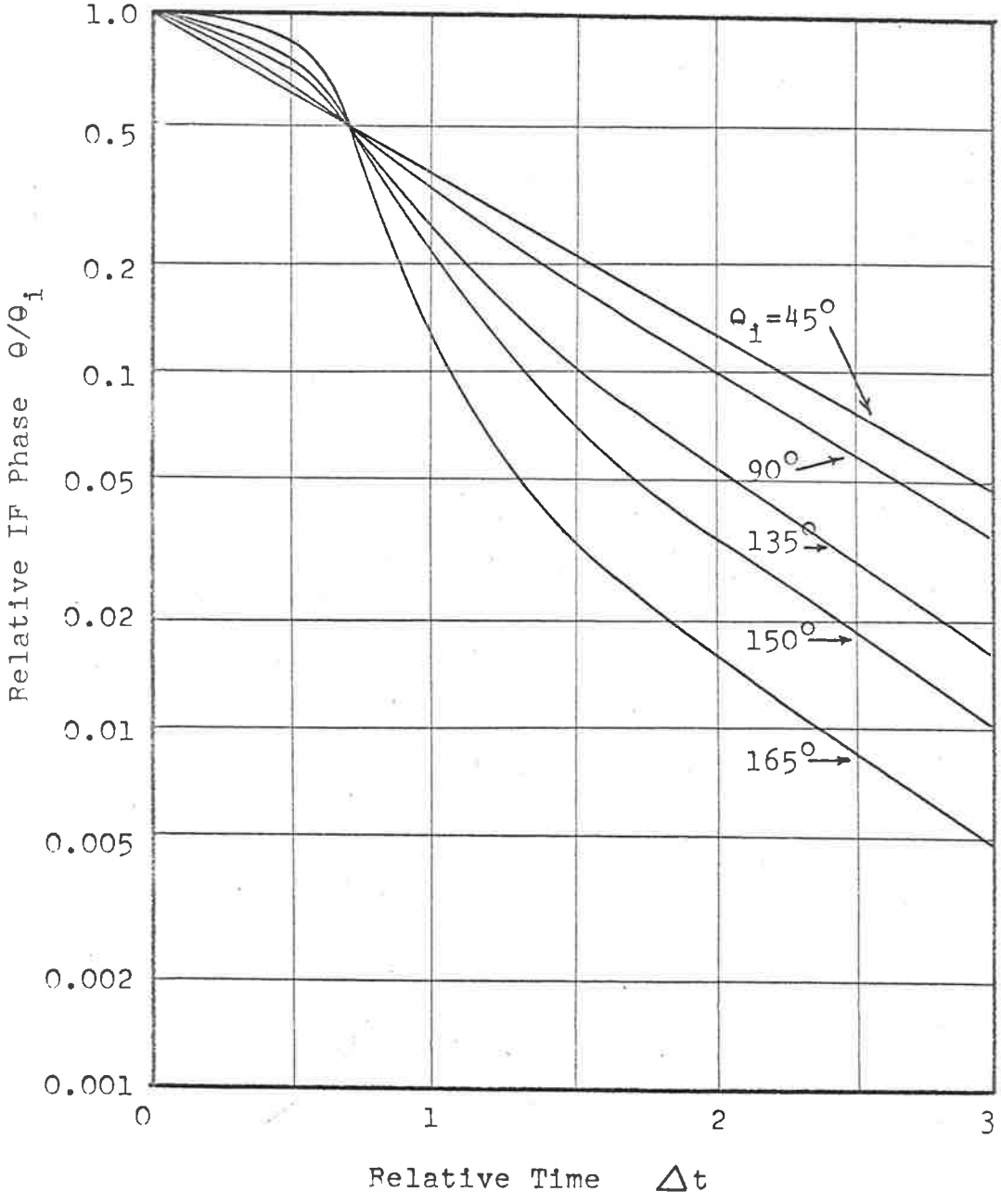

FIGURE 2.6: RESPONSE OF IF FILTER TO STEP CHANGE IN PHASE.

constant. This could be obtained from equation (20) by putting $x(t) = y(t) = \phi(t) = 0$ and using appropriate initial conditions for θ. However, in this case an exact analytical solution can be obtained from equation (18) using the initial condition $W(0) = e^{j\theta_i}$.

Hence:

$$W(t) = 1 - (1 - e^{j\theta_i}) e^{-\Delta t} \qquad \ldots\ldots (21)$$

and the phase $\theta(t)$ is given by the argument of $W(t)$.

$$\theta(t) = \arg \left\{ 1 - (1 - e^{j\theta_i}) e^{-\Delta t} \right\} \qquad \ldots\ldots (22)$$

Note that $\theta(t) = \frac{1}{2}\theta_i$ at $t = \frac{1}{\Delta} \ln 2$.

In the absence of local oscillator modulation, (i.e. $\phi(t) = 0$) it can be seen that if the response phasor $W(t)$ encircles the origin, then an impulse appears in the output. This corresponds to discriminator threshold and is conveniently analysed by using the fact that $W(t)$ is gaussian. (i.e. the cartesian components of $W(t)$ are jointly gaussian). This has been done by Rice [5].

In FMFB, $\phi(t)$ is not zero and in general $W(t)$ and $Z(t)$ are non-gaussian. However threshold occurs when there are phase jumps in $W(t)$, although these are not necessarily 2π in magnitude as will be seen shortly.

Figure 2.7 shows a model of FMFB equivalent to Figure 2.1. Inclusion of the amplifier of gain A+1 means $\theta_o(t)$ is equal to the incoming phase under ideal conditions. If the phasor $1+z(t)$ encircles the origin slowly enough that the loop follows it, then $\theta_o(t)$ will jump 2π,

the IF phase $\theta(t)$ will jump $2\pi/F$ and the local oscillator phase $\phi(t)$ will jump $2\pi(F-1)/F$.

In fact there are an infinite number of "rest" states for $\phi(t)$ separated by $2\pi(F-1)/F$, and a jump from one state to another is accompanied by an impulse in the output.

A difficulty arises here that even in the absence of feedback, a single pole IF filter has an infinite impulse rate. This is because the impulse rate is proportional to the RMS value of the derivative of the quadrature noise, which is unbounded for a single pole filter. In practice a single pole response is never actually obtained exactly and the impulse rate is always finite.

To avoid this difficulty it is necessary to consider an IF filter with a faster skirt roll-off. This could be provided by another tuned stage of wider bandwidth such that the response in the passband is still essentially single pole. Conventional IF stages (e.g. maximally flat) cannot be used because of loop stability problems and modulation dependent effects (see Chapter 3).

In the no feedback case, an IF channel consisting of two tuned stages of bandwidths B_1 and B_2, produces an impulse rate proportional to $\sqrt{B_1 B_2}$. The nett sensitivity of the threshold carrier level to changes in bandwidth ratio B_1/B_2, while still maintaining the same noise bandwidth, is relatively small, being about 0.7db difference for ratios of 1 and 100.

It is convenient therefore to assume the IF filter consists of the basic single pole filter plus a similar stage of wider

bandwidth. In FMFB the effect of the additional pole will be assumed to be compensated by a zero in the baseband filter (see Appendix E).

In considering the threshold of FMFB it is evident that in certain cases it is possible to say that this is caused predominantly either by effects similar to normal discriminator threshold or by effects related to the feedback. The external behaviour of the system is identical in either case, the impulses in the frequency detector output being caused by $2\pi/F$ jumps in the IF phase and $2\pi(F-1)/F$ jumps in the VCO phase.

2.5.2 Prediction of impulse rates.

A more convenient model of the FMFB system is obtained by introducing the noise at a different point in the circuit. In the absence of feedback, the incoming white noise passes through the mixer and the mixer output noise is also white. Passing through the IF filter only modifies its psd and hence the model of Figure 2.8 is obtained. The transfer of the noise input is also justified under feedback conditions because of the whiteness of the input noise n(t). This technique has been used in analyses of the phase locked loop [13] .

If the psd of n(t) is $\eta(f)$, then on the assumption that the mixer is an ideal multiplier and the VCO signal is given by $v_2 = R_e(2e^{j(\omega_2 t + \phi)})$, the psd of n'(t) is given by:

$$\eta'(f) = |H(j\omega)|^2 \quad \eta(f) \qquad \ldots\ldots (23)$$

where H(S) is the IF filter transfer function and use has been made of the fact that $\eta(f)$ = constant.

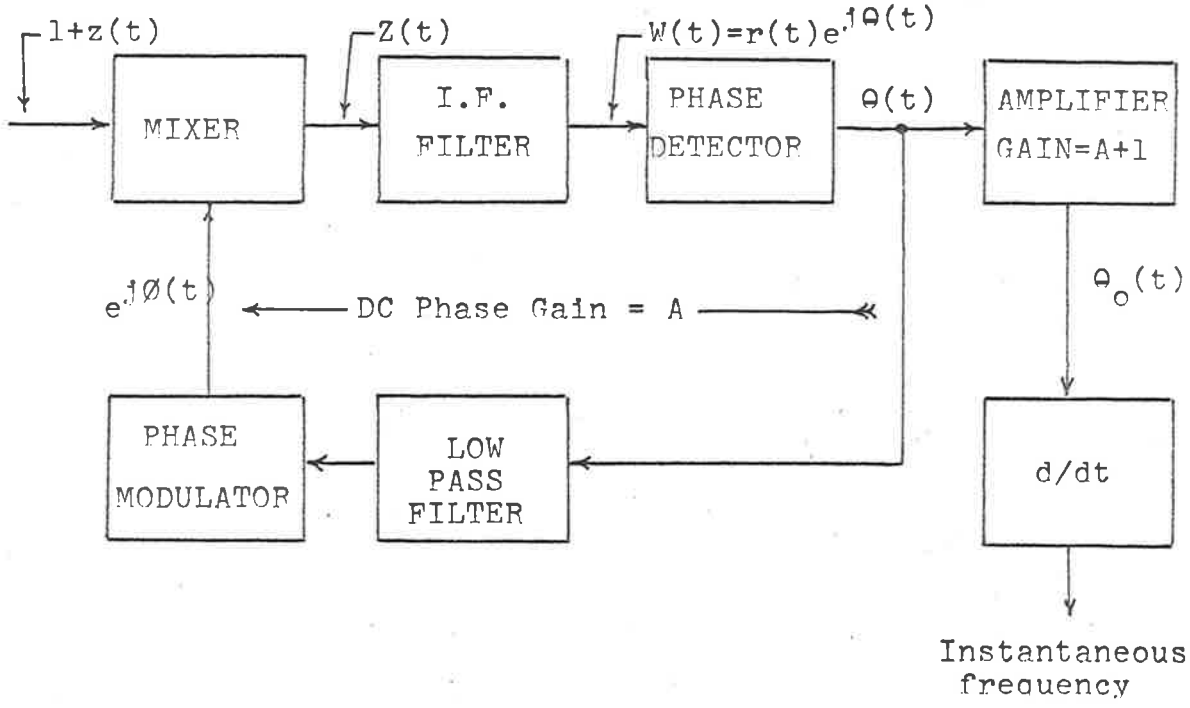

FIGURE 2.7: MODEL OF FMFB SYSTEM.

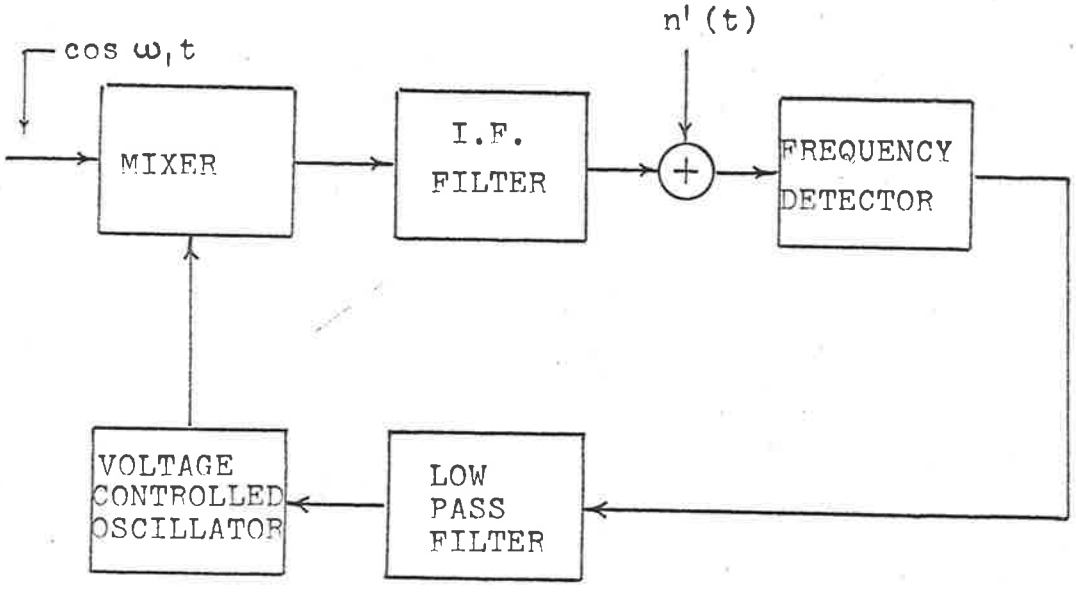

FIGURE 2.8: MODIFIED MODEL OF FMFB SYSTEM.

The advantage of this representation lies in the fact that we do not have the complication of interaction between the noise and the VCO phase modulation prior to IF filtering. Also the mean square value of n'(t) is finite and much less than unity if the system is above threshold.

Figure 2.5 shows the results of digital simulations on both the original model of Figure 2.1 (simulation 2) and the modified model of Figure 2.8 (simulation 3). The impulse rates obtained are not significantly different for the two models.

Figure 2.9 shows the phasor diagrams of an FMFB system at some time t for both the original model of Figure 2.1 and the modified model of Figure 2.8. The phasor z'(t) represents n'(t). The dotted lines with arrows indicate the paths the filter output phasors would follow if the input phasors were frozen. If the local oscillator phase deviation $\phi(t)$ is small, then impulses may occur due to n'(t) becoming large enough for the IF carrier plus noise phasor W(t) to encircle the origin.

The rest states are defined by the equations:

$$\phi_r + \theta_r = 2\pi k \quad (k \text{ an integer}) \qquad \ldots (24a)$$

$$\phi_r = A\,\theta_r \qquad \ldots (24b)$$

where θ_r and ϕ_r are the rest values of $\theta(t)$ and $\phi(t)$ in the absence of noise. In the presence of noise they may be regarded as the short term mean values of these quantities. Equation (24a) is the constraint imposed by the IF filter and (24b) corresponds to the feedback path.

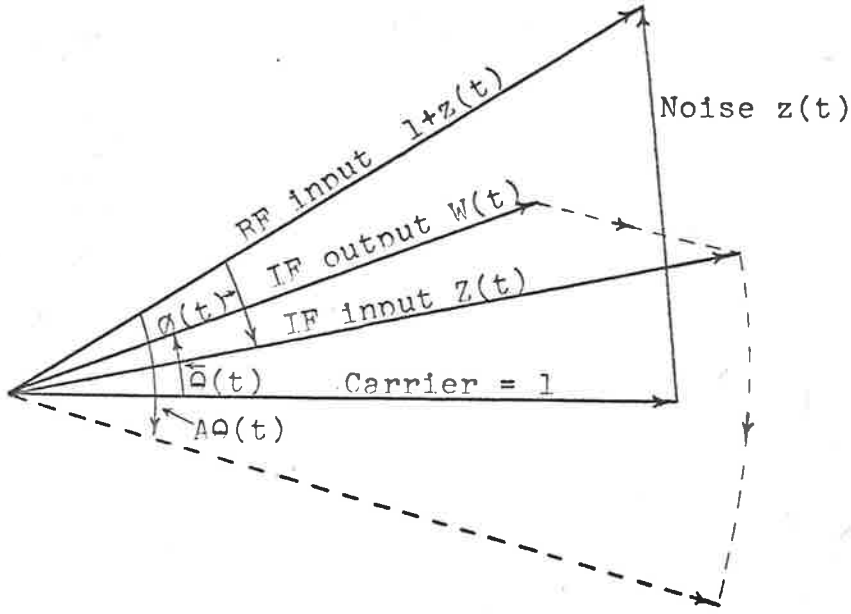

FIGURE 2.9a: PHASOR DIAGRAM OF ORIGINAL MODEL.

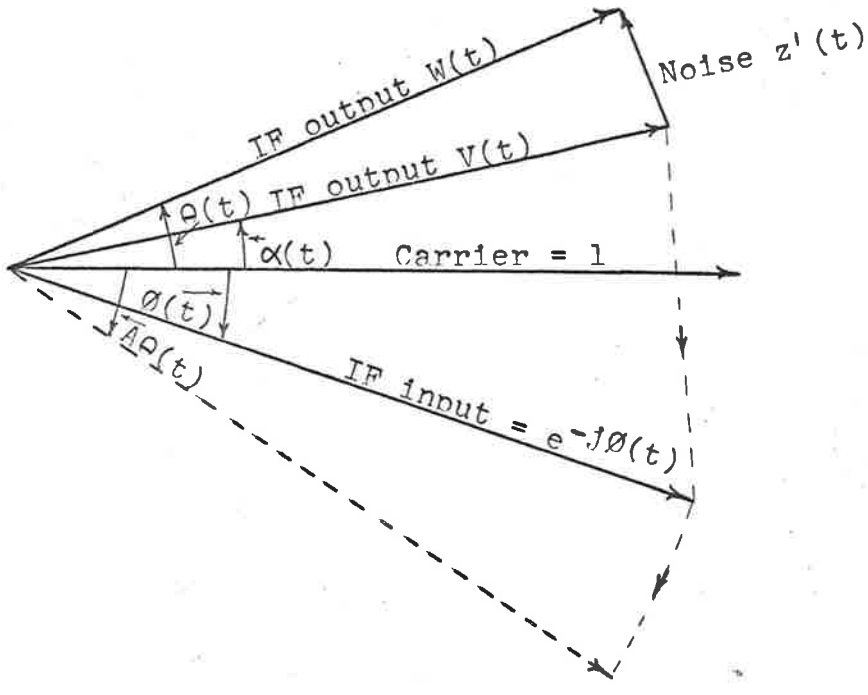

FIGURE 2.9b: PHASOR DIAGRAM OF MODIFIED MODEL.

If the phasor W(t) encircles the origin this introduces an extra 2π on the left hand side of (24a) due to the increase in $\theta(t)$. This is absorbed into new rest states $\theta_r' = \theta_r + 2\pi/F$ and $\phi_r' = \phi_r + 2\pi(F-1)/F$ in accordance with (24b). The nett IF phase jump is therefore $2\pi/F$. This effect produces results nearly identical to normal discriminator threshold in ordinary FM. The VCO phase $\phi(t)$ jumps $2\pi(F-1)/F$ even though its fluctuation about ϕ_r may be small initially.

If the VCO phase variation $\phi(t)$ is sufficiently large then impulses can occur, even though n'(t) be small. Due to the non-linear behaviour of the IF filter, if the angular difference between the IF input and output phasors increases to a magnitude greater than π, the output phasor approaches the input vector from the opposite direction. This results in the value of k in (21a) increasing or decreasing by 1 and the new rest states correspond to a $2\pi/F$ jump in θ_r and a $2\pi(F-1)/F$ jump in ϕ_r.

Note that both the above effects are due to the IF input and output phasors slipping relative to each other by an amount 2π radians. It is only the cause of this slip which distinguishes discriminator threshold from feedback threshold. Of course, in a practical system, it is not possible to accurately distinguish an impulse as being due to one or the other.

The impulse rate prediction of the first effect (called discriminator threshold) can be achieved using the results of Rice [5]

for normal FM. For the latter, the rate is evidently related to the magnitude of the deviation of the VCO phase $\phi(t)$. This corresponds to the feedback threshold.

(a) Discriminator impulse rate.

The discriminator impulse rate from Rice [5] will be derived. If the carrier is of unit amplitude and $x'(t) + j\, y'(t)$ is the phasor representation of $n'(t)$, then the impulse rate is given by:

$$\nu_d = \nu_{y'} \; P\,(x' \leqslant -1) \qquad \ldots\ldots (25)$$

where ν_d = total number of impulses / sec.

$\nu_{y'}$ = zero crossing rate of $y'(t)$.

The assumption is that every time the phasor crosses the negative real axis an impulse occurs. Now $\nu_{y'}$ is given by:

$$\nu_{y'} = m_{IF}/\pi \qquad \ldots\ldots (26)$$

where $m_{IF}^2 = \langle \dot{y}'^2 \rangle / \langle y'^2 \rangle$ and is a property of the IF filter alone if the incoming RF noise is white.

Also $x'(t)$ is gaussian of pdf:

$$p(x') = \frac{1}{\sqrt{2\pi \langle x'^2 \rangle}} \; e^{-x'^2 / 2\langle x'^2 \rangle} \qquad \ldots\ldots (27)$$

Hence $$\nu_d = \frac{m_{IF}}{\pi} \int_{-\infty}^{-1} p(x')\, dx'$$

i.e. $$\nu_d = \frac{m_{IF}}{2\pi} \; \mathrm{erfc}\,(\sqrt{\rho_{IF}}) \qquad \ldots\ldots (28)$$

where erfc is the complementary error function and $\rho_{IF} = 1/2\langle x'^2 \rangle$ is the CNR at the IF filter output.

(b) Feedback impulse rate.

A feedback impulse results when the IF output phasor fails to "track" the IF input phasor, and hence the critical point is where these phasors differ in argument by π radians. If this difference increases beyond π radians, the IF output phasor may approach the input by the shorter route, involving a slip of 2π radians. Feedback constraints redistribute this according to equations (24a) and (24b).

Referring to the phasor diagram of Figure 2.9b representing the modified model of Figure 2.8, we may consider that if the angular difference between the IF input and output phasors exceeds π radians, then a feedback impulse is almost certain to occur. (This is analogous to the impulse phenomenon in ordinary FM threshold, where an impulse almost certainly occurs if the argument of the signal plus noise phasor exceeds π radians in magnitude.)

If we denote the IF output before $n'(t)$ is added by the phasor:

$$V(t) = a(t)\, e^{j\alpha(t)} \qquad \ldots\ldots (29)$$

then if $n'(t)$ is represented by the phasor $z'(t) = x'(t) + j\, y'(t)$, the final IF output phasor after $n'(t)$ is added is given by:

$$W(t) = V(t) + z'(t) \qquad \ldots\ldots (30)$$

For the above model, the IF input phasor is simply the constant amplitude phasor $e^{-j\phi(t)}$. We may therefore state that the condition for an impulse to occur is that:

$$|\phi(t) + \alpha(t)| > \pi \qquad \ldots\ldots (31)$$

The fact that the distributions of $\phi(t)$ and $\alpha(t)$ are non-gaussian means that a prediction on the basis of gaussian pdf's is not likely to be accurate, particularly in view of the sensitivity of the impulse rate to the tails of the distribution.

Let us define $\gamma(t) = \phi(t) + \alpha(t)$ where $\gamma(t)$ is assumed continuous and not necessarily confined to the range $-\pi$ to π. (i.e. we take into account all 2π jumps in $\gamma(t)$). We are therefore interested in the rate at which $\gamma(t)$ crosses odd multiples of π, the even multiples of π corresponding to rest states.

If $p(\gamma, \dot{\gamma})$ is the joint pdf of $\gamma(t)$ and its time derivative, then the rate of crossing a level γ_k is given by: [18a]

$$\nu_{k+} = \int_0^\infty \dot{\gamma}\, p(\gamma_k, \dot{\gamma})\, d\dot{\gamma} \qquad \ldots\ldots (32)$$

where ν_{k+} = rate of crossing γ_k in a positive direction.

In particular, we are interested in the rate of crossing levels $\gamma_k = (2k+1)\pi$, k an integer. The total positive crossing rate is therefore:

$$\nu_+ = \sum_{k=-\infty}^{+\infty} \nu_{k+} = \int_0^\infty \dot{\gamma} \sum_{k=-\infty}^{+\infty} p((2k+1)\pi, \dot{\gamma})\, d\dot{\gamma} \qquad \ldots\ldots (33)$$

If we reduce $\gamma(t)$ modulo 2π to the range $-\pi < \gamma_r(t) \leq \pi$, then the joint pdf of $\gamma_r(t)$ and $\dot{\gamma}(t)$ is:

$$q(\gamma_r, \dot{\gamma}) = \sum_{k=-\infty}^{+\infty} p(\gamma_r + 2k\pi, \dot{\gamma}) \qquad \ldots\ldots (34)$$

Hence from (33) we obtain:

$$\nu_+ = \int_0^\infty \dot{\gamma}\ q(\pi, \dot{\gamma})\ d\dot{\gamma} \qquad \ldots\ldots (35)$$

If the distribution $q(\gamma_r, \dot{\gamma})$ is symmetrical in γ_r and $\dot{\gamma}$ then the negative crossing rate ν_- is equal to ν_+. This will normally be so under unmodulated conditions and correct tuning of the FMFB system. The nett impulse rate is therefore $\nu_f = 2\nu_+$.

If we write $q(\gamma_r, \dot{\gamma}) = q_1(\gamma_r)\ q_2(\dot{\gamma}/\gamma_r)$, where $q_1(\gamma_r)$ is the pdf of $\gamma_r(t)$ and $q_2(\dot{\gamma}/\gamma_r)$ the conditional pdf of $\dot{\gamma}(t)$, then from (35) we can express the impulse rate as:

$$\nu_f = q_1(\pi) < |\dot{\gamma}| >_{\gamma_r = \pi} \qquad \ldots\ldots (36)$$

Here we have assumed the symmetry requirements above are satisfied.

The assumption that $\gamma_r(t)$ and $\dot{\gamma}(t)$ are jointly gaussian leads to large errors in (36). The main source of error is in the factor $q_1(\pi)$, where because of the poor fit to the tails of the gaussian distribution, the error is extremely large. The factor $< |\dot{\gamma}| >_{\gamma_r = \pi}$ is also in error if evaluated in the gaussian assumption, although the error is not nearly so significant as that of $q_1(\pi)$.

We shall first consider the properties of the phase of a sinewave plus random gaussian noise. The properties of $\gamma(t)$ will be similar, although filtering and feedback will obviously have some effect.

The pdf of the instantaneous phase $\theta(t)$ of a sinewave plus gaussian noise is given by: [18b] .

$$p(\theta) = \frac{1}{2\pi}\left\{ e^{-\rho + \sqrt{\pi\rho}\cos\theta}\ e^{-\rho\sin^2\theta}\left(1+\mathrm{erf}\left(\sqrt{\rho}\cos\theta\right)\right)\right\} \quad \ldots\ldots (37)$$

where ρ is the CNR.

Hence:

$$p(\pi) = \frac{1}{2\pi}\left\{ e^{-\rho - \sqrt{\pi\rho}}\ \mathrm{erfc}\ \sqrt{\rho}\right\} \quad \ldots\ldots (38)$$

Using the asymptotic expansion for erfc $(\sqrt{\rho})$ [28], (38) becomes:

$$p(\pi) = \frac{e^{-\rho}}{4\pi}\left\{ \frac{1}{\rho} + O\left(\frac{1}{\rho^2}\right)\right\} \quad \ldots\ldots (39)$$

The high CNR gaussian approximation to the pdf of $\theta(t)$ gives:

$$p_g(\theta) = \sqrt{\frac{\rho}{\pi}}\ e^{-\rho\theta^2} \quad \ldots\ldots (40)$$

since $\langle\theta^2\rangle \approx \frac{1}{2\rho}$ for large ρ. Note that even though $\theta(t)$ becomes very nearly gaussian as $\rho \to \infty$, the expression (40) with $\theta = \pi$ does not converge to the correct value as given by (38). The fit to the tails of the gaussian distribution in terms of relative error is very poor.

We will also show that $\langle|\dot{\theta}|\rangle$ is different from $\langle|\dot{\theta}|\rangle_{\theta=\pi}$. These would be equal if $\theta(t)$ were gaussian. The first can be found from the pdf of $\dot{\theta}$ as derived in Appendix A. The result (from Appendix A) is:

$$\langle|\dot{\theta}|\rangle = m\, e^{-\frac{1}{2}\rho}\ I_0\left(\tfrac{1}{2}\rho\right) \quad \ldots\ldots (41)$$

where m is the radius of gyration of the IF filter characteristic (rad/sec).

The second can be found from the known impulse rate of sinewave

plus gaussian noise as given by equation (28): viz.

$$\nu = \frac{m}{2\pi} \operatorname{erfc}(\sqrt{\rho}) \qquad \ldots\ldots (42)$$

However we can also write (using (36)):

$$\nu = p(\pi) \langle |\dot{\theta}| \rangle_{\theta=\pi} \qquad \ldots\ldots (43)$$

where $p(\pi)$ is given by (38).

Hence:

$$\frac{\langle |\dot{\theta}| \rangle_{\theta=\pi}}{\langle |\dot{\theta}| \rangle} = \frac{\operatorname{erfc}(\sqrt{\rho})}{e^{-\frac{1}{2}\rho} I_0(\frac{1}{2}\rho) \left\{ e^{-\rho} - \sqrt{\pi\rho}\, \operatorname{erfc}(\sqrt{\rho}) \right\}} \qquad \ldots\ldots (44)$$

Using the asymptotic expansions for $\operatorname{erfc}(\sqrt{\rho})$ and $I_0(\frac{1}{2}\rho)$ [28] we obtain:

$$\frac{\langle |\dot{\theta}| \rangle_{\theta=\pi}}{\langle |\dot{\theta}| \rangle} = 2\rho \left(1 + O(\frac{1}{\rho})\right) \qquad \ldots\ldots (45)$$

This ratio diverges as $\rho \to \infty$.

Thus even though $\theta(t)$ tends to gaussian as $\rho \to \infty$, the impulse rate prediction assuming $\theta(t)$ is gaussian does not converge to the correct value.

If however, we assume $\theta(t)$ gaussian and that an impulse occurs whenever $|\theta(t)|$ exceeds some value θ_o, then to obtain the correct impulse rate, we require

$$\frac{m}{\pi} e^{-\rho \theta_o^2} = \frac{m}{2\pi} \operatorname{erfc}(\sqrt{\rho}) \qquad \ldots\ldots (46)$$

where the left hand side is the crossing rate of a gaussian process and the right hand side is as given by (42).

Hence:
$$\theta_o = \sqrt{\frac{1}{\rho} \ln \left\{ \frac{2}{\operatorname{erfc}(\sqrt{\rho})} \right\}} \qquad \ldots\ldots (47)$$

A plot of θ_o against ρ is shown in Figure 2.10. A prediction of the output noise (from a frequency demodulator) based on θ_o = constant is shown in Figure 2.11. i.e. the impulse rate is assumed to be given by the expression on the left hand side of (46). Also shown is the result given by the right hand side of (46), which is Rice's result. The IF transfer function is assumed rectangular of bandwidth $12f_a$ (corresponding to an FM system of modulation index 5.) (f_a = baseband bandwidth).

It can be seen that the gaussian model produces a curve of the correct shape, but one in which the rate of increase in noise is slightly higher than given by Rice's curve.

If we proceed in the same manner with $\gamma(t)$ (i.e. assume that $\gamma(t)$ is gaussian and an impulse occurs if $|\gamma(t)|$ exceeds γ_o), then the impulse rate is:

$$\nu_f = \frac{m_\gamma}{\pi} \; e^{-\gamma_o^2/2\langle\gamma^2\rangle} \qquad \ldots\ldots (48)$$

Since the threshold impulse rate is $\nu_f = 0.08\ \eta(f) f_a^2$ (from Appendix D), this yields the value of γ_o viz.

$$\gamma_o^2 = 2\langle\gamma^2\rangle \ln\left\{ \frac{m_\gamma}{0.08\pi\eta(f)\ f_a^2} \right\} \qquad \ldots\ldots (49)$$

The value of $\eta(f)$ can be found from the equation:

$$\langle\phi^2\rangle = 2\eta(f) \int_{-\infty}^{+\infty} |H_c(j\omega)|^2 \; df \qquad \ldots\ldots (50)$$

where $\langle\phi^2\rangle$ is assumed to be a value consistent with the results of Enloe. For the typical FMFB system of Appendix E, the value of γ_o is shown for various feedback factors and IF bandwidths in Figure 2.12.

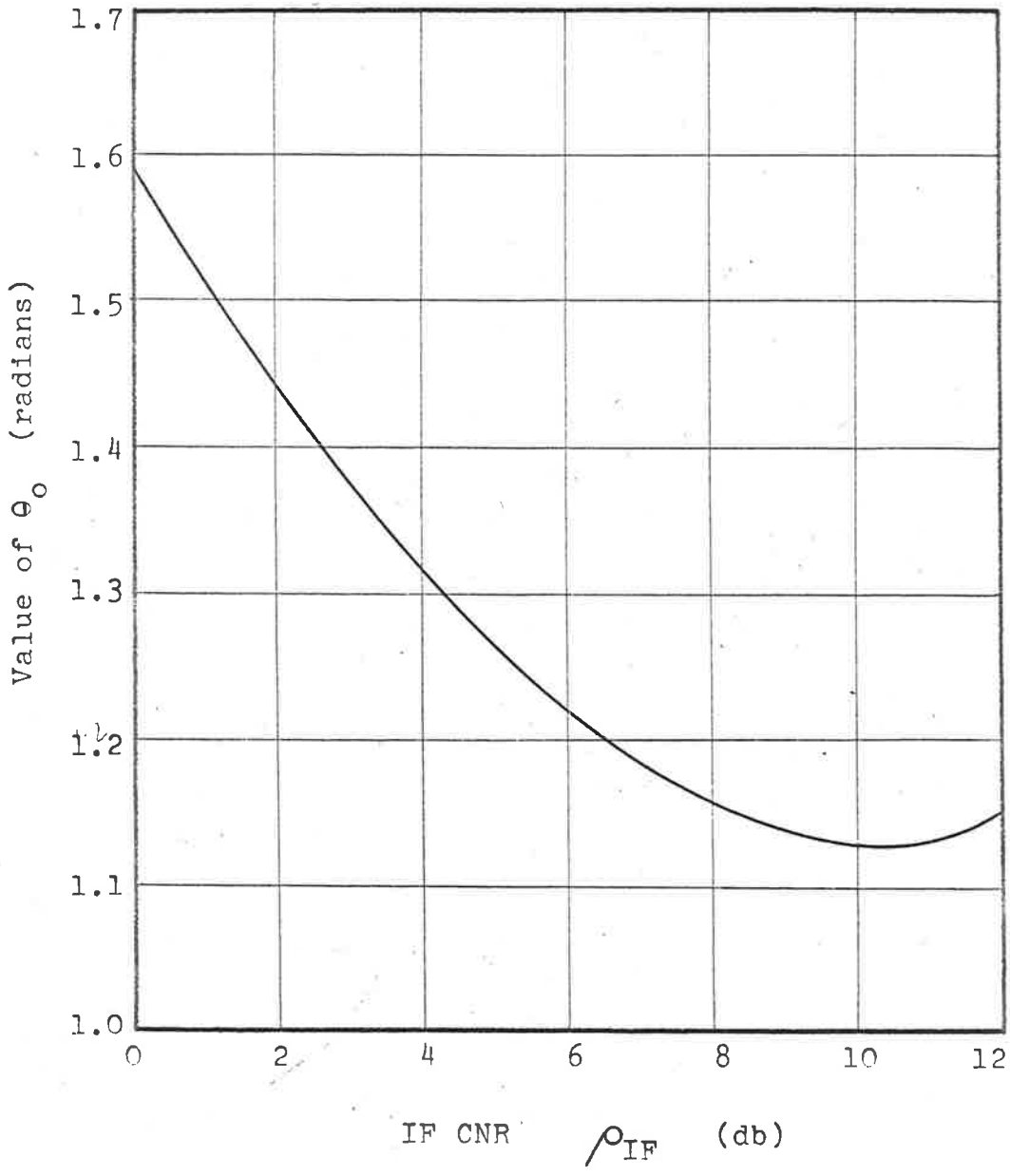

FIGURE 2.10: VARIATION OF θ_o WITH IF CNR.

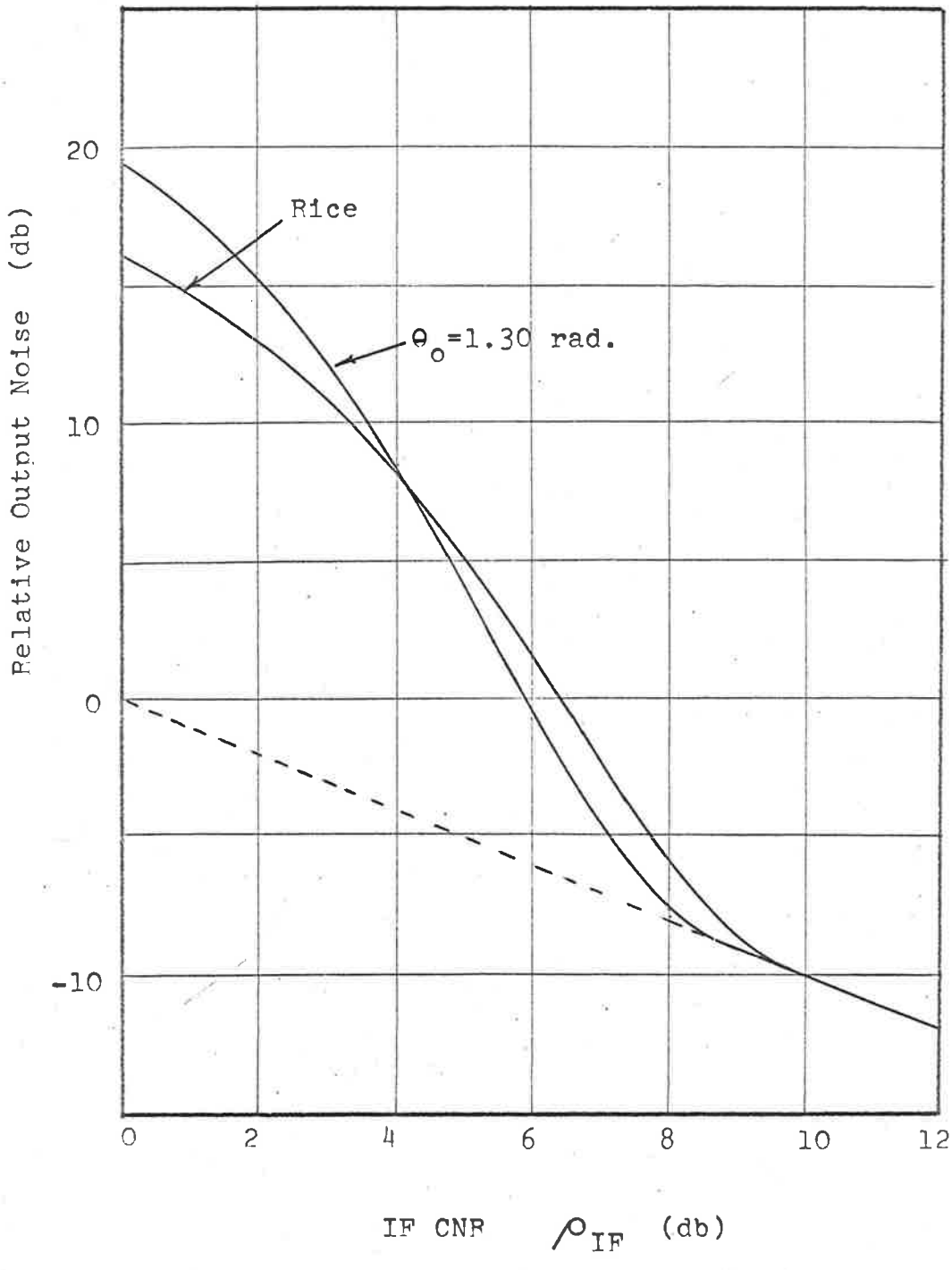

FIGURE 2.11: OUTPUT NOISE IN AN ORDINARY FM SYSTEM.

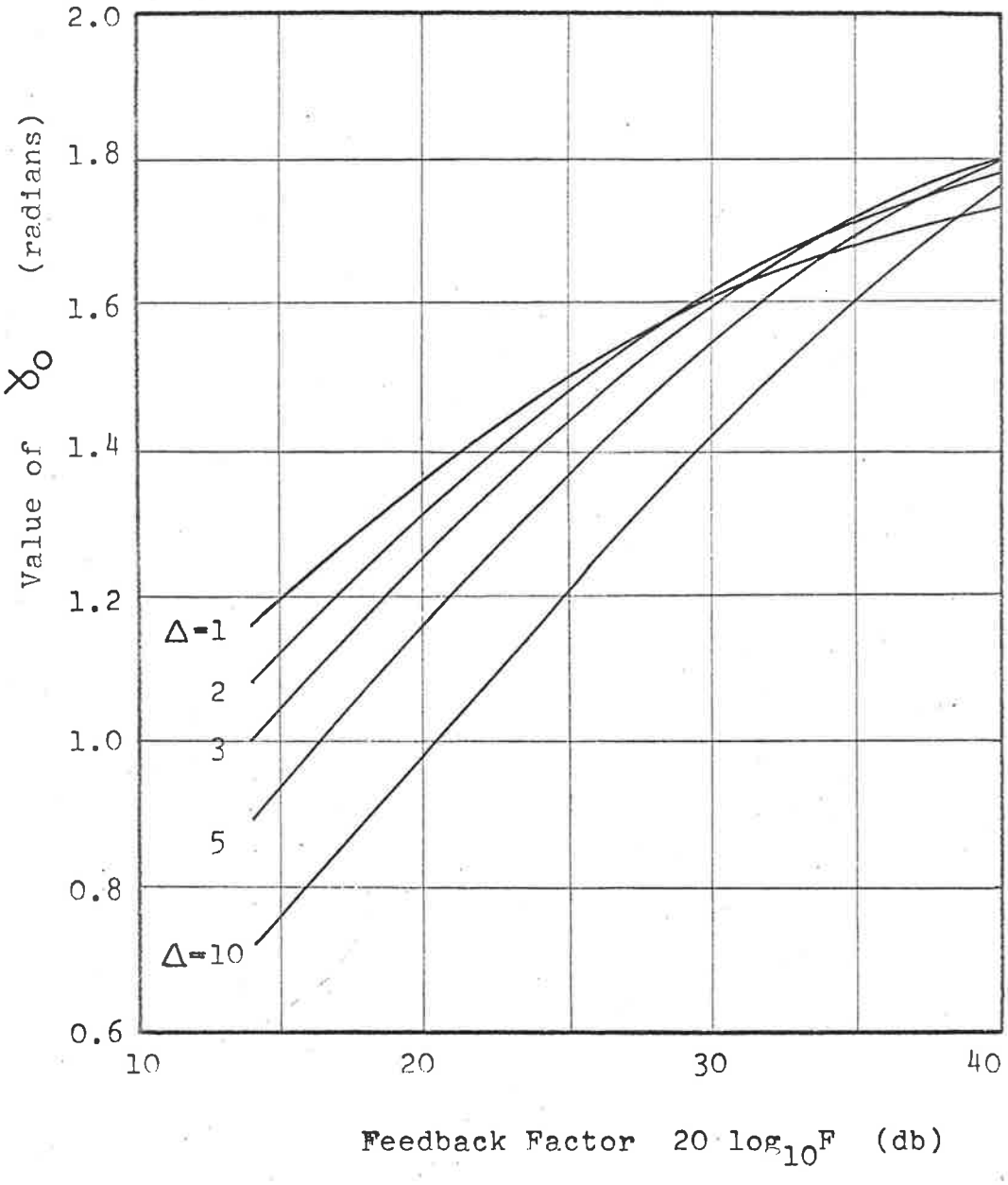

FIGURE 2.12: VARIATION OF γ_o WITH FEEDBACK AND IF BANDWIDTH.

The fact that γ_o is largest at high feedback factors is an indication that $\gamma(t)$ becomes more nearly gaussian as the feedback factor increases.

The power series approximation of Section 2.4 indicated that the magnitude of $\phi(t)$ was the factor which determined feedback threshold and this was supported by experimental evidence. [3],[29] .

If we assume an impulse occurs when $|\phi(t)|$ exceeds a certain magnitude ϕ_o, then the value of ϕ_o is given by an expression identical with (49) except that γ is replaced by ϕ. For the typical FMFB system of Appendix E, a plot of ϕ_o against F for various IF bandwidths is shown in Figure 2.13.

2.5.3 Threshold behaviour.

Using the previous results for ν_d and ν_f, the impulse rates due to discriminator and feedback effects respectively, the threshold performance of FMFB can be predicted.

Assuming that we may regard the discriminator and feedback impulse mechanisms as independent, the total output noise is given by: (Appendix D).

$$N_o = 16\pi^2 \eta(f) f_a^3/3 + 8\pi^2 (\nu_d + \nu_f) f_a \quad \ldots\ldots (51)$$

The first term is the above threshold gaussian noise (quadratic spectrum) and the second term is the impulse noise (flat spectrum).

Now ν_d is given by equation (28), whereas ν_f is given by (48) or by a similar expression involving ϕ. Hence:

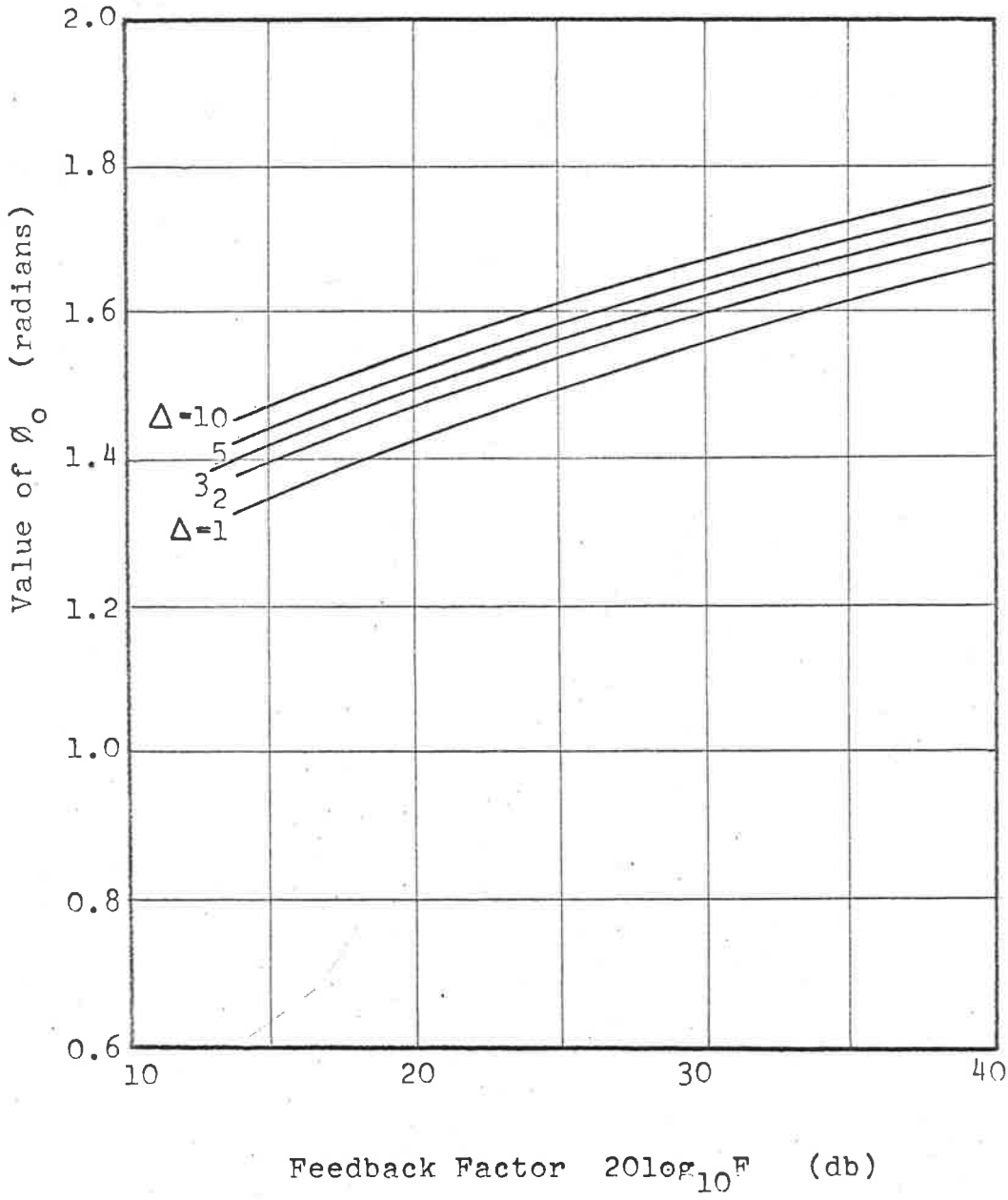

FIGURE 2.13: VARIATION OF ϕ_o WITH FEEDBACK AND IF BANDWIDTH.

$$N_o = 16\pi^2 \eta(f) f_a^3/3 + 8\pi^2 f_a \left\{ \frac{m_{IF}}{2\pi} \operatorname{erfc}(\sqrt{\rho_{IF}}) + \frac{m_\gamma}{\pi} e^{-\gamma_o^2/2\langle\gamma^2\rangle} \right\} \quad \ldots\ldots (52)$$

The total noise plotted against ρ_{IF} is shown in Figure 2.14 for the typical system of Appendix E. Also shown are experimental points from the working model of Appendix F. It can be seen that the agreement between experimental points and the theoretically predicted results is quite close, although the predicted rate of rise of noise is slightly greater than that obtained experimentally. This is similar to the results of Figure 2.11 for a normal frequency modulation system. The values of γ_o and ϕ_o were obtained from Figures 2.12 and 2.13 respectively, for the parameter values $F = 10$, $\Delta = 3$.

Comparison with the digital simulation results, as shown in Figure 2.5 , indicated that the impulse rates obtained by simulation were uniformly greater than predicted by the above theory. This was attributed to the poor approximation of the pseudo-random sequence to a gaussian distribution, even after filtering (see Appendix G). Also at carrier levels appreciably below threshold, the impulses tended to occur in bursts, similar to the effect observed in the phase-locked loop by Smith [26] . This means that the true output noise due to impulses will be less than given by the expression in Appendix D.

It is evident that the assumption that the rate of $|\phi(t)|$ crossing ϕ_o gives an adequately accurate representation of the impulse rate due to feedback. The spread in the values of ϕ_o encountered is less

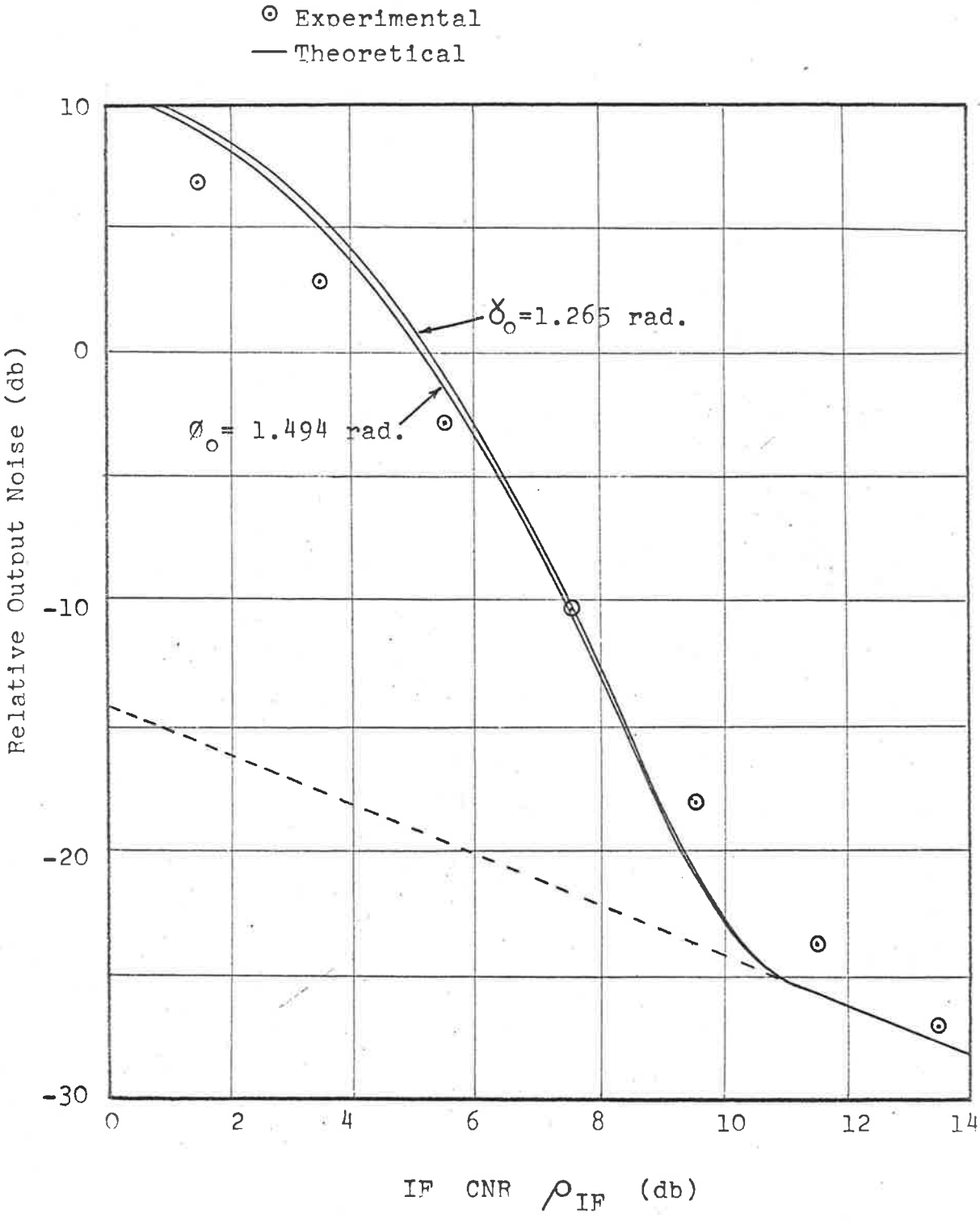

FIGURE 2.14: THRESHOLD BEHAVIOUR OF AN FMFB SYSTEM.

than that of the values of γ_o. Also in view of the fact that the necessar parameters involving $\phi(t)$ (e.g. m_ϕ , $<\phi^2>$) are more easily calculated than those involving $\gamma(t)$, the rate of crossing ϕ_o may be used in the prediction of feedback impulse rates.

2.6 Conclusions.

The threshold behaviour of FMFB is adequately explained in terms of impulse phenomena. Discriminator and feedback thresholds may be considered independently with little error. The discriminator threshold can be predicted using the results of Rice, and the feedback threshold can be predicted in terms of the rate of crossing a certain level by the local oscillator phase.

The fact that the loop is sluggish for large values of $\phi(t)$ results in the assumption of $\phi(t)$ being gaussian being in error. For this reason, a critical level ϕ_o less than π was computed on the basis of $\phi(t)$ being gaussian.

The treatment of threshold in this section has been confined to unmodulated conditions. The effect of modulation is considered in Chapter 3.

CHAPTER 3: MODULATION DEPENDENT THRESHOLD.

It has been shown that the carrier level at which threshold occurs in ordinary FM is practically the same for modulated and unmodulated conditions, although the behaviours below threshold may differ. [5]

Observations on FMFB indicated that modulation could affect the threshold point, but care in design could minimise modulation dependent effects.

3.1 The IF filter.

3.1.1 The IF non-linearity.

The IF filter is non-linear to phase for large excursions, but its small signal transfer function also changes in the presence of modulation. If the IF filter transfer function is H(S), then the small signal transfer function to phase or frequency modulation on a carrier of frequency ω_c is [3] :

$$H_1(S) = \frac{1}{2}\left\{ \frac{H(S + j\omega_c)}{H(j\omega_c)} + \frac{H(S - j\omega_c)}{H(-j\omega_c)} \right\} \quad \ldots\ldots (1)$$

As shown in Appendix B, a high Q tuned circuit of resonant frequency ω_o has a transfer function to phase given by:

$$H_1(S) = \frac{S\Delta + \Delta^2 + \lambda^2}{(S+\Delta)^2 + \lambda^2} \quad \ldots\ldots (2)$$

where Δ = semi 3db bandwidth (rad/sec)

$\lambda = \omega_c - \omega_o$

The pole-zero pattern is shown in Figure 3.1. The single pole at $S = -\Delta$ for $\lambda = 0$ splits into two conjugate

complex poles and a real zero, all lying on a circle passing through the origin.

The effect on an FMFB system is that as the carrier frequency moves away from the resonant frequency, the gain and phase margins of the feedback loop are reduced and an increase in loop noise occurs. This increase may be calculated in typical cases. If a single pole baseband filter is assumed, then the open loop transfer function is:

$$H_o(S) = \frac{A(S\Delta + \Delta^2 + \lambda^2)}{\{(S+\Delta)^2 + \lambda^2\}\{S+1\}} \quad \ldots\ldots (3)$$

The closed loop transfer function is given by:

$$H_c(S) = \frac{H_o(S)}{1 + H_o(S)} \quad \ldots\ldots (4)$$

For the transfer function (3) this is:

$$H_c(S) = \frac{A(S\Delta + \Delta^2 + \lambda^2)}{S^3 + (1+2\Delta)S^2 + (\lambda^2+\Delta^2+F\Delta+\Delta)S + F(\Delta^2+\lambda^2)} \quad .. (5)$$

The mean square local oscillator phase is given by:

$$\langle\phi^2\rangle = \int_{-\infty}^{+\infty} 2\eta(f) \mid H_c(j\omega) \mid^2 df \quad \ldots\ldots (6)$$

This integration may be performed with the aid of standard tables [25].

$$\langle\phi^2\rangle = \frac{\eta(i)(F-1)^2\{2\Delta^3 + (F+1)\Delta^2 + 2\lambda^2\Delta + \lambda^2\}}{F\{2\Delta^3 + (F+3)\Delta^2 + (2\lambda^2+F+1)\Delta + \lambda^2(1-F)\}} \quad .. (7)$$

This reduces to the expected form for $\lambda = 0$ viz.

$$\langle \phi^2 \rangle_{\lambda=0} = \frac{\eta(f_c)(F-1)^2\Delta}{F(1+\Delta)} \qquad \ldots\ldots (8)$$

A plot of equation (7) for typical parameter values is shown in Figure 3.2.

This indicates a 2db increase in $\langle \phi^2 \rangle$ when $\lambda = \Delta$, and hence the threshold carrier level would be 2db higher. The increase in $\langle \phi^2 \rangle$ is mainly at frequencies above baseband and the output noise is not greatly affected if the system is above threshold. If the system is near threshold, however, the increase in $\langle \phi^2 \rangle$ may be sufficient to cause feedback threshold, with a consequent rise in output noise.

Previously we assumed a two pole IF transfer function with a compensating zero in the baseband filter. Since the extra IF pole corresponds to a much wider bandwidth than the main pole at $S = -\Delta$ the effect of carrier detuning is negligible for the values of λ of interest. Inclusion of this pole produced negligible corrections to equation (7) for $|\lambda| < 2\Delta$.

Since frequency modulation may be regarded as a quasistatic variation of the carrier frequency, it is evident that modulation will affect the point at which threshold occurs. For more complex IF filters the system may even become unstable on the modulation peaks.

3.1.2 The IF CNR effect.

As the IF filter response is not flat if a single tuned circuit (or the two pole modification mentioned in Chapter 2) is

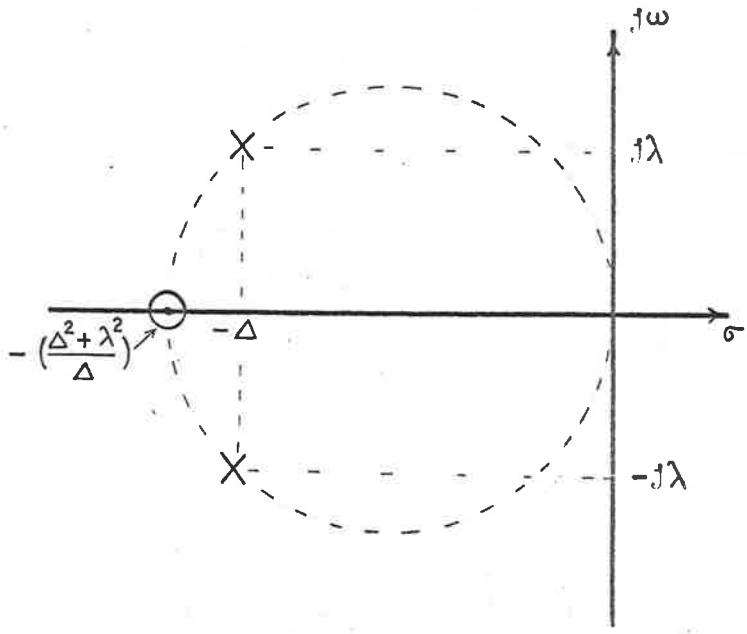

FIGURE 3.1: TRANSFER FUNCTION OF IF FILTER TO PHASE.

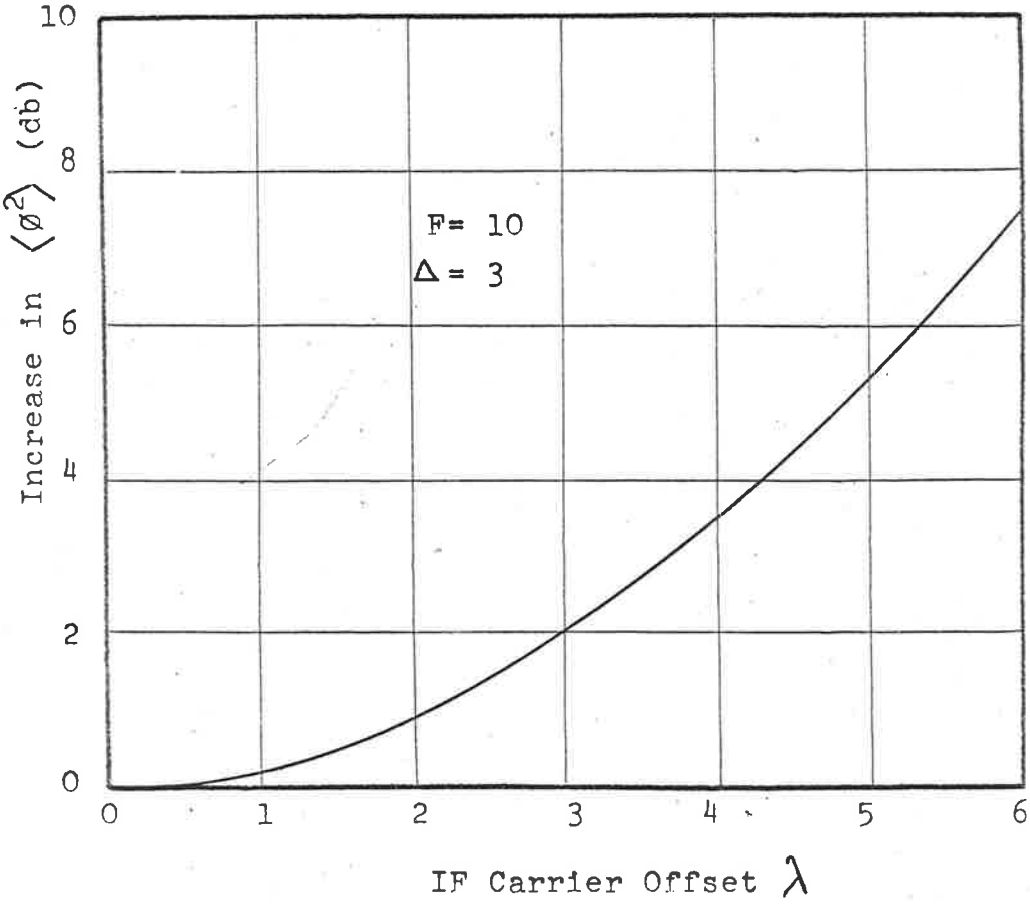

FIGURE 3.2: VARIATION OF LOOP NOISE WITH CARRIER DETUNING.

used, the IF CNR falls as the carrier is detuned. The IF CNR will be 3db lower at an IF carrier deviation equal to the 3db point of filter (i.e. at $\lambda = \Delta$). In the vicinity of threshold therefore, carrier detuning may reduce the IF CNR to a point where discriminator threshold occurs.

Thus in general, the unmodulated CNR must be above threshold by up to 3db in order to prevent threshold occurring under modulated conditions. This IF CNR effect can be minimised by reducing the IF deviation (which sacrifices most of the improvement achieved by FMFB), or by use of a more complex IF filter in which the response is flat over the IF passband. However, the latter may involve problems in loop stability and further aggravate the effect discussed in the previous section.

The above threshold output noise may be calculated from the transfer functions derived in the previous section. If the output voltage is assumed taken from the output of the baseband filter (see Figure 2.1) then this corresponds to the time derivative of $\phi(t)$.

The spectral density of this voltage is given by:

$$G_o(f) = \frac{2\eta(f)\omega^2}{K_2^2} \left| H_c(j\omega) \right|^2 \qquad \ldots\ldots (9)$$

where K_2 is the VCO gain constant (rad/sec/volt).

The mean square output noise in a baseband bandwidth fa is given by:

$$N_o = \int_{-fa}^{+fa} G_o(f)\, df \qquad \ldots\ldots (10)$$

where for the model considered fa has been normalised to $\frac{1}{2\pi}$ H_z.

Numerical integration of (10) for the typical values used in Figure 3.2 (i.e. F = 10, Δ = 3) indicated less than 0.2 db change in output noise over the range $|\lambda| \leq 6$.

Figure 3.3. shows the variation of output noise with carrier detuning for the experimental system of Appendix F. This was plotted for three different carrier levels, corresponding to -2db, +2db and +6db relative to the threshold carrier level under unmodulated conditions.

This illustrates that the output noise varies little with modulation if the system is well above threshold. In the vicinity of threshold, however, the system can go below threshold on the modulation peaks and the output noise rises.

The two effects involving the IF filter are essentially independent, except that attempts to improve one is usually at the expense of the other. The optimum condition is where they are equal in effect, since this gives the minimum deterioration of threshold level under modulated conditions. For the system considered, the single pole IF (or its two pole modification) is close to optimum, giving a threshold deterioration of the order of 3db at the maximum frequency excursions.

These two effects do not explain the extremely rapid rise

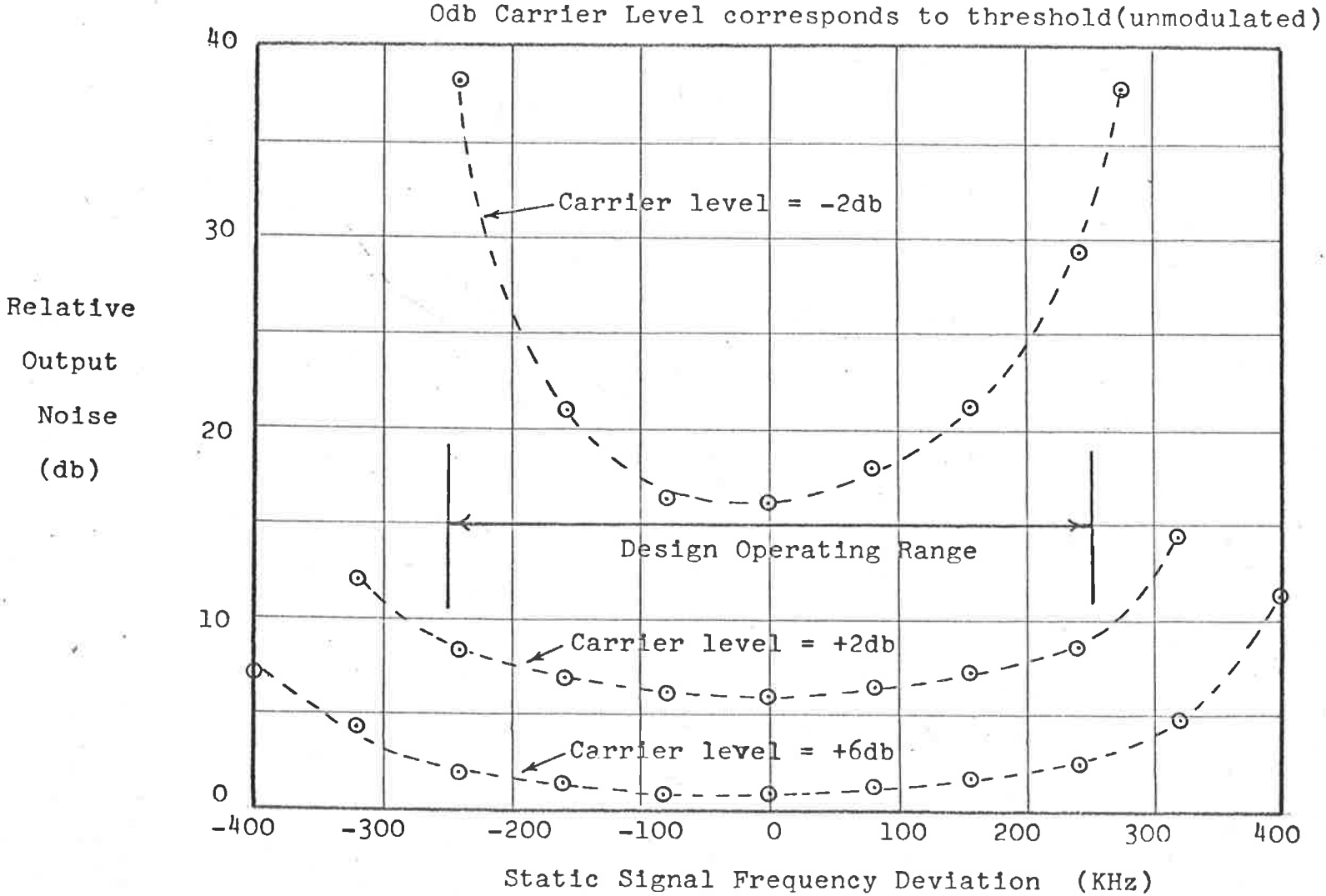

FIGURE 3.3: VARIATION OF OUTPUT NOISE WITH CARRIER DETUNING (EXPERIMENTAL).

in noise at the extremities of the curves of Figure 3.3, especially the one corresponding to -2db carrier level. The other carrier levels exhibit this effect, but at greater frequency offsets as the carrier level increases.

Observations indicated that this was a result of the feedback loop losing synchronism. It was found by Davis [7] that this was closely related to the frequency detector. A study of this effect is found in the following section.

3.2 The frequency detector.

In an FMFB system the frequency detector converts the instantaneous frequency of the signal at the output of the IF filter into a voltage. There are several means of doing this, but the characteristics are generally similar to the form of Figure 3.4.

In ordinary FM it is only necessary that the linearity of the detector achieve the quality required in the output signal.

In FMFB however, the instantaneous IF frequency depends on the voltage output via the baseband filter and voltage controlled oscillator. Hence feedback is applied around the characteristic in Figure 3.4, being negative in the operating region but reversing to positive on the tails of the characteristic. This results in a characteristic of the form of Figure 3.5.

This characteristic has an extended linear range, but also has unstable regions. Under low noise conditions, a peak RF deviation of the order of ω_1 can be used. However in the range of deviations

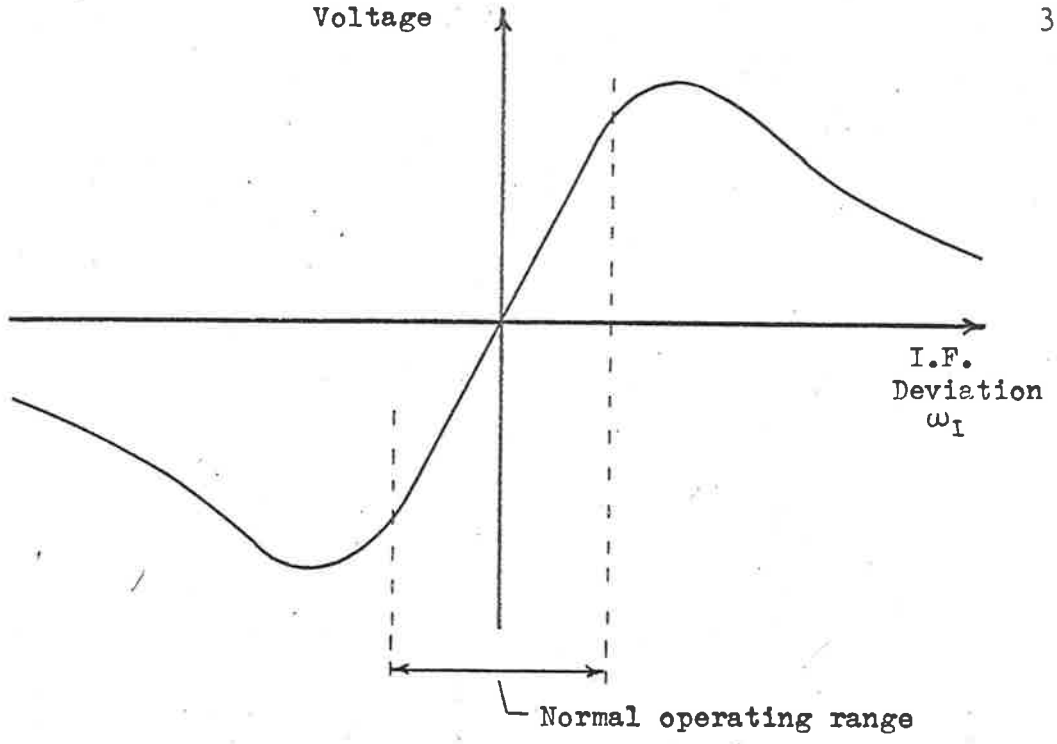

FIGURE 3.4: TYPICAL CHARACTERISTIC OF A FREQUENCY DETECTOR.

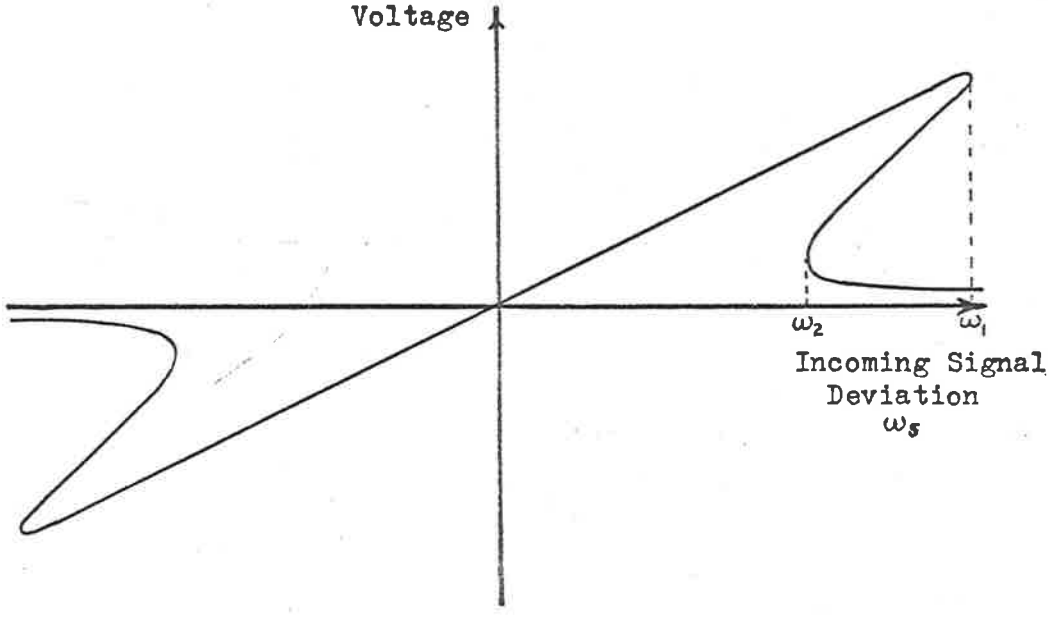

FIGURE 3.5: EFFECT OF FEEDBACK ON DETECTOR CHARACTERISTIC.

between ω_2 and ω_1 there exists the possibility of another stable state, which can easily be achieved during the relatively high noise conditions near threshold.

In the vicinity of threshold, the peak RF deviation is limited to the order of ω_2, otherwise jumps from one stable state to the other produce rapid deterioration of the output signal.

It was shown by Davis [7] that even for an ideal frequency detector (i.e. one in which output voltage is proportional to instantaneous frequency), the above effect occurs due to the suppression of signal by noise. The relation between the output voltage and IF carrier frequency is non-linear and of the form of Figure 3.4.

In the case of a practical discriminator, the effect of suppression of signal by noise is more complex. This problem can be approached by considering the pdf of the instantaneous frequency of a sinewave plus gaussian noise and using this in conjunction with the discriminator characteristic to find the mean output voltage.

3.2.1 Frequency distribution method.

The pdf of the instantaneous frequency is (from Appendix A):

$$p(\Omega_i) = \frac{e^{y-\rho}}{2(1+\Omega_i^2)^{3/2}} \left\{ (1+\mu) I_0(y) + \mu I_1(y) \right\} \quad \ldots\ldots (11)$$

where $\Omega_i = \omega_i / m$

$d = \omega_I / m$

$\mu = \rho (1 + d\Omega_i)^2 / (1 + \Omega_i^2)$

$y = \frac{1}{2}(\mu - \rho d^2)$

ρ = IF CNR

ω_o = IF filter centre frequency (rad/sec)

ω_c = carrier frequency (rad/sec)

m = radius of gyration of IF filter characteristic about ω_o (rad/sec)

$\omega_i(t)$ = instantaneous frequency with respect to ω_o (rad/sec). This is a random time variable.

ω_I = IF carrier deviation = $(\omega_c - \omega_o)$.

For the purpose of illustration a simple stagger tuned discriminator will be considered. This consists of two high Q tuned circuits of bandwidth 2α separated by $2\sqrt{2}\,\alpha$ where α is a frequency scaling constant. This gives better than 1% linearity in the range $-\alpha$ to $+\alpha$.

The voltage-frequency characteristic of this discriminator is:

$$v(\omega_i) = \frac{1}{\sqrt{1 + (\sqrt{2} - \omega_i/\alpha)^2}} - \frac{1}{\sqrt{1 + (\sqrt{2} + \omega_i/\alpha)^2}} \quad \ldots (12)$$

The mean output voltage is therefore:

$$\langle v(\omega_i) \rangle = \int_{-\infty}^{+\infty} v(\Omega_i)\, p(\Omega_i)\, d\Omega_i \quad \ldots\ldots (13)$$

where $v(\Omega_i)$ is given by (12) with $\Omega_i = \omega_i/m$ and $p(\Omega_i)$ is given by (11).

Equation (13) was integrated numerically for the case $m = \alpha$. The result is shown in Figure 3.6. This curve assumes the CNR is constant (at 12db), whereas in fact it falls as the carrier frequency moves away from the IF filter centre frequency. For a filter of power transfer characteristic:

$$|H(j\omega)|^2 = e^{-\omega^2/2\alpha^2} \qquad \ldots\ldots (14)$$

which has $m = \alpha$ and is only 2.2db down at $\omega = \alpha$, the result is also shown in Figure 3.6.

These curves are only approximations since the discriminator is not a lagless device. However they do indicate that the discriminator characteristic at threshold may be markedly different from that at higher CNR's.

The digital simulation results on Figure 3.6 are from section 3.2.3.

3.2.2 Amplitude distribution method.

An alternative approach used was to consider that the discriminator circuit produced an output corresponding to the difference of the envelopes of the signals appearing at the outputs of the stagger tuned pair.

On the assumption that the noise is gaussian, and the carrier of amplitude A, the joint pdf of envelope r(t) and phase $\theta(t)$ is:

$$p(r,\theta) = \left\{\frac{r}{2\pi\sigma^2}\right\} e^{-\frac{(r^2 - 2Ar\cos\theta + A^2)}{2\sigma^2}} \qquad \ldots\ldots (15)$$

where σ = RMS noise.

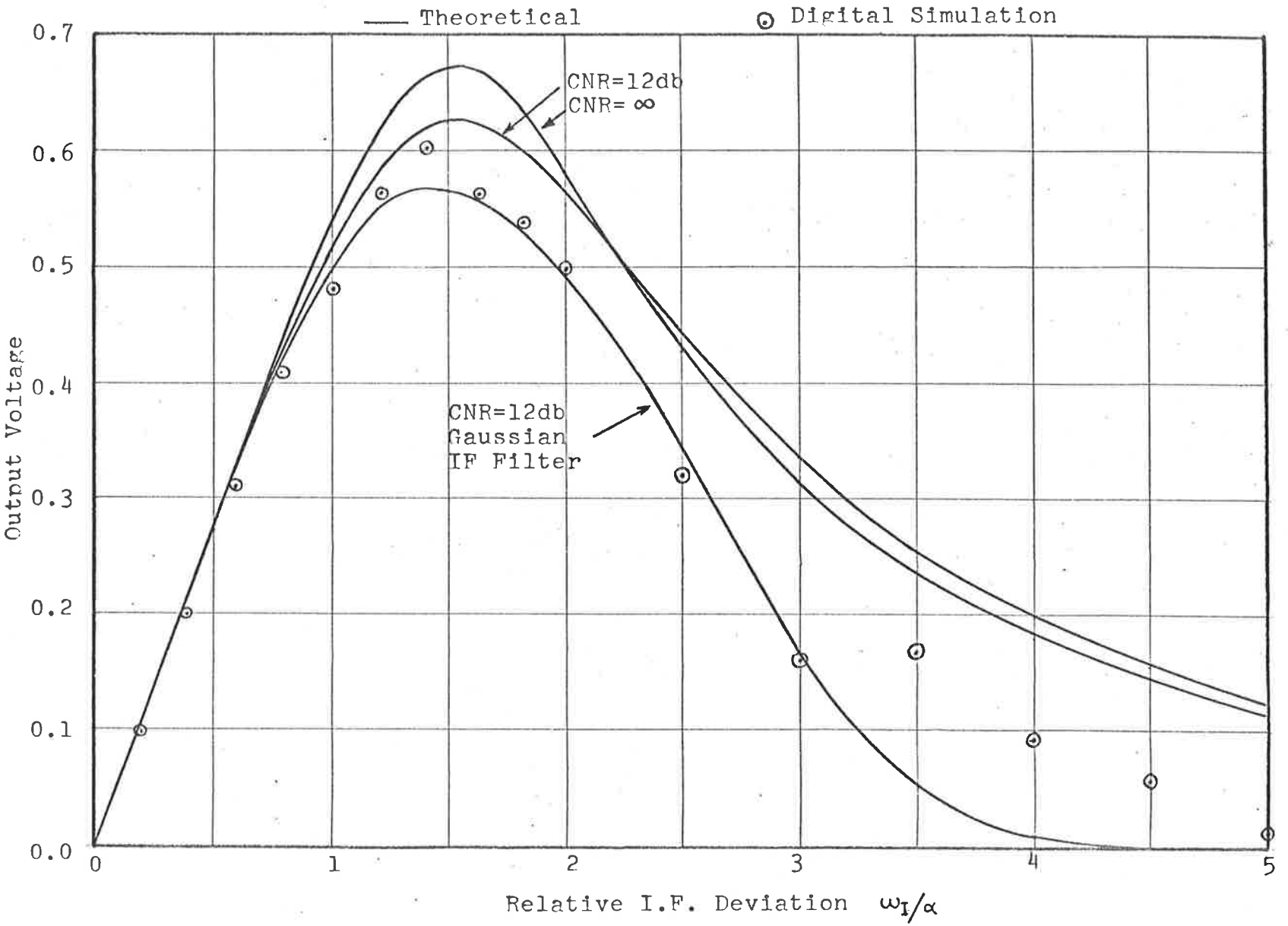

FIGURE 3.6: DISCRIMINATOR CHARACTERISTIC - FREQUENCY DISTRIBUTION METHOD.

This may be used to find the mean envelope amplitude <r> (see Appendix C) viz:

$$\langle r \rangle = \sigma\sqrt{\pi/2}\left\{ (1+\rho) I_0(\rho/2) + \rho I_1(\rho/2) \right\} e^{-\rho/2} \quad \ldots\ldots (16)$$

where ρ = CNR = $A^2/2\sigma^2$.

For the stagger tuned discriminator used previously and assuming a single stage IF filter of bandwidth 2α, the difference of the two envelope averages from the stagger tuned pair was calculated. The action of the limiter was assumed to maintain the carrier amplitude constant at the output of the IF filter, although the CNR altered as the carrier frequency moved from the centre frequency. The results are shown in Figure 3.7.

3.2.3 Simulation.

To check the validity of the previous calculations the system was simulated digitally. A low pass equivalent circuit was used, as an RF simulation by digital means was impractical because of the inefficient use of computer time. Figure 3.8 shows the actual model and the low pass equivalent which was simulated. The transfer functions $H_{ij}(S)$ are defined in Appendix G.

The solution involved the solving of 12 simultaneous first order differential equations. A shift register code was used to generate the noise components x(t) and y(t).

The results are plotted as points in Figures 3.6 and 3.7 showing agreement within the statistical limits expected. Also

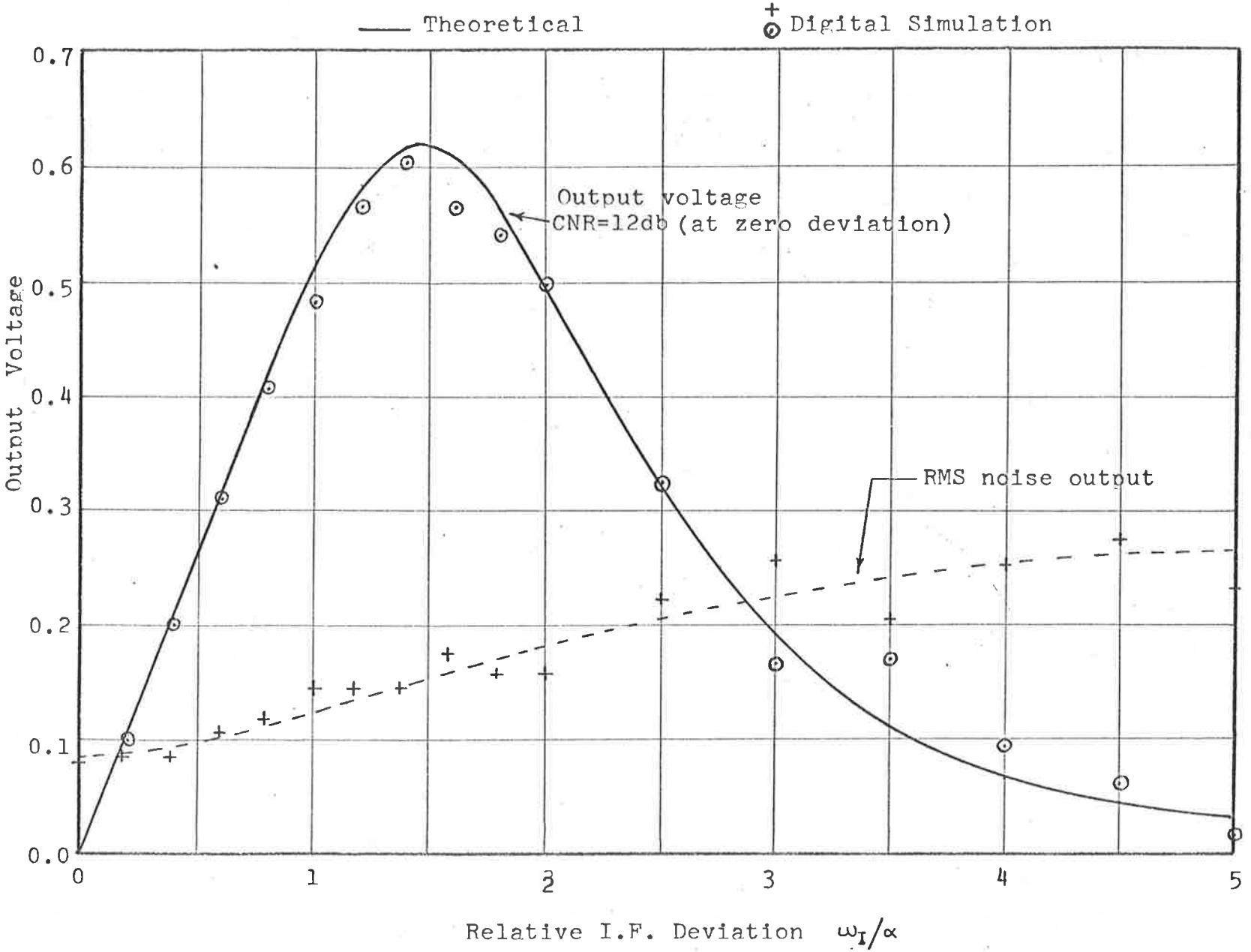

FIGURE 3.7: DISCRIMINATOR CHARACTERISTIC - ENVELOPE DIFFERENCE METHOD.

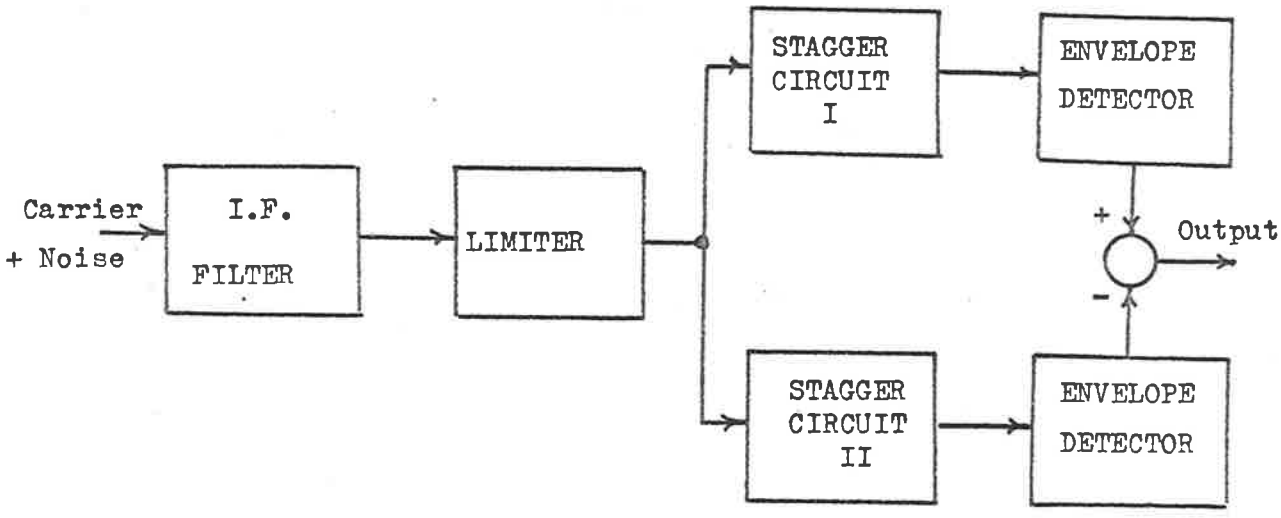

FIGURE 3.8a: IF FILTER AND STAGGER TUNED DISCRIMINATOR.

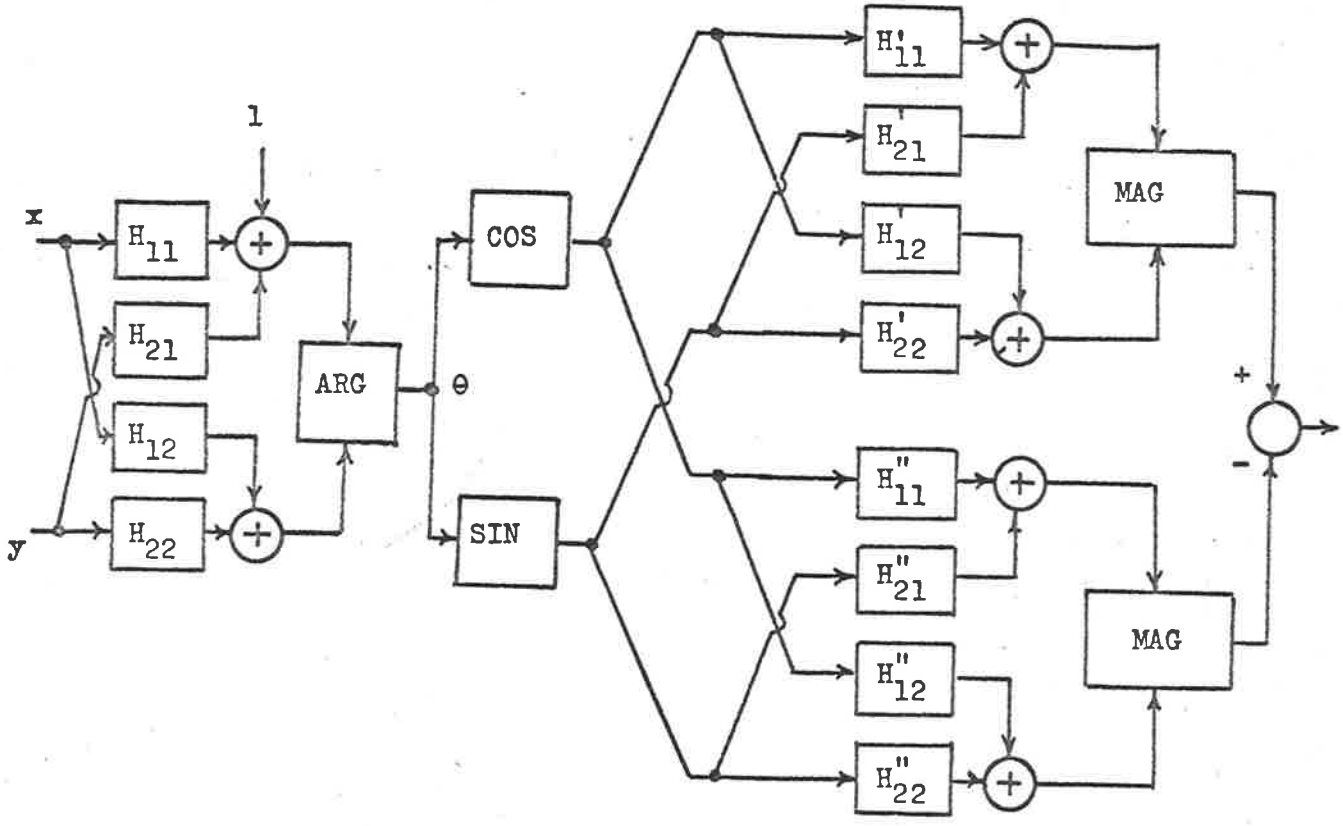

FIGURE 3.8b: LOW PASS MODEL USED IN DIGITAL SIMULATION.

plotted on Figure 3.7 is the R.M.S. output noise.

The agreement between the digital simulation results and the results of the previous section indicated that the idealisation concerning the limiter was justified in this application.

3.2.4 Evaluation.

Following the method used in [7] , the IF deviations when the signal deviation equals ω_2 and ω_1 are plotted against feedback factor in Figure 3.9, both for the ideal frequency detector and the discriminator characteristic obtained previously by digital simulation.

For the ideal discriminator, $\omega_s = \omega_2$ is not encountered in normal operation (i.e. $|\omega_I| \leq \Delta$) until F = 36 db. For the practical discriminator however this is F = 13.5 db which is well within the range normally used. An IF deviation corresponding to $\omega_s = \omega_1$ is not normally reached in either case, since this corresponds to operation well outside the linear region.

The preceding gives a qualitative notion of the limitations of the frequency detector, whereas a quantitative result would be more useful. Analysis based on the pdf of instantaneous frequency is complicated by the fact that a single pole IF filter has an infinite radius of gyration m. The inclusion of an extra pole as done previously and the use of the high CNR gaussian approximation removes this difficulty.

We shall show that the probability of the loop losing synchronism is sufficiently high that, if $\omega_s > \omega_2$ then the performance deteriorates rapidly.

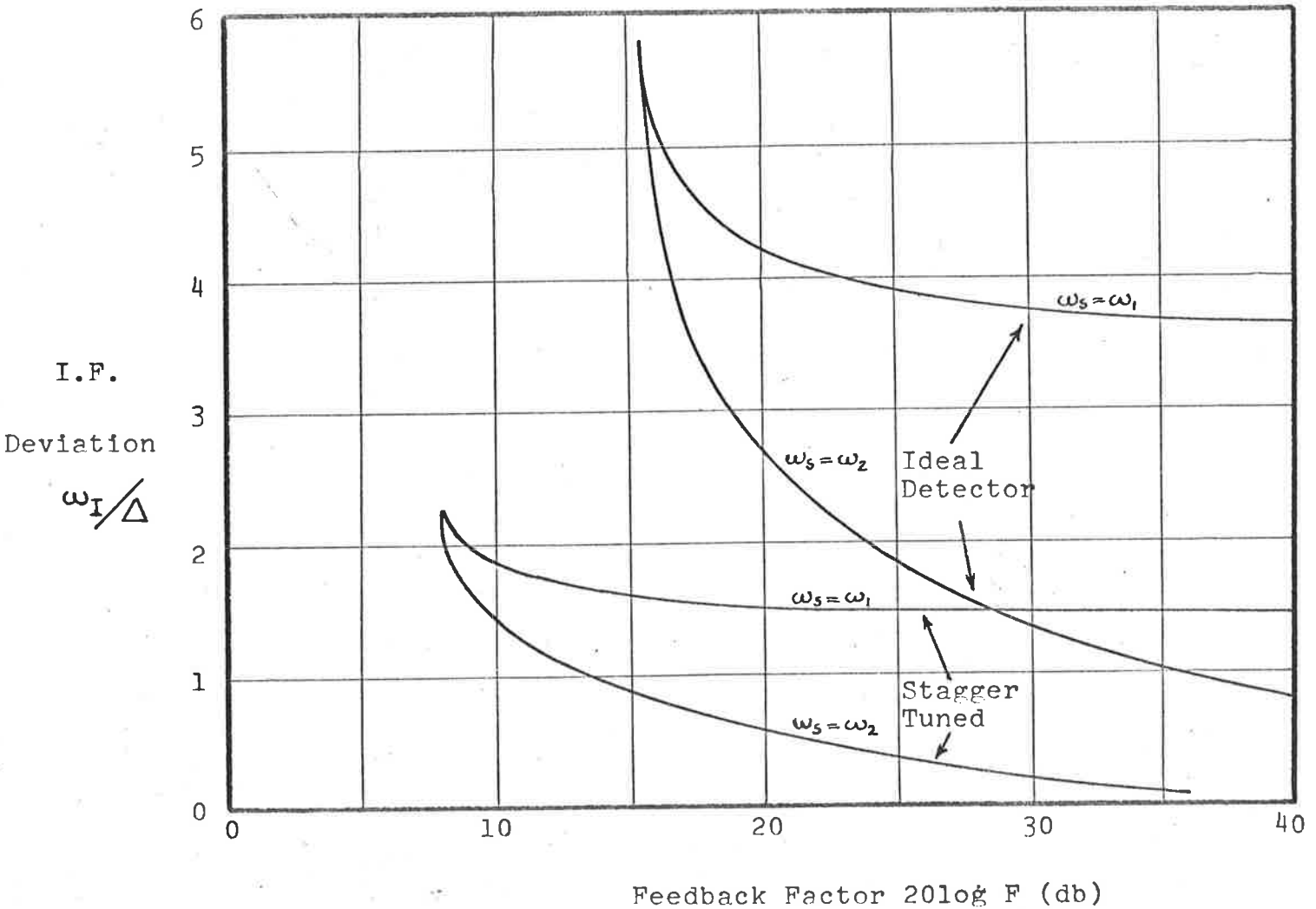

FIGURE 3.9: VARIATION OF CRITICAL IF DEVIATIONS WITH FEEDBACK FACTOR.

If the IF frequency noise is considered to be gaussian (high CNR approximation) the rate of crossing a certain level can be found. In particular, the rate of crossing the critical IF deviation ω_{cr} corresponding to a signal deviation of ω_1 is of interest. If this occurs, the loop jumps to a new stable state and is said to have lost synchronism.

The crossing rate is given by:

$$\nu_+ = \frac{m_\omega}{2\pi} \; e^{-\omega_{cr}^2 / 2 \langle \omega_i^2 \rangle} \qquad \ldots\ldots (17)$$

where ν_+ = number of upward crossings per sec.

$$m_\omega^2 = \langle \dot{\omega}_i^2 \rangle \; / \langle \omega_i^2 \rangle$$

For a two pole IF response, $\langle \omega_i^2 \rangle$ is finite but $\langle \dot{\omega}_i^2 \rangle$ is not. In order to obtain a finite value for the latter, it is necessary to have at least a 3 pole response.

In a typical practical system, the rate of crossing ω_{cr} is sufficiently high in the vicinity of threshold to restrict the peak modulation deviation to less than ω_2. For the system considered earlier, $\langle \omega_i^2 \rangle$ is $0.371\,\Delta^2$ for an IF CNR of 12db. A stagger tuned discriminator as considered earlier has $\omega_{cr} = 1.50\Delta$ and the probability of ω_i exceeding ω_{cr} is shown in Figure 3.10 for various quasistatic IF deviations.

This probability is high and the crossing rate (17) would also be high for a system in which $\langle \dot{\omega}_i^2 \rangle$ is defined. Any static IF deviation beyond the smaller critical frequency (e.g. 0.55Δ for

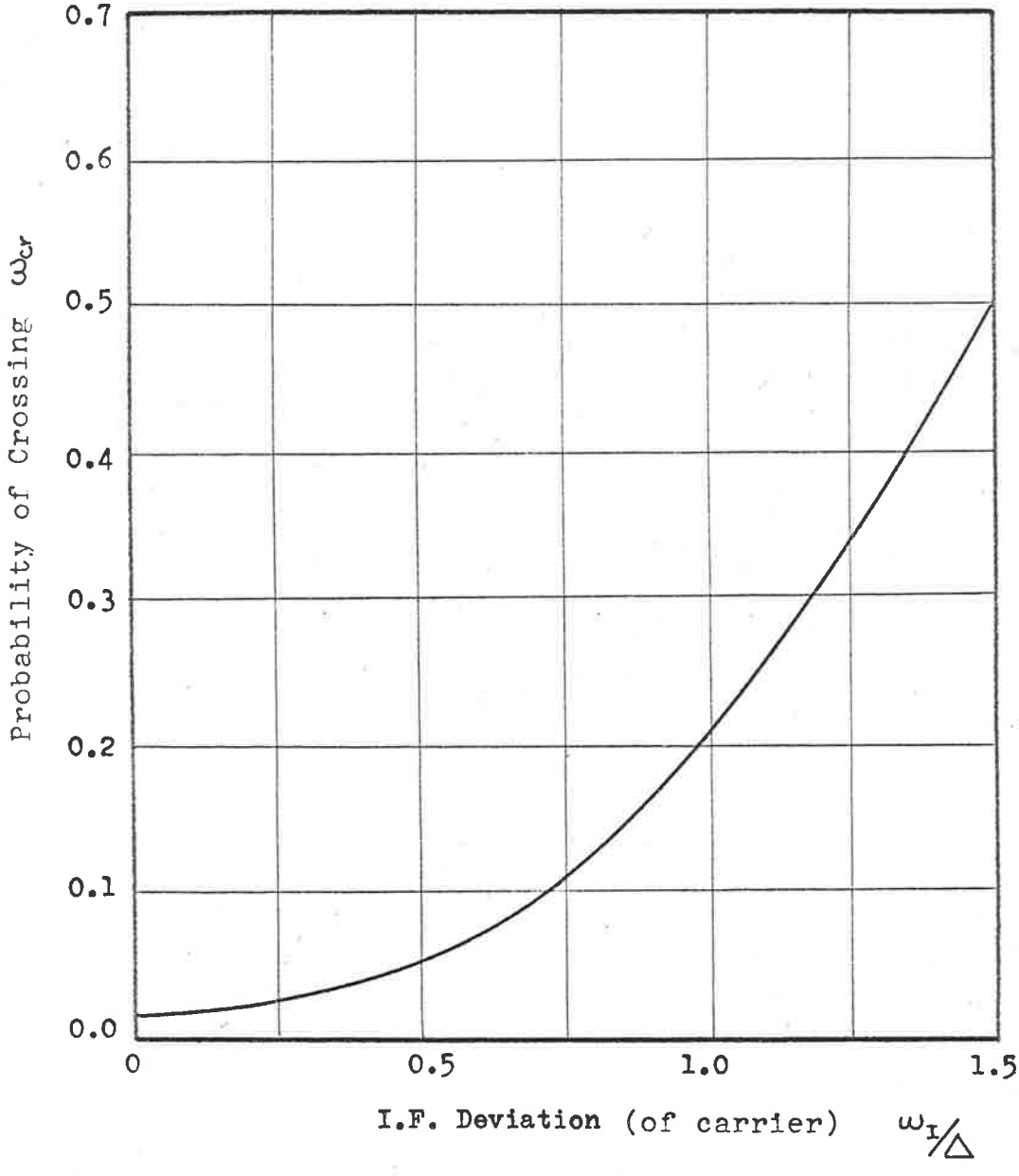

FIGURE 3.10: PROBABILITY OF LOSS OF SYNCHRONISM.

above) will result in the second stable state being achieved for long periods of time, with consequent signal deterioration.

3.2.5 Quasilinearisation.

A possible technique of analysis is the quasilinearisation method [8]. In this, the non-linear device is replaced by a linear amplifier of gain such as to minimise the mean square error made by the substitution.

If a lagless non-linearity f(x) is replaced by an amplifier of gain G, the error is minimum if:

$$G = \frac{1}{\langle x^2 \rangle} \int_{-\infty}^{+\infty} x\, p(x)\, f(x)\, dx \qquad \ldots\ldots (18)$$

where p(x) is the pdf of the input signal x(t). If x(t) is gaussian, then

$$G = \int_{-\infty}^{+\infty} f'(x)\, p(x)\, dx \qquad \ldots\ldots (19)$$

In the case of FMFB, x is the instantaneous IF frequency ω_i which has an unbounded mean square value for all IF filters and CNR's. This is a consequence of the finite probability of a frequency impulse when the carrier plus noise phasor encircles the origin. However we may use the high CNR gaussian approximation with little error.

Equation (19) then gives a relation between the gain G and the mean square frequency deviation $\langle \omega_i^2 \rangle$. An analysis of the linearised system gives $\langle \omega_i^2 \rangle$ in terms of G. This may be obtained from Appendix E by putting $1 + (F-1)G$ instead of F.

For the discriminator characteristic defined by equation (12), equation (19) was integrated numerically for various values of $\langle\omega_i^2\rangle$ and static carrier deviations ω_I. (For $\omega_I \neq 0$ we interpret $\langle\omega_i^2\rangle$ as the mean square fluctuation of ω_i about its mean value. This mean is ω_I in the high CNR approximation). The frequency scaling constant of the discriminator was chosen to be $\alpha = \Delta$, giving 1% linearity over the normal operating range.

Figure 3.11 shows a plot of G versus $\langle\omega_i^2\rangle$ for $\omega_I = 0$ and $\omega_I = \Delta$. Also shown are the family of curves relating $\langle\omega_i^2\rangle$ to G for various IF CNR's. These curves are strictly only valid for $\omega_I = 0$ as the IF detuning effect causes an increase in $\langle\omega_i^2\rangle$, possibly of the order of several db for $\omega_I = \Delta$.

Figure 3.11 indicates a fall in loop gain below an IF CNR of about 13db. With the carrier detuned this fall in gain occurs at a higher IF CNR. However, the gain G must be correctly interpreted. It is in fact the effective gain of the non-linear device to random fluctuations about static or quasistatic quantities. The modulation is assumed quasistatic and this obeys the non-linear characteristic given by equation (13). The modification to this characteristic has already been considered in sections 3.2.1 , 3.2.2 and 3.2.3.

Develet's analysis of the phase-locked loop [12] by this technique revealed a critical carrier level below which no solution was obtained, indicating threshold in the form of loss of lock. In the case of FMFB there is no such phenomenon and the quasilinearisation method

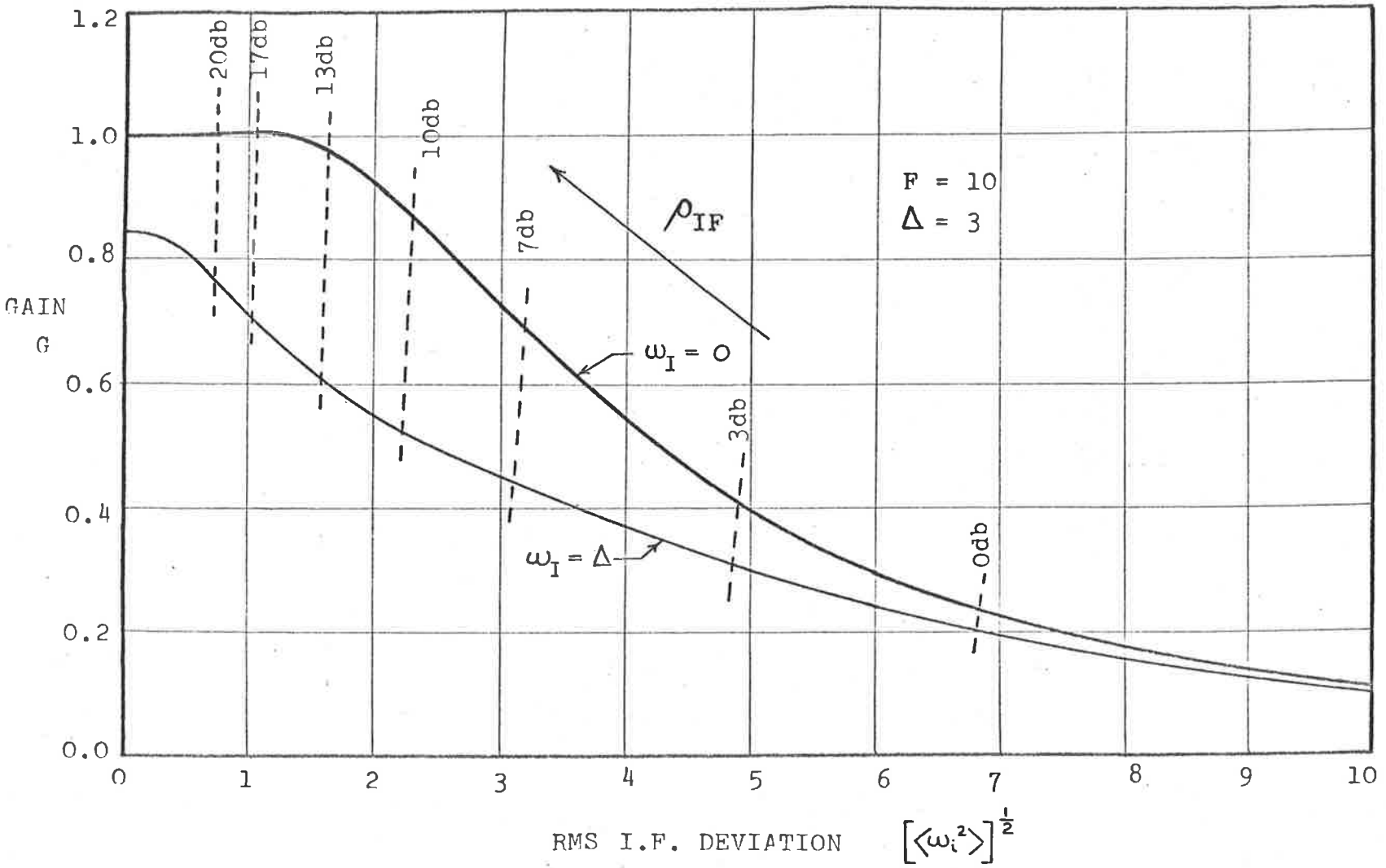

FIGURE 3.11: RESULTS OF QUASILINEARISATION OF DISCRIMINATOR.

does not predict any marked increase in loop noise.

This points to the basic limitation of the quasilinearisation technique, which, while well suited to the analysis of small non-linearities, is inadequate for the type of characteristic involved here. The fact that the loop switches from conditions of negative feedback to positive feedback indicates that an approach postulating an equivalent loop gain is unlikely to be successful. This is evident from a calculation of the mean square error, which is not negligible in the range of $<\omega_i^2>$ of interest.

3.3 Conclusions.

It has been shown that the natures of the IF filter and the frequency discriminator can affect the performance of FMFB significantly under modulated conditions. The performance is mainly affected near the modulation peaks, resulting in deterioration of the signal in this region.

The IF filter has the effect of increasing the threshold carrier level in the presence of modulation, whereas the frequency discriminator limits the peak frequency deviation of the signal.

Particular attention must be paid to obtaining a discriminator which is linear well outside the normal operating range in order to reduce the latter effect, particularly at high feedback factors.

CHAPTER 4: OPTIMISATION OF FMFB.

4.1 Analogue Systems.

In an analogue FM system the performance parameter used may be the output SNR required. It is convenient, but not necessary, to specify this for sinusoidal modulation. SNR requirements for other forms of modulation can be expressed as an equivalent SNR for sinusoids.

Optimisation of FMFB entails choosing the system parameters to achieve the required performance so that a cost parameter is minimised. The simplest cost parameter is the transmitter power required, although other factors such as bandwidth may also be of importance.

The optimisation of FMFB involves choosing the system parameters such that the two thresholds occur at the same carrier level [3]. Although the optimum loop transfer function is physically unrealisable, very little degradation in performance occurs if the open loop response is a simple two pole response, one pole from the IF filter and another from an RC baseband filter. The results are shown in Figure 4.1 and are similar to those obtained by others. [3, 9, 10].

The threshold limit is calculated from Shannon's result that in an ideal system the encoding at RF and baseband should be ideal viz.

$$C = f_a \log_2 (1 + S_o/N_o) = B \log_2 (1 + S_i/N_i) \quad \ldots\ldots (1)$$

where B is the RF bandwidth and f_a the baseband bandwidth.

This relation may be solved for ρ_o (the CNR in a bandwidth $2f_a$) in terms of the output SNR, S_o/N_o. It is interesting to note that FMFB is only 5 -6db above this curve at the point of closest approach.

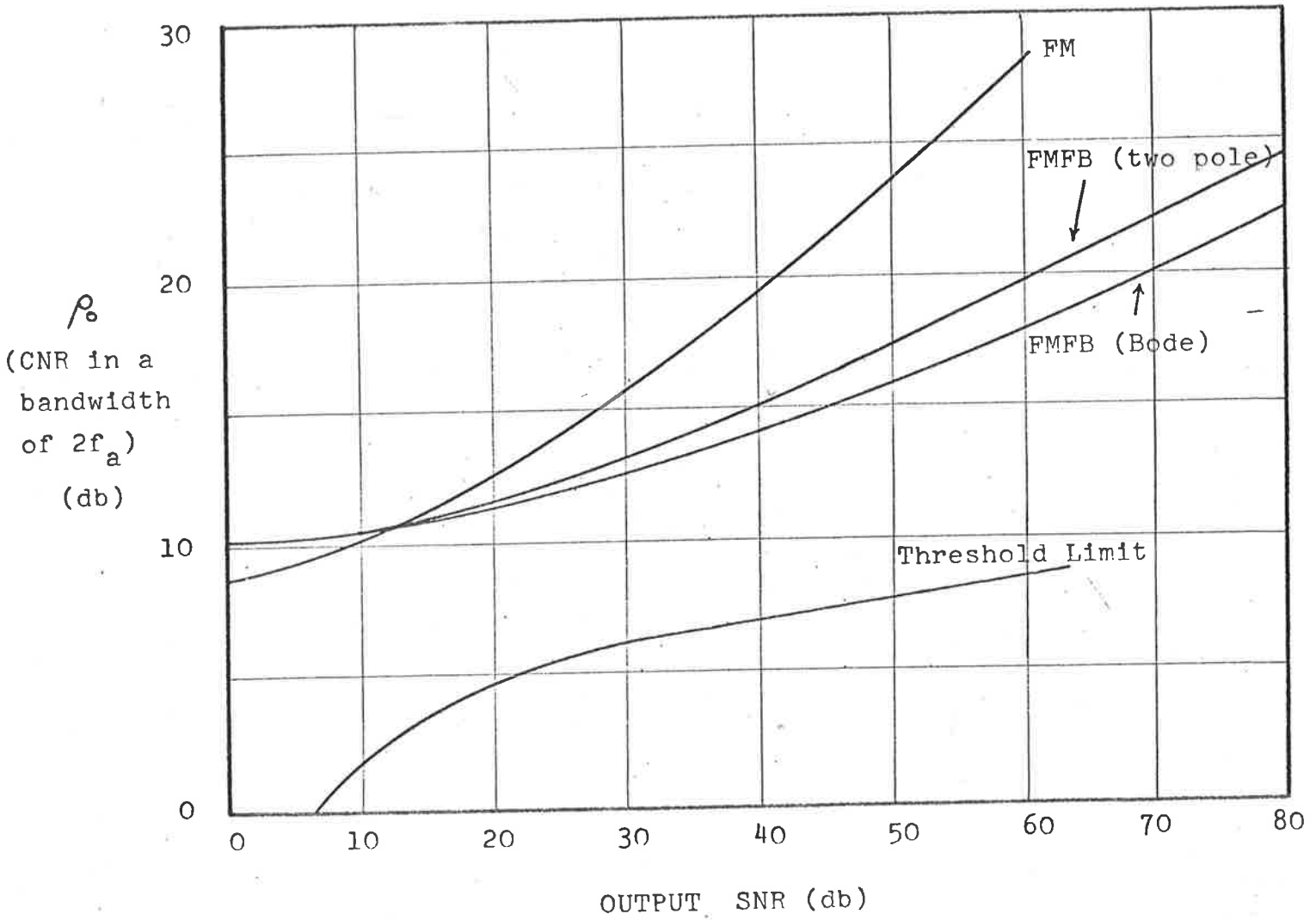

FIGURE 4.1: OPTIMUM PERFORMANCE OF FREQUENCY MODULATION SYSTEMS.

4.2 Communication efficiency.

A figure of merit proposed for comparing communication systems is communication efficiency, defined by Sanders [11] to be :

$$\beta = \frac{\text{Energy per bit}}{\text{Noise spectral density}} \qquad \ldots\ldots (2)$$

For the purposes of calculation, the equivalent form

$$\beta = \frac{S_i}{N_i} \cdot \frac{B}{C} \qquad \ldots\ldots (3)$$

is more convenient, where S_i/N_i is the incoming CNR, C the information rate and B the RF bandwidth. If the baseband bandwidth f_a were encoded perfectly, then $C = f_a \log_2(1 + S_o/N_o)$ bits/sec, where S_o/N_o is the output SNR at baseband. The noise spectral density referred to in equation (2) is the so called "one sided" spectral density, which is double the "two sided" spectral density used elsewhere in this thesis.

The communication efficiency may be calculated for both FM and FMFB and the results are shown in Figure 4.2. The efficiency varies with the output SNR required, being best at about 20db SNR for FM and 30db for FMFB.

It is apparent from both Figures 4.1 and 4.2 that FMFB realises its full capabilities of threshold improvement at high output SNR's. An ideal system using infinite bandwidth has $\beta = -1.6$db.

4.3 Telemetry applications.

4.3.1 General.

In this section a typical FM time multiplex telemetry

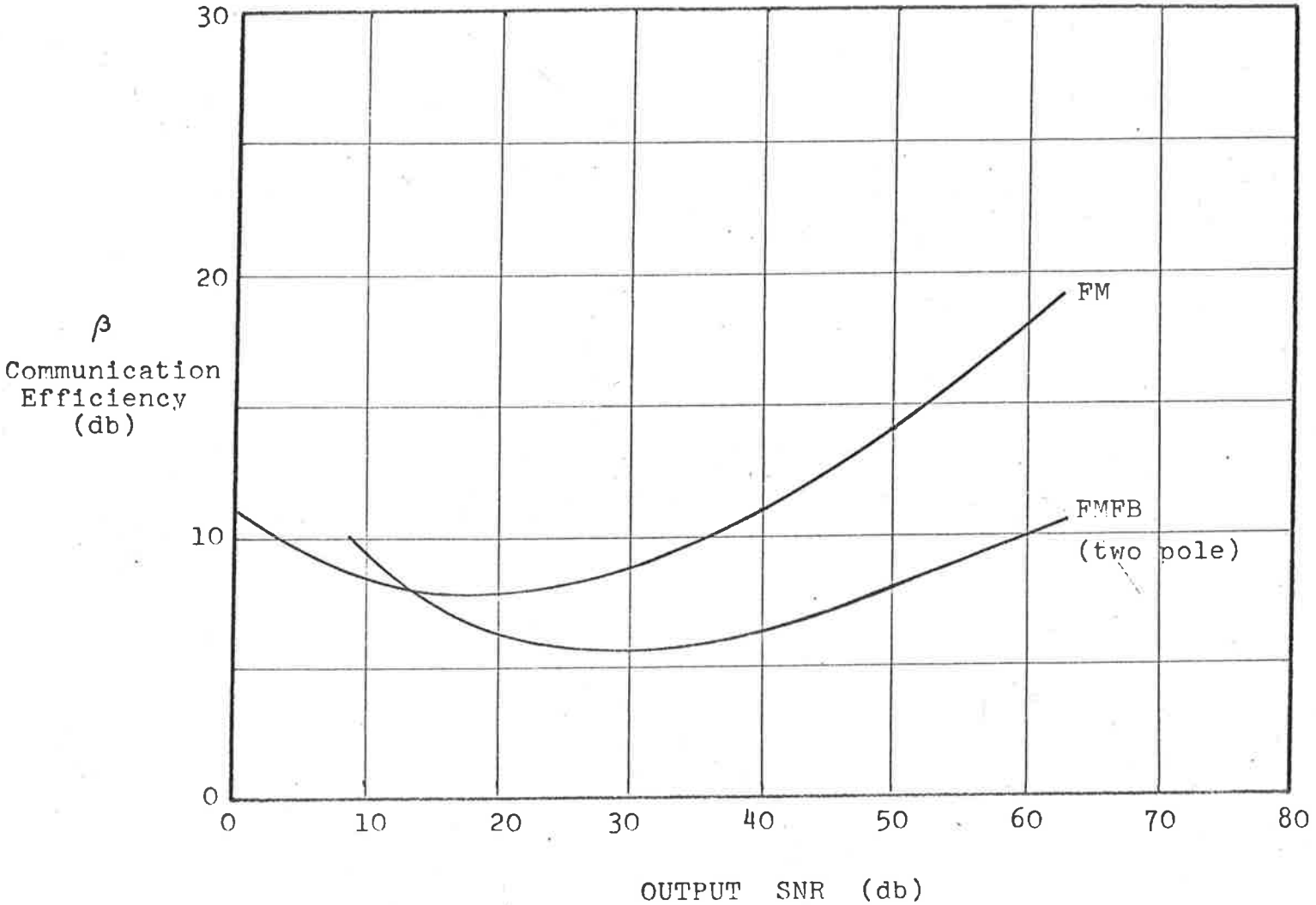

FIGURE 4.2: COMMUNICATION EFFICIENCY OF FM SYSTEMS.

system is considered and a comparison is made between the performances of FM and FMFB.

It is assumed that the various signals are sampled at a high rate and stored in a hold circuit until the next sample. The resulting "histogram" or "boxcar" waveform is then applied to an FM transmitter.

At the receiver, a filter is required which will minimise the errors due to noise and those due to signal degradation. Usually a filter is chosen such that the histogram becomes a set of exponential curves, and the value reached at the end of the sample period is different from the true value by only a small amount. At this point the histogram is sampled, the small signal error being tolerated to reduce the noise error. The filter is chosen to minimise the overall error.

The specification of a telemetry system is usually in terms of the overall accuracy required. In the following, the minimum carrier level required to achieve this accuracy at a given sample rate is derived.

4.3.2 Choice of filter.

The ideal filter is one which provides maximum noise rejection combined with a minimum rise time to a step input. The gaussian filter is one which, (in the class of linear filters without overshoot) has the shortest rise time for a given bandwidth. The gaussian filter is not physically realisable, but may be approximated by the Simmonds filter [19, 24], the accuracy of the approximation depending on the number of sections used.

It has been shown that a 5 section Simmonds filter gives the fastest rise time for errors in the range 0.1% to 10% [19]. Filters with fewer sections have a longer rise time, whereas those with more sections tend to have a time delay.

The transfer function of an n section Simmonds filter has n identical real poles. For the telemetry system considered, a 5 section filter will be assumed.

If T is the time constant of the common pole, then

$$\left.\begin{aligned} B_o &= 0.0905/T \text{ Hz} \\ B_{3db} &= 0.0615/T = 0.680\, B_o \text{ Hz} \end{aligned}\right\} \quad \ldots\ldots (4)$$

where B_o = integrated bandwidth to quadratic FM noise

B_{3db} = 3db bandwidth.

The signal error is related to the difference between the excitation and the response at a time t_s (the sample period). If it is assumed all sample levels are equally probable, then the RMS error is $1/\sqrt{6}$ times the peak error. [19]. A plot of the RMS error (relative to the maximum peak to peak signal) against t_s is shown in Figure 4.3. This is commonly called the crosstalk error.

4.3.3 Optimum ratio of crosstalk and noise errors.

The total mean square error $\langle \varepsilon_t^2 \rangle$ is equal to the sum of the mean square crosstalk error $\langle \varepsilon_c^2 \rangle$ and the mean square noise error $\langle \varepsilon_n^2 \rangle$. The noise error is proportional to B_o^3. Figure 4.3 shows the total RMS error plotted against $B_o t_s$ for various levels of noise.

The minimum noise occurs when the ratio of the RMS noise

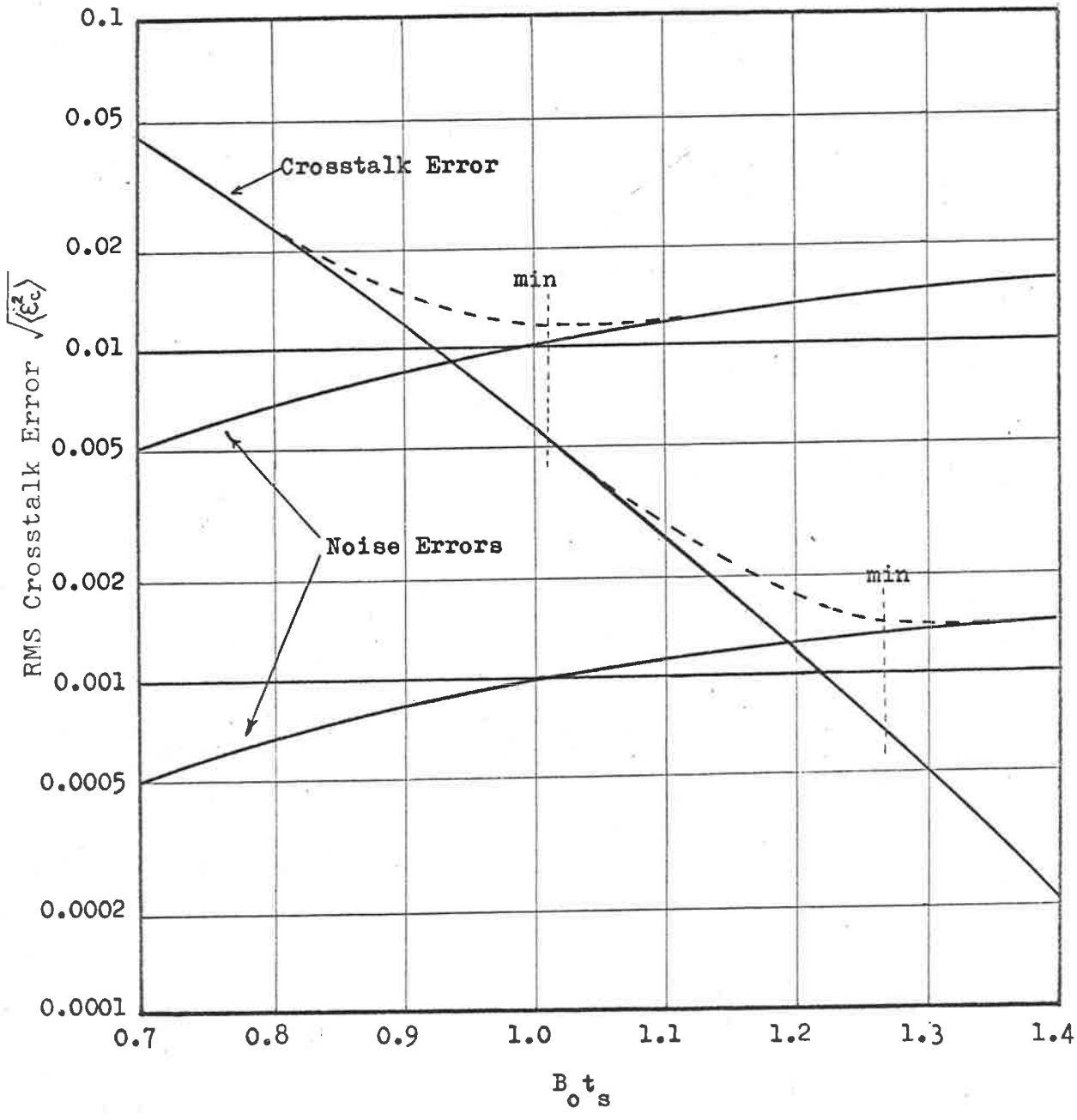

FIGURE 4.3: ERROR VARIATION WITH FILTER BANDWIDTH.

error to RMS crosstalk error is approximately 2:1 and this value will be assumed optimum. Because of the very broad minima in Figure 4.3, errors in this assumption will have negligible effect.

4.3.4 Design of an FM telemetry system.

For convenience the following symbols are defined:

S = ratio of IF 3db bandwidth and twice baseband bandwidth

ρ_t = threshold value of the IF CNR (discriminator threshold)

m = modulation index = ratio of peak frequency deviation and baseband bandwidth.

The well known bandwidth rule for FM will be assumed viz.

$$S = 1 + m \qquad \text{..... (5)}$$

(a) Noise errors.

In an FM system of peak frequency deviation f_d, the mean square noise error (relative to peak to peak signal of $2f_d$) is given by:

$$\langle \varepsilon_n^2 \rangle = \eta B_o^3 / 6 P_c f_d^2 \qquad \text{..... (6)}$$

where P_c = carrier power

η = noise spectral density (assumed constant).

B_o = Simmonds filter integrated FM bandwidth.

This may be rewritten in the form:

$$\langle \varepsilon_n^2 \rangle = (B_o/f_a)^3 / 24 \rho_o (f_d/f_a)^2 \qquad \text{..... (7)}$$

where $\rho_o = \dfrac{P_c}{4 \eta f_a}$ = CNR in bandwidth $2f_a$.

f_a = nominal baseband bandwidth of system.

Putting in terms of the parameters defined earlier,

$$\langle \varepsilon_n^2 \rangle = (B_o/f_a)^3/24S\,\rho_t\,(S-1)^2 \qquad \ldots\ldots (8)$$

(b) Filter bandwidth.

If a total error $\langle \varepsilon_t^2 \rangle$ is specified, then $\langle \varepsilon_n^2 \rangle = 0.8\ \langle \varepsilon_t^2 \rangle$ on the assumption of a 2:1 ratio of RMS noise error to RMS crosstalk error. Hence for a given value of $\langle \varepsilon_t^2 \rangle$ and values of S and ρ_t, equation (8) can be solved for B_o/f_a. Also from $\langle \varepsilon_c^2 \rangle = 0.2\ \langle \varepsilon_t^2 \rangle$, the value of $B_o t_s$ can be determined from Figure 4.3.

(c) Minimum carrier level.

The carrier level is expressed in terms of the parameter $\rho_c = \dfrac{P_c\, t_s}{4\eta}$, which is equal to the CNR in an RF bandwidth equal to twice the sample rate.

$$\rho_c = S\rho_t\,(B_o t_s)/(B_o/f_a) \qquad \ldots\ldots (9)$$

Hence from previously calculated results, ρ_c may be found.

(d) Optimisation procedure.

(i) A range of values of S was chosen.

(ii) The values of ρ_t were obtained by using results obtained by others. [3, 14].

(iii) A range of values $\langle \varepsilon_t^2 \rangle$ was chosen, and hence the values of $\langle \varepsilon_n^2 \rangle$ and $\langle \varepsilon_c^2 \rangle$ (such that $\langle \varepsilon_n^2 \rangle = 4 \langle \varepsilon_c^2 \rangle$).

(iv) The parameter B_o/f_a was calculated from (8).

(v) The parameter $B_o t_s$ was obtained from Figure 4.3.

(vi) The parameter ρ_c was calculated from (9).

(vii) For each value of $\langle \varepsilon_t^2 \rangle$, the value of S which gave the minimum

value of ρ_c was chosen, provided B_o/f_a was less than 1.5. (This latter condition is necessary to prevent the 3db bandwidth of the Simmonds filter exceeding the nominal baseband bandwidth.)

The results of this calculation are shown in Figure 4.4.

4.3.5 Considerations in FMFB telemetry.

Because of the nature of the feedback FM system, it is not able to follow rapid changes in signal frequency satisfactorily. The histogram modulation consists of a set of step changes in frequency. Due to the finite response time of the feedback loop, a large change in frequency can cause loss of synchronism in the system.

The problem is to confine the IF carrier within the IF passband at all times. One obvious (but inefficient) method is to reduce the peak frequency deviation of the signal. Alternatively the modulating waveform may be passed through a prefilter ahead of the frequency modulator, thus reducing the rate of change of frequency to a value that the loop can track without difficulty; or the feedback loop may be modified so that it can handle step changes in frequency without difficulty. [15].

4.3.6 FMFB telemetry system with transmitter filter.

In this section, the FMFB receiver will be assumed to be the optimum analogue system with a two pole loop transfer function. At the transmitter end, a filter is used to limit the maximum rate of change of frequency. This filter affects the histogram modulation, and since it is effectively in series with the Simmonds filter

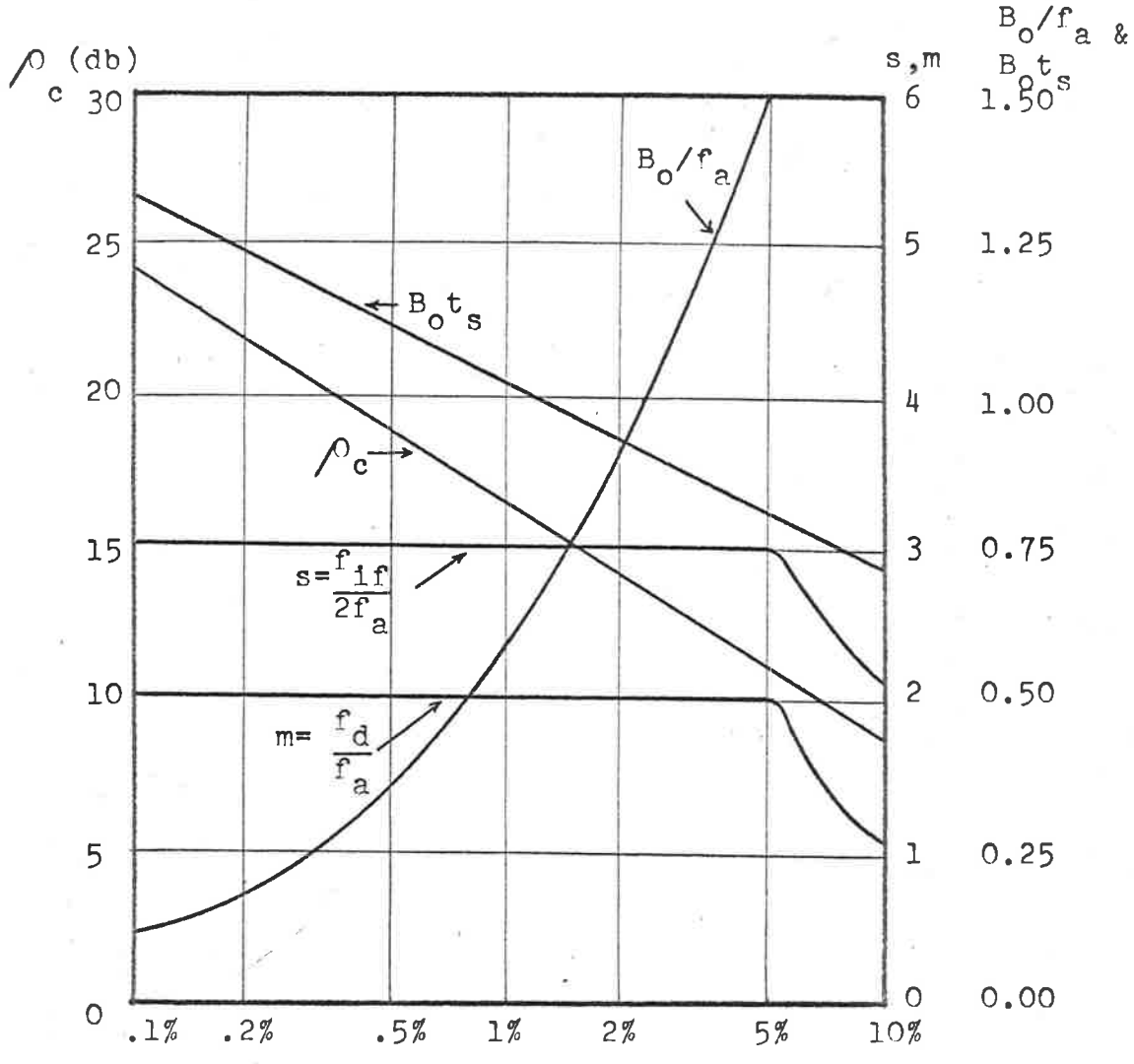

FIGURE 4.4: OPTIMUM PARAMETERS FOR AN FM TELEMETRY SYSTEM.

it causes an additional crosstalk error. It will be assumed that the overall receiver transfer function is that of a 5 section Simmonds filter. There is very little error in this assumption, since the closed loop bandwidth is usually much larger than the Simmonds filter bandwidth. Alternatively, the overall receiver transfer function can be made that of a 5 section Simmonds filter by suitable baseband filtering.

(a) The transmitter filter.

The object of the transmitter filter is to reduce the overshoot of the IF frequency when a step change in the modulating voltage occurs. An overshoot in the step response of a network is generally related to a rise in the amplitude response at high frequencies.

The closed loop response of the FMFB system with the output taken after the baseband filter tends to be fairly flat. The response at the output of the frequency detector corresponds to this response multiplied by the inverse of the baseband filter, giving a rising response of frequencies beyond baseband. The transmitter filter is chosen to be identical to the baseband filter in order to keep the overall frequency response relatively flat.

From the resulting transfer function, the overshoot e_o may be calculated (relative to an excitation of a unit step). The peak IF deviation will be slightly larger than the compressed signal deviation. The worst case gives:

$$(f_d)_{IF} = \frac{f_d}{F}(1 + 2e_o) \qquad \ldots\ldots (10)$$

The IF bandwidth is given by:

$$B_{IF} = 2(f_a + (f_d)_{IF}) \qquad \ldots\ldots (11)$$

and hence the relation between modulation index m and the parameter $S = B_{IF}/2f_a$ is:

$$m = \frac{F(S - 1)}{1 + 2e_o} \qquad \ldots\ldots (12)$$

(b) Noise errors.

The mean square noise error is the same as for the FM telemetry system and is given by (7). Substituting for $m = f_d/f_a$ from (12) gives:

$$\langle \varepsilon_n^2 \rangle = (1 + 2e_o)^2 (B_o/f_a)^3/24S\rho_t F^2(S - 1)^2 \qquad \ldots\ldots (13)$$

(c) Filter bandwidth.

Given a total error $\langle \varepsilon_t^2 \rangle$, equation (13) can be solved for B_o/f_a assuming the other parameters (viz. e_o, S, ρ_t, F) are known.

Figure 4.3 cannot be used to obtain $B_o t_s$ since the overall response is modified by the inclusion of the transmitter filter. Figure 4.5 shows the crosstalk error as a function of $B_o t_s$ for various ratios of B_o/f_a.

From this figure, the value of $B_o t_s$ can be obtained.

(d) Minimum carrier level.

As in the previous case, equation (9) is used to calculate the carrier power parameter ρ_t.

(e) Optimisation procedure.

This is essentially the same as before except that from the values of S and ρ_t chosen, it is necessary to calculate the feedback factor

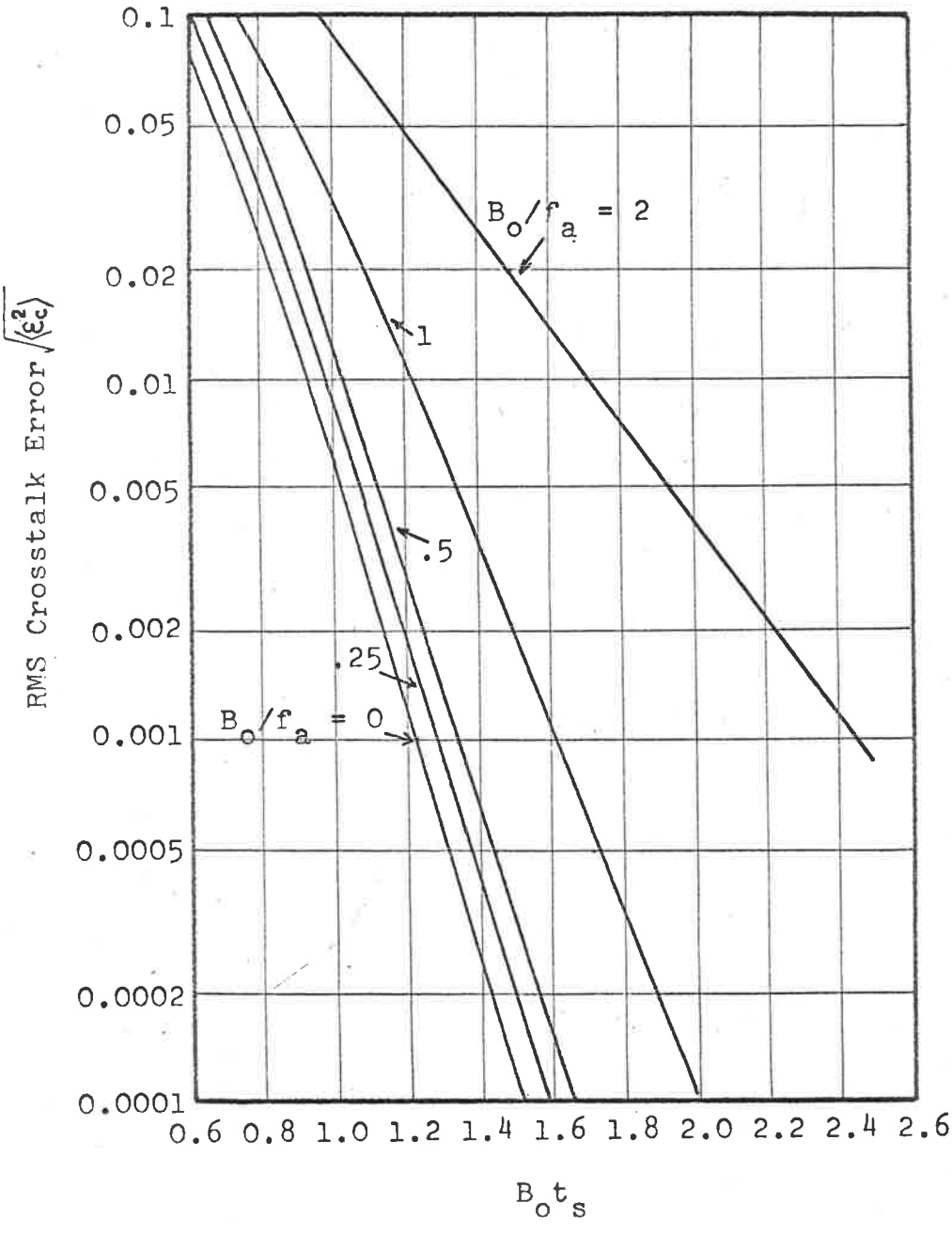

FIGURE 4.5: ERROR VARIATION WITH FILTER BANDWIDTH.

F which optimises the loop performance under analogue conditions and also the overshoot e_o which is dependent on the loop transfer function.

The results of this optimisation are shown in Figure 4.6.

4.3.7 FMFB telemetry system with modified loop.

(a) Requirements.

The feedback loop must be able to follow the rapid changes in input frequency without losing synchronism. This is achieved by making the baseband filter of wider bandwidth, or omitting it entirely. In doing so, however, the feedback threshold is enhanced so the performance deteriorates. There is no additional crosstalk error introduced, however.

As in the previous section, the overall receiver transfer function is assumed to be that of a 5 section Simmonds filter.

The IF deviation is again limited by the overshoot e_o and the relation between m and S is given by equation (12).

(b) Receiver optimisation.

It is necessary to know the optimum feedback factor and the baseband filter bandwidth before the overshoot can be calculated.

If the filter bandwidth is known then the feedback factor which optimises the loop can be found and the overshoot e_o obtained. Using equation (12) the value of m may be found. The optimum value of the baseband filter bandwidth is that which gives the maximum value of m.

For a range of values of S, the optimum baseband filter bandwidth was calculated, with the corresponding values of e_o, F, m.

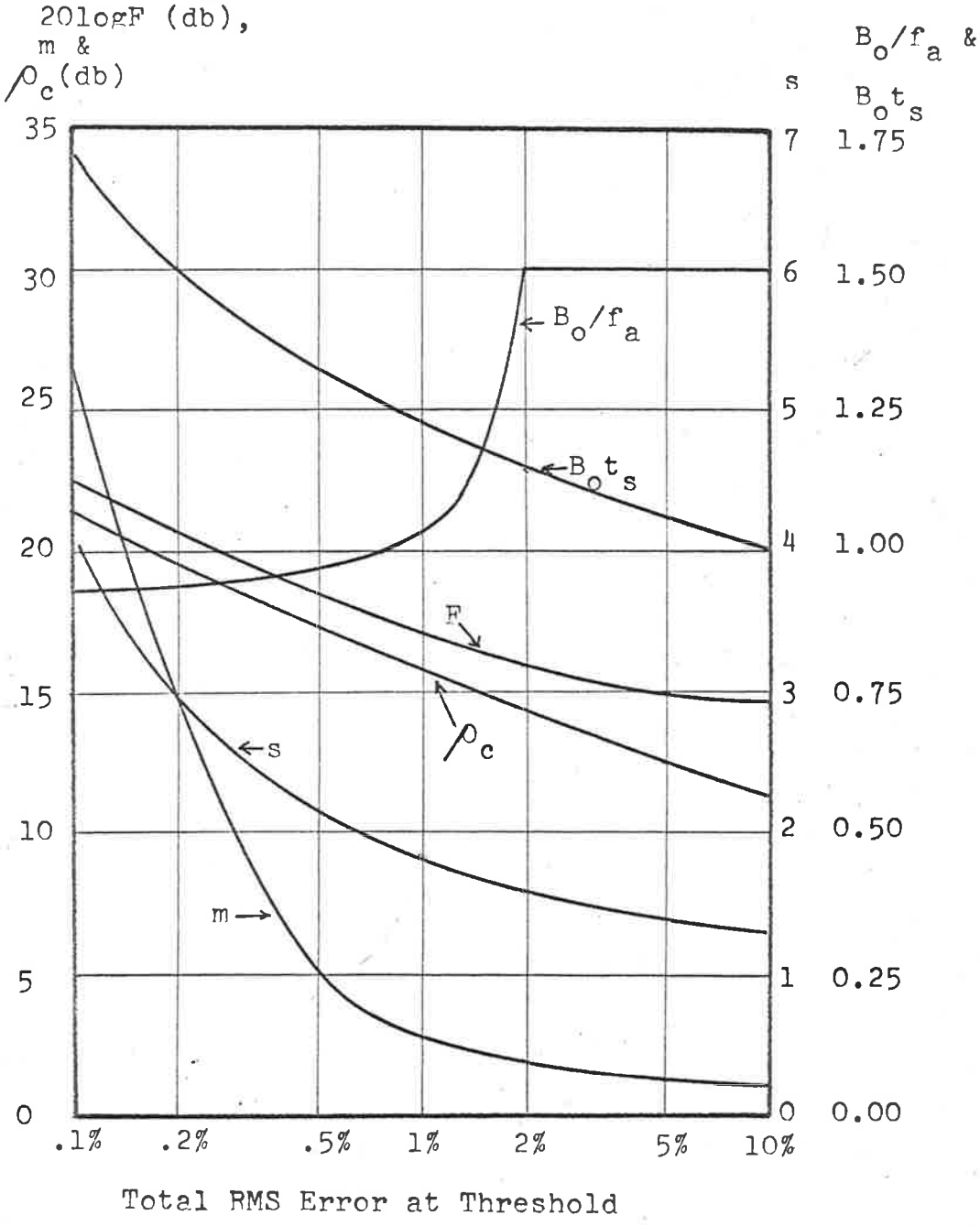

FIGURE 4.6: OPTIMUM PARAMETERS FOR FMFB TELEMETRY SYSTEM. (TRANSMITTER FILTER).

(c) Noise errors.

The expression is the same as previously given in equation (13).

(d) Filter bandwidth.

Solving (13) for B_o/f_a and using Figure 4.3 to obtain $B_o t_s$ enables the minimum carrier level to be calculated.

(e) Minimum carrier level.

Using equation (9) the parameter ρ_c may be calculated.

(f) Optimisation procedure.

This is the same as for FM except that for each value of S, the optimum values of F, e_o and m must be calculated. This involves finding the baseband filter bandwidth which gives maximum m.

The results are shown in Figure 4.7.

4.3.8 FMFB with transmitter filter and modified loop.

If a wider baseband filter is assumed and a transmitter filter identical to it is used, then the telemetry system may be designed along the lines of the previous section. However it was found that the optimum baseband filter bandwidth was equal to the nominal baseband bandwidth f_a and hence the system was identical to the transmitter filter system of section 4.3.6.

4.3.9 Comparison of FM telemetry systems.

Figure 4.8 shows the value of ρ_c required for the three FM telemetry systems considered. It can be seen that the modified loop system is marginally superior to the transmitter filter system and both

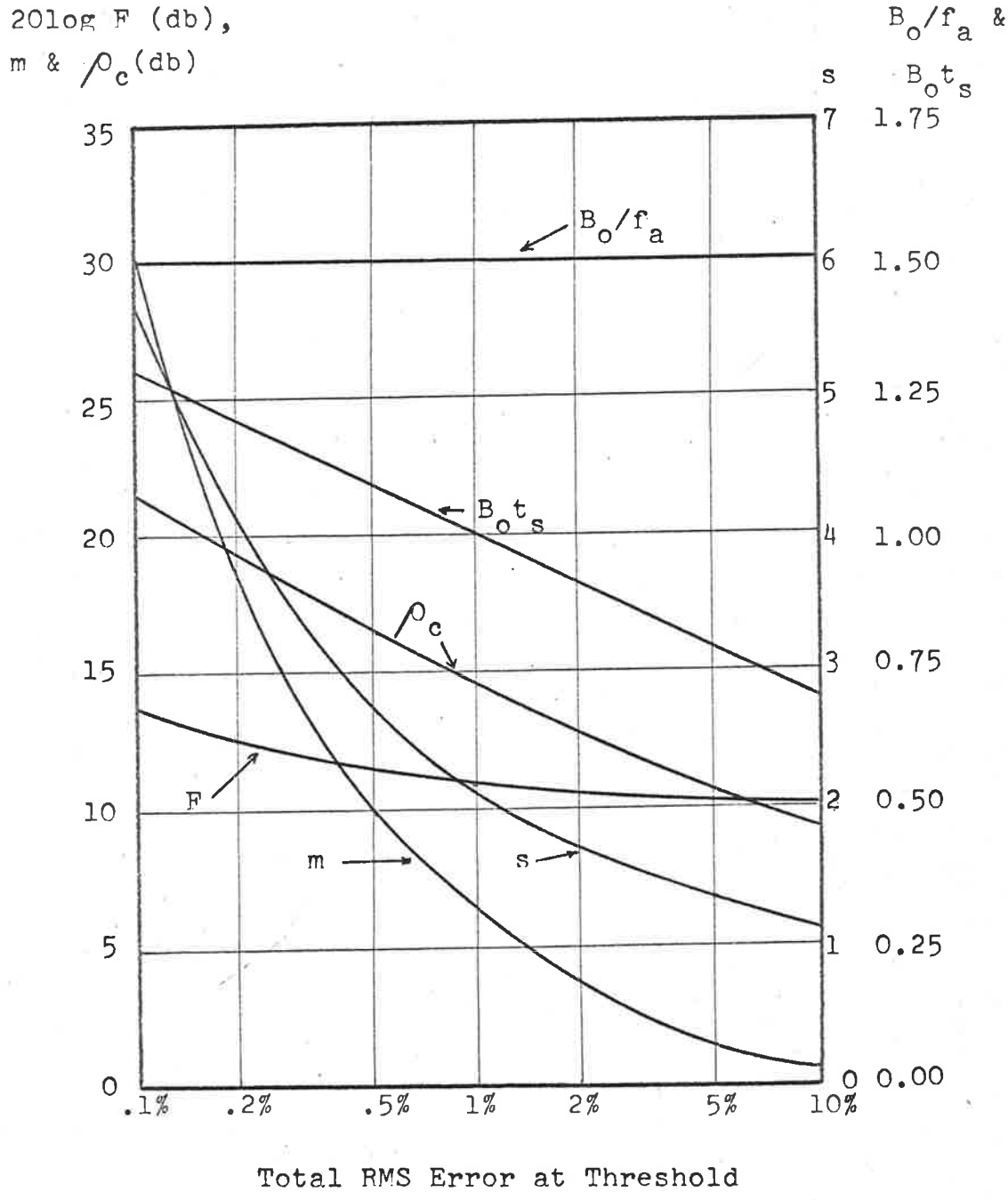

FIGURE 4.7: OPTIMUM PARAMETERS FOR FMFB TELEMETRY SYSTEM. (MODIFIED LOOP).

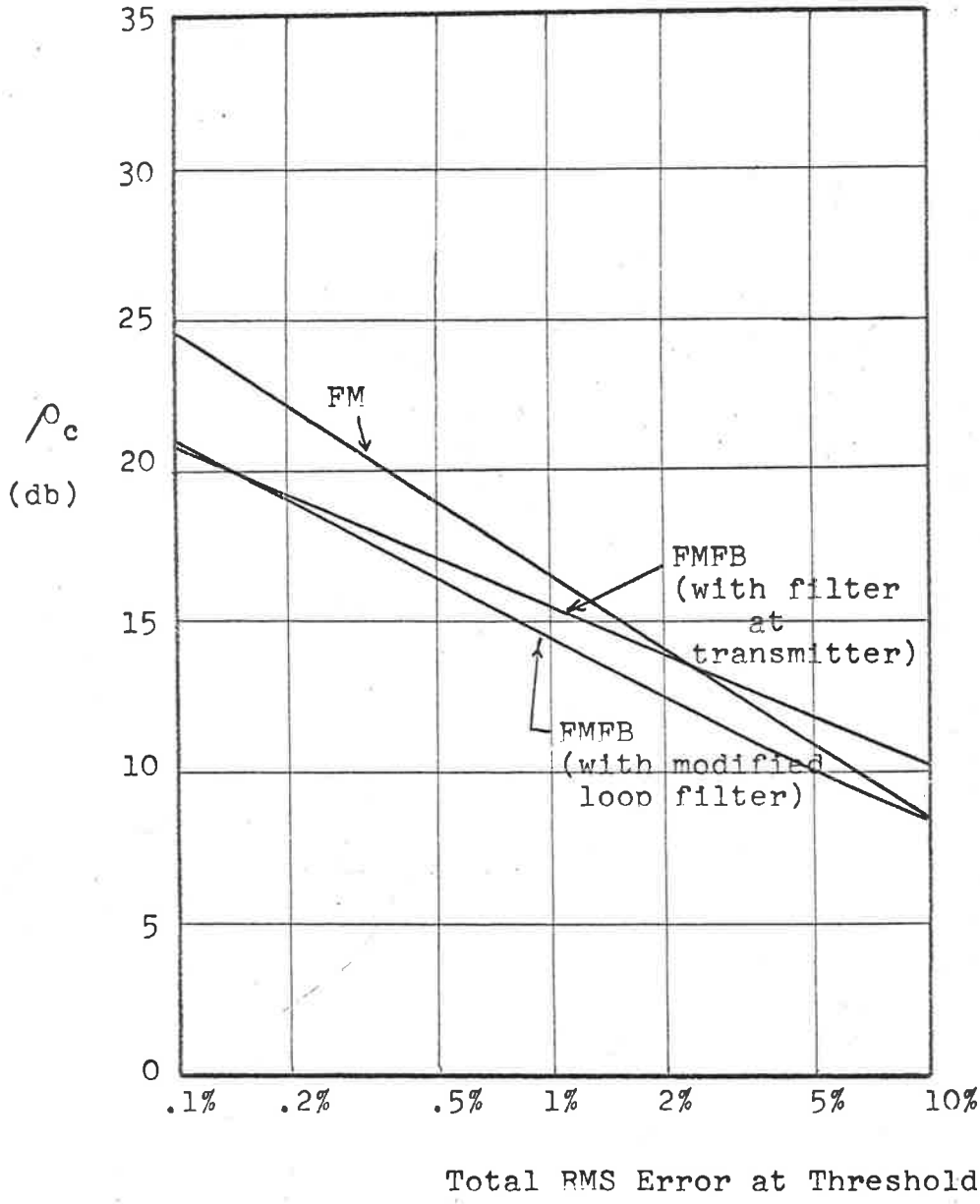

FIGURE 4.8: COMPARISON OF FM TELEMETRY SYSTEMS.

are better than ordinary FM for errors less than 1%.

In all the foregoing calculations, distortion due to the non-linear behaviour of the IF filter has been ignored. This would probably be significant at low error levels and reduction of these errors would require an IF bandwidth greater than assumed.

4.4 Conclusions.

FMFB produces the largest improvement in threshold in analogue systems at high output SNR's. This is evident from the fact that compression of the modulation index below unity does not achieve any worthwhile saving of IF bandwidth. The improvement on a narrow band system is therefore small. At high SNR's the carrier power saving can be as high as 5-10db which is a very significant saving in terms of transmitter installation, or alternatively a large increase in useful propagation distance can be achieved for the same transmitter power.

The application of FMFB to telemetry does produce some carrier power saving of the order of 2db at 1% error and 3db at .1% error. However the nature of FMFB does not really suit it to the type of modulation encountered in the time multiplex system considered. Possibly the use of pulses of narrower spectral width than the rectangular pulses would enable higher gains to be made in this regard.

CHAPTER 5: SYSTEMS RELATED TO FMFB.

In this section the results of a preliminary investigation into systems related to FMFB is presented. FMFB is in fact only one member of a class of frequency compressive systems, the aim of all being to reduce the effective frequency deviation of an FM signal, but each differing in the means of achieving it.

The two systems which will be considered in this chapter are the dynamic filter and the phase locked frequency divider. The former is a type of tracking filter and the second a frequency compressive system where no conversion to baseband occurs within the feedback loop.

5.1 The dynamic filter.

5.1.1 Introduction.

In FMFB the receiver is made to track the incoming instantaneous frequency by means of a voltage controlled oscillator and a fixed IF channel. The tracking is achieved by an error sensor (the frequency detector) providing a correction voltage to the VCO in order to minimise the error.

An alternative method of tracking the signal is to actually alter the resonant frequency of the IF channel and use a fixed frequency oscillator. In this case, of course, an oscillator/mixer combination is not necessary in theory, but since in practice it is easier to manipulate signals at IF rather than at RF they will normally be included.

The possibility of altering the IF resonant frequency gives rise to the so called "dynamic filter". A threshold improvement

achieved by such a system is based on the same principle as FMFB, namely a reduction in IF bandwidth and a consequent reduction in noise.

5.1.2 Dynamic filter response to FM.

If a normal tuned circuit is excited by a sinusoid whose frequency differs from the resonant frequency by a fixed amount, then the output signal is a replica of the input signal except for an amplitude change and a phase shift, both of which depend only on the frequency difference.

It has been shown [16] that if a dynamic filter whose centre frequency is varying sinusoidally is excited by a frequency modulated signal such that the difference of the instantaneous excitation frequency and the instantaneous centre frequency is constant, then the output signal is a replica of the input except for an amplitude change and a phase shift. Also the amplitude and phase modifications are dependent only on the frequency difference.

The response of the dynamic filter to an arbitrary signal is most conveniently found by resolving the incoming signal into components which differ in frequency from the filter centre frequency by constant amounts. This is analogous to Fourier analysis in the case of fixed tuned circuits.

5.1.3 Dynamic filter FM detectors.

One form of FM detector suggested by Baghdady [17] is shown in Figure 5.1. This is a dynamic selector circuit which uses the output of the frequency detector to tune the dynamic filter to the instantaneous frequency of the FM signal.

Although in theory this will give a threshold improvement, it is found in practice that maintaining perfect tracking in amplitude and phase for the whole modulation bandwidth is extremely difficult [16]. This is because the system is essentially an open loop system, the tuning of the dynamic filter having no direct effect on the instantaneous frequency of the signal. However such a technique has some application in the separation of two FM signals [20].

A closed loop system similar to FMFB might be as shown in Figure 5.2. A possibility for the detector is to measure the phase difference between the input and output signals of the dynamic filter [16].

Such a system as Figure 5.2 is identical to FMFB as far as processing the signal is concerned and has the same threshold performance. It is interesting to note, however, that there is no parameter equivalent to the VCO phase, although the integral of the dynamic filter instantaneous frequency does represent this.

5.1.4 Conclusions.

In view of the similarity of the dynamic filter to the VCO/fixed IF system, it is evident that the performance of a feedback type detector using a dynamic filter is identical to an FMFB system.

Practical difficulties associated with the system of Figure 5.2 are in obtaining a linear variation of frequency with voltage without bandwidth alteration and in obtaining a linear off-tune detector. These difficulties make such a system an unattractive alternative to FMFB.

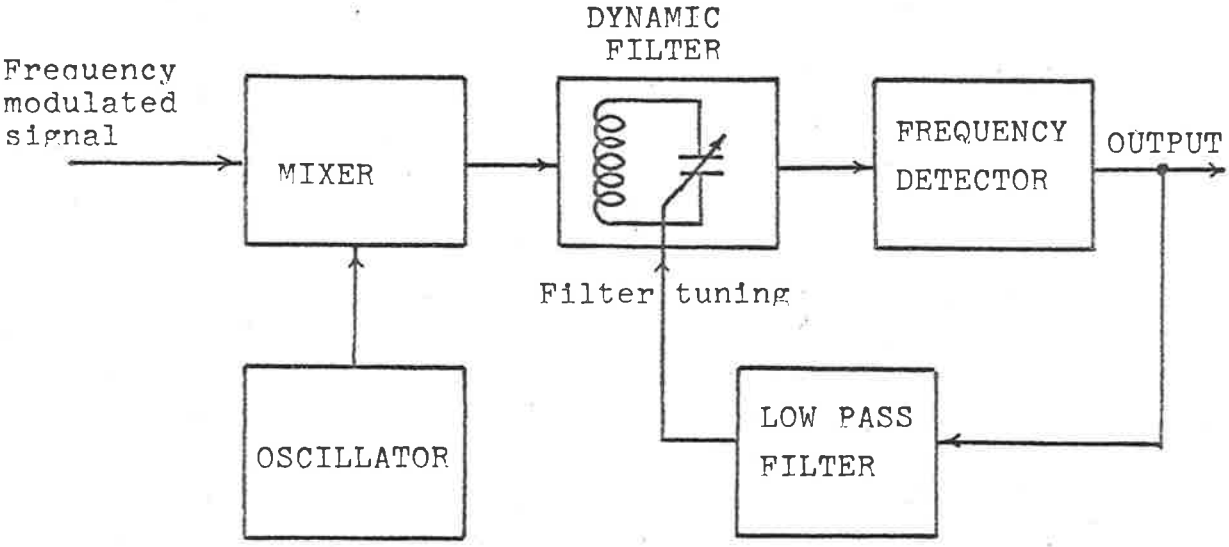

FIGURE 5.1: DYNAMIC SELECTOR SYSTEM.

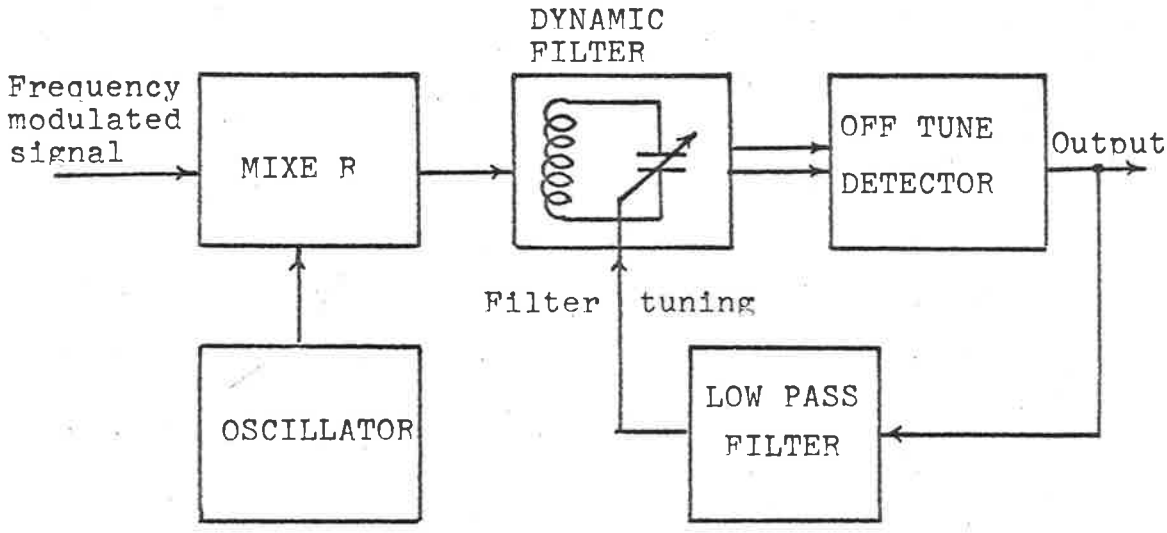

FIGURE 5.2: DYNAMIC FILTER SYSTEM.

5.2 The phase-locked frequency divider.

5.2.1 Introduction.

This system has properties similar to FMFB but has the additional constraint that it is phase synchronous. The basic block diagram is shown in Figure 5.3.

The system has several applications, the most common being as an accurate frequency divider. However since frequency division achieves frequency compression also, the possibility of using it as an FMFB type detector also arises. A system of this form was studied by Beers [21] , although he found it necessary to supplement the frequency compression by means of FMFB in order to obtain a workable system.

Although similar to FMFB in its processing of the frequency modulation, it is evident that the physical operation of the system is markedly different. Firstly, in the absence of signal there is no local oscillator signal and hence arises the question of whether the system is self starting or not, and secondly, the fact that it is phase synchronous may impose additional constraints.

5.2.2 Relation to time varying systems.

It is evident from Figure 5.3 that because of the inclusion of non-linear elements such as the mixer and frequency multiplier, the describing equations will be non-linear.

Consider a simplified form of Figure 5.3 in which the mixer is a perfect multiplier, the IF a single tuned circuit and the frequency multiplier a lagless non-linear device. See Figure 5.4

The differential equation describing the circuit is:

$$LC\frac{d^2v}{dt^2} + RC\frac{dv}{dt} + v = v_i(t)f(v) \qquad \ldots\ldots (1)$$

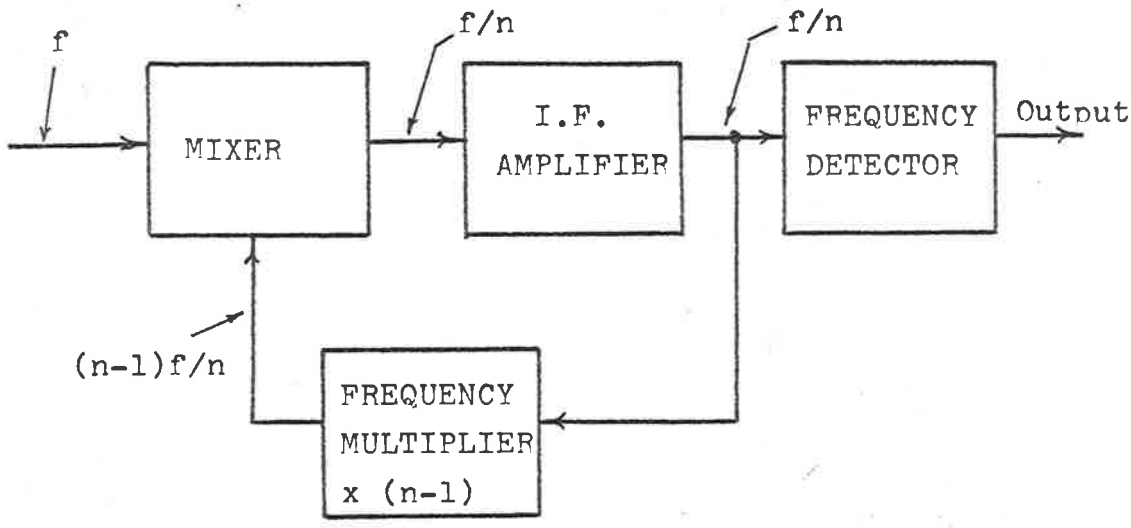

FIGURE 5.3: THE PHASE-LOCKED FREQUENCY DIVIDER.

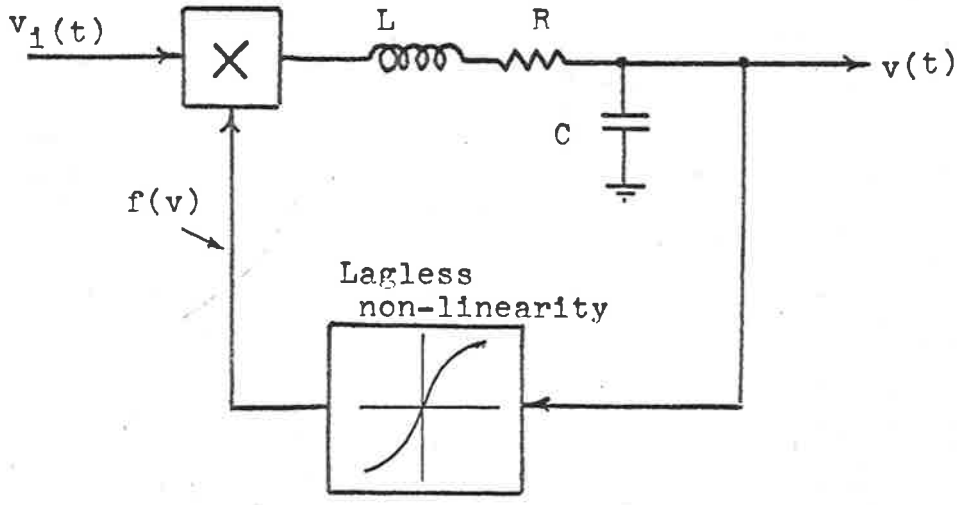

FIGURE 5.4: SIMPLE FREQUENCY DIVISION SYSTEM.

In the particular case where $f(v) = v$, (1) becomes a linear time varying differential equation. If $v_i(t)$ is sinusoidal, (1) can be transformed into the Mathieu equation. Normalising the resonant frequency to 1 rad/sec and defining the following:

$$LC = 1$$

$$\varepsilon = \frac{R}{2L} = \frac{1}{2Q} \ll 1$$

$$v_i(t) = A \cos pt$$

then equation (1) becomes:

$$\frac{d^2v}{dt^2} + 2\varepsilon \frac{dv}{dt} + v(1 - A \cos pt) = 0 \qquad \ldots\ldots (2)$$

whereby on change of variables:

$$\frac{d^2w}{d\tau^2} + w\,(a - 2q \cos 2\tau) = 0 \qquad \ldots\ldots (3)$$

where $2\tau = pt$

$$w(\tau) = v(t)\, e^{\varepsilon t}$$

$$a = \frac{4}{p^2}(1 - \varepsilon^2)$$

$$q = \frac{2A}{p^2}$$

Equation (3) is the standard Mathieu equation. The particular solutions of interest are exponentially growing oscillatory solutions when $a \approx 1$. This corresponds to frequency division by a factor of 2.

To obtain a periodic solution in $v(t)$, it is necessary to find an oscillatory solution for $w(\tau)$ with an exponential growth rate of ε sec^{-1}. From the theory of the Mathieu equation, for small ε

the required value of q is given by:

$$q^2 = (\varepsilon^2 + a - 1)^2 + 4\varepsilon^2 \qquad \ldots\ldots (4)$$

In terms of the parameters of Figure 5.4 this becomes:

$$4A^2 = (1 - \varepsilon^2)^2 (4 - p^2)^2 + 4\varepsilon^2 p^4 \qquad \ldots\ldots (5)$$

Since the range of interest for p is in the vicinity of p=2 we put $p=2(1 + \mu\varepsilon)$ and (5) becomes:

$$A = 4\varepsilon \sqrt{1 + \mu^2} + O(\varepsilon^2) \qquad \ldots\ldots (6)$$

When $\mu = \pm 1$ this corresponds to the IF filter operating at its 3db point, since for small ε, the 3db points are $1 \pm \varepsilon$ and the IF signal is a sinusoid of frequency $p/2 = 1 + \mu\varepsilon$.

If $v_i(t)$ is a quasistationary frequency modulated wave then (6) gives the condition for sustained oscillations. A practical realisation of Figure 5.4 would require an A greater than that given by (6), with a limiter of some form in the feedback loop to maintain the oscillation amplitude at a finite value.

The simplest form of limiter is the ideal hard limiter $f(v) = \text{sign}\ (v)$. The describing differential equation is now:

$$\frac{d^2v}{dt^2} + 2\varepsilon \frac{dv}{dt} + v = v_i(t)\ \text{sign}\ (v) \qquad \ldots\ldots (7)$$

This may split into three linear differential equations for the three regions $v(t) > 0$, $v(t) < 0$ and $v(t) = 0$, or alternatively the oscillation amplitude may be found by using a harmonic balance technique. Assuming the output wave is approximately sinusiodal of frequency p (due to the high Q tuned circuit) the limiter output is a square wave.

If:

$$v(t) = e\cos(pt + \phi)$$

then $$\text{sign}(v) = \frac{4}{\pi}\left(\cos(pt+\phi) - \tfrac{1}{3}\cos 3(pt+\phi) + \cdots\right) \quad \ldots\ldots (8)$$

If $v_i(t) = A\cos 2pt$ then the component at frequency p resulting from $v_i(t)\,\text{sign}(v)$ is:

$$v_p(t) = \frac{2A}{\pi}\left\{\cos(pt-\phi) - \tfrac{1}{3}\cos(pt+3\phi)\right\} \quad \ldots\ldots (9)$$

When $v_p(t)$ is filtered by the IF filter, it must give v(t). At frequency p the IF filter has a response:

$$H(jp) = \frac{1}{1 - p^2 + j\,2\varepsilon p} \quad \ldots\ldots (10)$$

Hence $$e^2 = \frac{4A^2}{\pi^2}\,\frac{(\cos\phi - \tfrac{1}{3}\cos 3\phi)^2 + (\sin\phi + \tfrac{1}{3}\sin 3\phi)^2}{(1-p^2)^2 + 4\varepsilon^2 p^2} \quad \ldots (11)$$

$$\phi = \arg\left[e^{-j\phi} - \tfrac{1}{3}e^{j3\phi}\right] - \arctan\frac{2\varepsilon p}{1-p^2} \quad \ldots\ldots (12)$$

The solutions to (11) and (12) are shown in Figure 5.5. The device is theoretically self-starting although in practice hysteresis or backlash in the limiter may prevent reliable self-starting. However provided A is large enough, the system should always self start.

For the divide by two circuit there is also the possibility of instability due to multiplier imperfections. Unless the mixer is ideal or at least balanced, a direct feedback path at the IF frequency exists and oscillations independent of the excitation may occur.

5.2.3 The divide by three system.

In Figure 5.4 if f(v) is such that the second harmonic of v is favoured then the circuit will divide the frequency by three. A

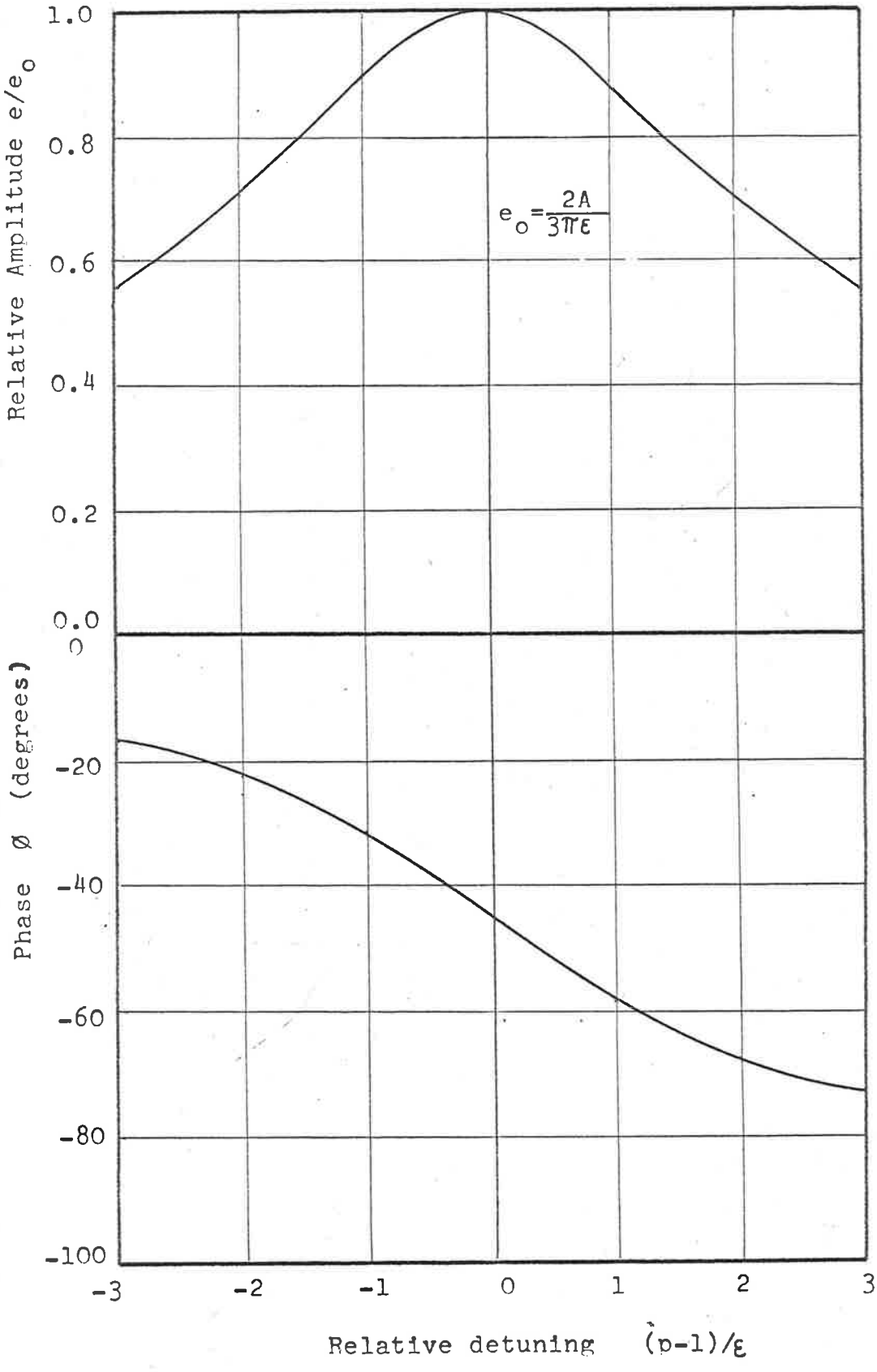

FIGURE 5.5: OUTPUT AMPLITUDE AND PHASE OF DIVIDE BY TWO SYSTEM.

logical choice for f(v) might be a quadratic device $f(v) = \alpha v^2$, followed by a high pass filter to reject the D.C. component.

Using the technique of harmonic balance to generate a solution $v = e \cos(pt + \phi)$ with an excitation $v_i = A \cos 3pt$, it is found that the solutions for the high Q case are:

$$e = \frac{\alpha A e^2}{4} \cdot \frac{1}{\sqrt{(1-p^2)^2 + 4\varepsilon^2 p^2}} \qquad \ldots\ldots (13)$$

$$\phi = -\tfrac{1}{2} \arg (1 - p^2 + j2\varepsilon p) \qquad \ldots\ldots (14)$$

There are two solutions to (13) one of which is $e = 0$. The other solution $e = e_s$ is a separatrix between exponentially increasing and exponentially decreasing oscillatory solutions. This indicates the system is not self starting and unless the amplitude of the solution is greater than e_s the output will be exponentially decreasing. Also a momentary decrease in the excitation amplitude may cause the oscillations to stop.

The exponentially increasing solution can be restricted to a finite amplitude by placing a limiter in the loop. In practice it would be desirable to have a self-starting system. This could be done by making the frequency multiplier a free running oscillator which is synchronised with the IF output when this reaches a certain magnitude. This technique was used by Beers [21]. Alternatively, self starting could be achieved by modifying f(v) so that the second harmonic output is proportional to e for small e rather than e^2 as for the quadratic device.

A suitable non-linear device is $f(v) = |v|$. The resulting

divide by three circuit has similar characteristics to the divide by two circuit, in that there is a minimum input amplitude required for growing solutions.

5.2.4 The divide by n system.

In a practical frequency compression system a large compression ratio (typically 10-50) is required in order to obtain significant improvement in performance.

In its simplest form of Figure 5.4 it is evident that the function f(v) must be such that the harmonic output is at least linearly related to the input voltage for small inputs. This is not usually satisfied by conventional multipliers.

It is evident that if f(v) is continuous and continuous in all its derivatives then the above condition will not be satisfied, since the amplitude of the K^{th} harmonic will vary as the K^{th} power of the input.

The simplest solutions for f(v) which contain only one point of discontinuity are:

$$f(v) = \begin{cases} \text{sign}(v) & ; \text{ n even} \\ |v| & ; \text{ n odd} \end{cases} \qquad \ldots\ldots (15)$$

remembering that a divide by n system requires an (n-1) frequency multiplier.

The function sign (v) produces odd harmonics of constant amplitude for all input amplitudes and the output of the system reaches a steady value given by the harmonic balance equations (under unmodulated

conditions.)

The function $|v|$ produces even harmonics of amplitude directly proportional to the input amplitude. The system will excite provided the input exceeds a threshold value. To limit the exponentially growing output, some form of AGC is required. The simplest method is to modify f(v) e.g.

$$f(v) = \begin{cases} |v| & ; \ |v| \leq v_o \\ v_o & ; \ |v| > v_o \end{cases} \qquad \ldots\ldots (16)$$

In practice of course, the harmonic output would be filtered to eliminate the unwanted components, and also to shape the loop response into a desirable form as for FMFB.

Practical difficulties associated with this type of system are self-starting of the system and adequate operating range (to accommodate videband FM). The first can be eliminated by using a free running oscillator which is synchronised with the IF signal. However it it difficult to obtain reliable synchronisation over the frequency range required, e.g. Beers [21] found it necessary to supplement his system with FMFB.

5.2.5 Phase stability.

In a circuit of the form of Figure 5.3 there are n stable subharmonic phases for which the circuit operates. These stable phases are $2\pi/n$ apart. In this property the system is identical to FMFB and in fact the low pass linear approximations are the same. This indicates immediately that an n + 1 frequency multiplier is not possible

for successful operation, as this corresponds to positive feedback in the phase equivalent circuit.

In the FMFB system some of the filtering is done by the IF filter and some by the baseband filter. The IF filtering is non-linear to phase whereas the baseband filter is linear. The IF non-linearity is the primary cause of threshold effects in the system.

In the phase-locked frequency divider all filtering is done by bandpass circuits, and the modulation dependent threshold effects will therefore be accentuated. Jumps from one stable state to another result in frequency impulses at the frequency detector output and threshold occurs in a similar manner to that in FMFB.

5.2.6 Comparison with FMFB.

The phase locked frequency divider is similar in its effect to that of an FMFB system, except for some restrictions on the system parameters. It is necessary to examine these restrictions to see whether they produce any advantages or not.

One restriction is that the feedback factor must be an integer. This may be a disadvantage in that system optimisation may require a non-integral feedback factor. However the performance is unlikely to be affected significantly by using the nearest integer value.

Another restriction is that the system is phase synchronous, although this is another implication of an integral feedback factor. In a sense FMFB is also phase-synchronous, the limit of its accuracy being determined only by the stability of the loop gain. An

arbitrary constant is introduced in FMFB due to the operations of differentiation (frequency detector) and integration (V.C.O). Phase synchronism does not therefore produce any advantages or disadvantages as far as threshold improvement is concerned.

The restriction that all filtering must be done by RF circuits is one which puts the phase-locked frequency divider at a disadvantage compared with FMFB, as the modulation dependent threshold effects will be much more predominant, and loop stability difficulties may be encountered.

From a hardware point of view the phase locked frequency divider is probably more difficult to realise than FMFB and does not lend itself to easy alteration of the feedback factor, should this be required.

5.2.7 Conclusions.

The phase-locked frequency divider has a performance comparable with FMFB, but cannot better it. It has some practical disadvantages, although the property of exact frequency and phase synchronism may be of use in some applications.

APPENDIX A: The pdf of the instantaneous frequency of sinewave plus random noise.

Let $v(t) = \cos 2\pi f_c t + n(t)$ ..... (1)

where $n(t)$ is bandlimited gaussian noise of spectral density $G_n(f)$. If $G_n(f) = 0$ for $|f| > 2f_c$ then the resolution of (1) into inphase and quadrature components is unique. viz.

$$v(t) = (1 + x(t)) \cos 2\pi f_c t - y(t) \sin 2\pi f_c t \quad \ldots\ldots (2)$$

where $x(t)$ and $y(t)$ are low pass gaussian time variables in quadrature.

The instantaneous phase $\theta(t)$ of $v(t)$ is:

$$\theta(t) = \arctan\left\{\frac{y(t)}{1+x(t)}\right\} \quad \ldots\ldots (3)$$

and the instantaneous frequency deviation from ω_c is:

$$\dot{\theta}(t) = \frac{(1 + x(t))\,\dot{y}(t) - \dot{x}(t)\,y(t)}{(1 + x(t))^2 + y(t)^2} \quad \ldots\ldots (4)$$

To find the pdf of $\dot{\theta}$ we need the joint pdf of $x(t)$ and $y(t)$ and their derivatives. Let $u_1 = x(t)$, $u_2 = y(t)$, $u_3 = \dot{x}(t)$ and $u_4 = \dot{y}(t)$. Then:

$$p(u_1, u_2, u_3, u_4) = \frac{1}{(2\pi)^2 |A|^{\frac{1}{2}}} e^{-\frac{1}{2}u' A^{-1} u} \quad \ldots\ldots (5)$$

where u = column vector $[u_i]$

u' is its transpose

A is the matrix $[a_{ij}]$ where $a_{ij} = \langle u_i\ u_j \rangle$

A^{-1} is its inverse

$|A|$ is its determinant.

If $R_{ij}(\tau) = \langle u_i(t)\, u_j(t+\tau) \rangle$ is the cross correlation function of u_i and u_j then

$$a_{ij} = R_{ij}(0) \qquad \ldots\ldots (6)$$

The cross correlation function is related to the power spectral density by the relation:

$$R_{ij}(\tau) = \int_{-\infty}^{+\infty} G_{ij}(f)\, e^{j2\pi f \tau}\, df \qquad \ldots\ldots (7)$$

and hence:

$$R_{ij}(0) = \int_{-\infty}^{+\infty} G_{ij}(f)\, df \qquad \ldots\ldots (8)$$

We know

$$\begin{aligned} G_{xx}(f) &= G_{yy}(f) = G_n(f-f_c) + G_n(f+f_c) \\ G_{xy}(f) &= j(G_n(f-f_c) - G_n(f+f_c)) \end{aligned} \qquad \ldots\ldots (9)$$

Also we have the relations:

$$\begin{aligned} G_{x\dot{x}}(f) &= j2\pi f\ G_{xx}(f) \\ G_{\dot{x}\dot{x}}(f) &= 4\pi^2 f^2\ G_{xx}(f) \\ G_{x\dot{y}}(f) &= j2\pi f\ G_{xy}(f) \\ G_{\dot{x}\dot{y}}(f) &= 4\pi^2 f^2 G_{xy}(f) \end{aligned} \qquad \ldots\ldots (10)$$

Hence:

$$A = \sigma^2 \begin{bmatrix} 1 & 0 & 0 & h \\ 0 & 1 & -h & 0 \\ 0 & -h & k^2 & 0 \\ h & 0 & 0 & k^2 \end{bmatrix}$$

where σ^2 = mean square value of $n(t)$ = $2\int_0^\infty G_n(f)df$

$$k^2 = \frac{2}{\sigma^2}\int_{\rho\infty}^{\infty} (\omega - \omega_c)^2 G_n(f)\, df$$

$$h = \frac{2}{\sigma^2}\int_{\rho\infty}^{\infty} (\omega - \omega_c)\, G_n(f)\, df$$

If we define ω_o and m^2 as follows:

$$\omega_o = \frac{2}{\sigma^2}\int_0^\infty \omega\, G_n(f)\, df$$

$$m^2 = \frac{2}{\sigma^2}\int_0^\infty (\omega - \omega_o)^2\, G_n(f)\, df$$

then:

$$h = \omega_o - \omega_c$$

$$k^2 = m^2 + h^2$$

It is convenient to introduce a change of variables to v_1, v_2, v_3 and v_4 such that

$$u = T\,v \qquad \ldots\ldots (11)$$

where T is a lower triangular matrix such that $TT' = A$. This factorisation is possible since A is a real symmetric matrix. The pdf of v_1, v_2, v_3, v_4 is

$$p(v_1, v_2, v_3, v_4) = \frac{1}{(2\pi)^2}\, e^{-\frac{1}{2} v'v} \qquad \ldots\ldots (12)$$

Now $T = \sigma$

$$\begin{bmatrix} 1 & 0 & 0 & 0 \\ 0 & 1 & 0 & 0 \\ 0 & -h & m & 0 \\ h & 0 & 0 & m \end{bmatrix} \qquad \ldots\ldots (13)$$

From (4):

$$\dot{\theta} = \frac{(1 + u_1)\, u_4 - u_2\, u_3}{(1 + u_1)^2 + u_2^2} \qquad \ldots\ldots (14)$$

Substituting for u from (11) and (13) and defining:

$$d = -h/m = \text{normalised carrier offset}$$

$$\Omega_i = \frac{\dot{\theta}-h}{m} = \text{normalised frequency deviation from } \omega_o$$

$$\lambda = \frac{1}{\sigma}$$

then

$$\Omega_i = \frac{(v_1+\lambda)(v_4+\lambda d) - v_2 v_3}{(v_1+\lambda)^2 + v_2^2} \qquad \ldots\ldots (15)$$

To find the pdf of Ω_i we substitute for v_3 in the pdf (12) and integrate over the variables not required. The limits are assumed $-\infty$ to $+\infty$ unless otherwise stated.

$$p(\Omega_i) = \iiint p(v_1, v_2, v_3, v_4)\, J\, dv_1\, dv_2\, dv_4 \qquad \ldots\ldots (16)$$

$$\text{where} \quad J = \left| \frac{\partial v_3}{\sigma\, \Omega_i} \right| = \left| \frac{(v_1+\lambda)^2 + v_2^2}{v_2} \right| \qquad \ldots\ldots (17)$$

The exponent in (12) is given by:

$$\tfrac{1}{2} v'v = \tfrac{1}{2}\left\{ v_1^2 + v_2^2 + v_3^2(v_1, v_2, v_4, \Omega_i) + v_4^2 \right\}$$

$$= \tfrac{1}{2} B^2 (v_4 + C)^2 + \tfrac{1}{2} D$$

where B, C, D are functions of v_1, v_2, Ω_i.

Performing the v_4 integration in (16) gives:

$$p(\Omega_i) = \frac{1}{(2\pi)^{3/2}} \iint \frac{J\, e^{-\frac{1}{2}D}}{|B|}\, dv_1\, dv_2 \qquad \ldots\ldots (18)$$

$$\text{Now } B = \frac{\sqrt{(v_1+\lambda)^2 + v_2^2}}{v_2}$$

$$\text{and } D = v_1^2 + v_2^2 + \frac{\left[-\lambda d(v_1+\lambda) + \Omega_i \left\{ (v_1+\lambda)^2 + v_2^2 \right\} \right]^2}{(v_1+\lambda)^2 + v_2^2}$$

Hence:

$$p(\Omega_i) = \frac{1}{(2\pi)^{3/2}} \iint + \sqrt{(v_1+\lambda)^2 + v_2^2}\; e^{-\frac{1}{2}D}\, dv_1\, dv_2 \quad \ldots\ldots (19)$$

Convert to polar co-ordinates r, ϕ.

$$v_1 + \lambda = r \cos\phi .$$

$$v_2 = r \sin\phi .$$

$$\therefore p(\Omega_i) = \frac{1}{(2\pi)^{3/2}} \int_{\phi=0}^{\pi} \int_{r=-\infty}^{+\infty} r^2\, e^{-\frac{1}{2}\left\{ r^2 - 2\lambda r \cos\phi + \lambda^2 + (\Omega_i r - \lambda d \cos\phi)^2 \right\}} dr\, d\phi \quad \ldots\ldots (20)$$

Performing the r integration:

$$p(\Omega_i) = \frac{e^{-\rho}}{2\pi(1+\Omega_i^2)^{3/2}} \int_{\phi=0}^{\pi} (1 + 2\mu \cos^2\phi)\, e^{2y \cos^2\phi}\, d\phi \quad \ldots\ldots (21)$$

where $\rho = \lambda^2/2$ = CNR in IF bandwidth

$$\mu = \rho (1+\Omega_i d)^2/(1+\Omega_i^2)$$

$$y = \tfrac{1}{2}(\mu - \rho d^2)$$

Finally performing the ϕ integration by putting $\chi = 2\phi$;

$$p(\Omega_i) = \frac{e^{y-\rho}}{4\pi(1+\Omega_i^2)^{3/2}} \int_{\chi=0}^{2\pi} (1+\mu+\mu\cos\chi)\, e^{y\cos\chi} d\chi$$

$$p(\Omega_i) = \frac{e^{y-\rho}}{2(1+\Omega_i^2)^{3/2}} \left\{ (1+\mu)\, I_0(y) + \mu\, I_1(y) \right\} \quad \ldots\ldots (22)$$

where I_0 and I_1 are modified Bessel functions of order 0 and 1 respectively.

It is interesting to note that as $\rho \to \infty$ the asymptotic form

of $p(\Omega_i)$ is not gaussian except for Ω_i in the vicinity of d. i.e. As $\rho \to \infty$ the instantaneous frequency is distributed normally about the carrier frequency only for small deviations from the carrier. The deviation from gaussian form can be attributed to the finite probability of an origin encirclement by the carrier plus noise phasor, at which time $\dot{\theta}$ is very large (an impulse).

We also require $<|\Omega_i|>$ for the case when the carrier is centrally tuned (i.e. d=0). We start from the expression for $p(\Omega_i)$ given by equation (20). Hence:

$$<|\Omega_i|> = \frac{2}{(2\pi)^{3/2}} \int_0^{\pi} \int_{-\infty}^{+\infty} \int_0^{\infty} r^2 \Omega_i \, e^{-\frac{1}{2}(r^2 - 2\lambda r \cos\phi + \lambda^2 + r^2\Omega_i^2)} \, d\Omega_i \, dr \, d\phi \quad \ldots\ldots (23)$$

Performing the Ω_i integration:

$$<|\Omega_i|> = \frac{2}{(2\pi)^{3/2}} \int_0^{\pi} \int_{-\infty}^{+\infty} e^{-\frac{1}{2}(r^2 - 2\lambda r \cos\phi + \lambda^2)} \, dr \, d\phi$$

Performing the r integration:

$$<|\Omega_i|> = \frac{2}{2\pi} \int_0^{\pi} e^{-\frac{1}{2}\lambda^2 \sin^2\phi} \, d\phi$$

$$= \frac{e^{-\frac{1}{2}\rho}}{2\pi} \int_0^{2\pi} e^{\frac{1}{2}\rho \cos\chi} \, d\chi$$

where $\rho = \frac{1}{2}\lambda^2 = \text{CNR}$, $\chi = 2\phi$.

$$\therefore <|\Omega_i|> = e^{-\frac{1}{2}\rho} \, I_0(\tfrac{1}{2}\rho) \quad \ldots\ldots (24)$$

APPENDIX B: Incremental phase response of a tuned circuit.

The transfer function of a parallel LGC tuned circuit may be written in the form:

$$H(S) = \frac{2S\Delta}{(S+\Delta)^2+\omega_o^2} \qquad \ldots\ldots (1)$$

where $\Delta = G/2C$ = semi 3db bandwidth (rad/sec)

$$\omega_o^2 = \frac{1}{LC} - \Delta^2$$

The small signal transfer function to phase modulation on a carrier frequency ω_c is:

$$H_1(S) = \tfrac{1}{2}\left[\frac{H(S+j\omega_c)}{H(j\omega_c)} + \frac{H(S-j\omega_c)}{H(-j\omega_c)}\right] \qquad \ldots\ldots (2)$$

For the transfer function (1) this becomes:

$$H_1(S) = \frac{2\Delta S^3 + (3\Delta^2+\lambda_1\lambda_2)S^2 + \left\{2\Delta^3+\Delta(\lambda_1^2+\lambda_2^2)\right\}S + (\Delta^2+\lambda_1^2)(\Delta^2+\lambda_2^2)}{\left\{(S+\Delta)^2+\lambda_1^2\right\}\left\{(S+\Delta)^2+\lambda_2^2\right\}} \qquad \ldots\ldots (3)$$

where $\lambda_1 = \omega_c - \omega_o$

$\lambda_2 = \omega_c + \omega_o$

If ω_c is not greatly different from ω_o then under high Q conditions $\lambda_2 >> \lambda_1$ and $\lambda_2 >> \Delta$.

The transfer function (3) can be then approximated by:

$$H_1(S) = \frac{\Delta S + \Delta^2 + \lambda^2}{(S+\Delta)^2+\lambda_1^2} \qquad \ldots\ldots (4)$$

This approximation is valid for frequencies $\omega << \lambda_2$.

The approximate location of the other two zeros may be found from the root relations of the numerator of (3) and the knowledge that one root is approximately $-\frac{\Delta^2 + \lambda_1^2}{\Delta}$. In particular:

$$\text{Sum of roots} \quad \doteq \quad -\frac{\lambda_1 \lambda_2}{2\Delta}$$

$$\text{Product of roots} \quad \doteq \quad -\frac{(\Delta^2 + \lambda_1^2)\lambda_2^2}{2\Delta}$$

This yields the values of the other two zeros as:

$$S_1 , S_2 \doteq -\frac{\lambda_1 \lambda_2}{4\Delta} \pm \sqrt{\frac{\lambda_1^2 \lambda_2^2}{16\Delta^2} - \frac{\lambda_2^2}{2}} \qquad \ldots\ldots (5)$$

The pole-zero diagram is shown in Figure B-1. The approximation (4) includes only those singularities in the vicinity of the origin.

In the special case of $\lambda_1 = 0$, the approximation (4) reduces to:

$$H_1(S) = \frac{\Delta}{S+\Delta} \qquad \ldots\ldots (6)$$

which is the transfer function of a low pass RC filter.

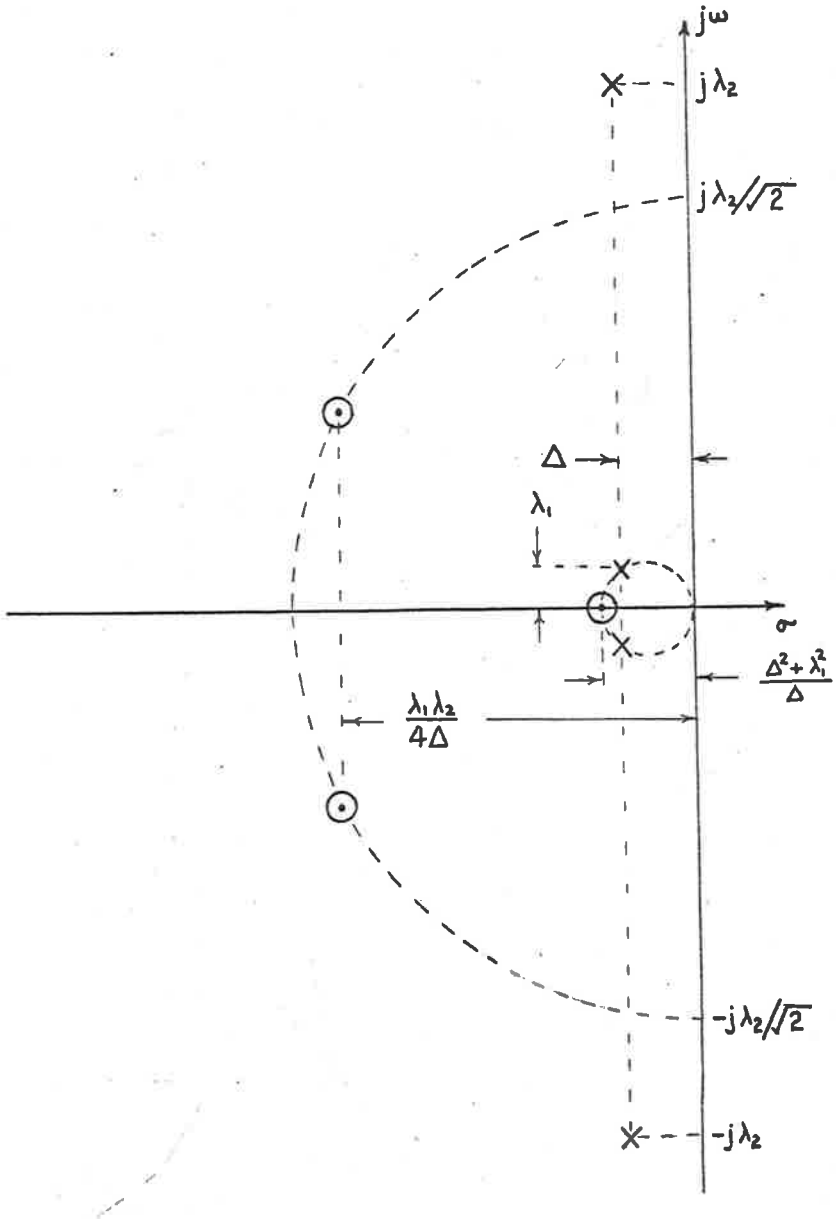

FIGURE B-1: COMPLETE TRANSFER FUNCTION OF A SINGLE TUNED CIRCUIT TO PHASE.

APPENDIX C: Mean amplitude of sinewave and gaussian noise.

If a sinewave plus narrow band noise is put in the form:

$$v(t) = \left\{ 1 + x(t) \right\} \cos \omega_c t - y(t) \sin \omega_c t = r(t) \cos \left\{ \omega_c t + \theta(t) \right\} \quad \ldots (1)$$

then since $x(t)$ and $y(t)$ are jointly gaussian, the pdf of $r(t)$ and $\theta(t)$ is:

$$p(r, \theta) = \frac{r}{2\pi\sigma^2} e^{-\frac{r^2 - 2r\cos\theta + 1}{2\sigma^2}} \quad \ldots\ldots (2)$$

Hence:

$$\langle r \rangle = \frac{1}{2\pi\sigma^2} \int_{\theta=0}^{2\pi} \int_{r=0}^{\infty} r^2 \, e^{-\frac{r^2 - 2r\cos\theta + 1}{2\sigma^2}} \, dr \, d\theta$$

$$= \frac{1}{2\pi\sigma^2} \int_{\theta=0}^{\pi} \int_{r=-\infty}^{+\infty} r^2 \, e^{-\frac{r^2 - 2r\cos\theta + 1}{2\sigma^2}} \, dr \, d\theta$$

Performing the r integration gives:

$$\langle r \rangle = \frac{1}{\sigma\sqrt{2\pi}} \int_{\theta=0}^{\pi} (\sigma^2 + \cos^2\theta) \, e^{-\frac{\sin^2\theta}{2\sigma^2}} \, d\theta$$

$$= \frac{1}{\sigma\sqrt{2\pi}} \int_{\theta=0}^{\pi} (\sigma^2 + \tfrac{1}{2} + \tfrac{1}{2}\cos 2\theta) \, e^{-\frac{(1 - \cos 2\theta)}{4\sigma^2}} \, d\theta$$

$$= \frac{e^{-1/4\sigma^2}}{2\sigma\sqrt{2\pi}} \int_{\phi=0}^{2\pi} (\sigma^2 + \tfrac{1}{2} + \tfrac{1}{2}\cos\phi) \, e^{\frac{\cos\phi}{4\sigma^2}} \, d\phi \text{ where } \phi = 2\theta$$

$$= \frac{e^{-1/4\sigma^2}}{\sigma} \sqrt{\pi/2} \left\{ (\sigma^2 + \tfrac{1}{2}) \, I_0\left(\frac{1}{4\sigma^2}\right) + \tfrac{1}{2} I_1\left(\frac{1}{4\sigma^2}\right) \right\}$$

$$\langle r \rangle = \sigma\sqrt{\frac{\pi}{2}} \, e^{-\frac{1}{2}\rho} \left\{ (1+\rho) \, I_0(\tfrac{1}{2}\rho) + \rho \, I_1(\tfrac{1}{2}\rho) \right\} \quad \ldots\ldots (3)$$

where $\rho = 1/2\sigma^2$ = CNR

APPENDIX D: Threshold in FM and FMFB.

If the RF noise psd is $\eta(f)$ = constant and carrier amplitude = 1, then the gaussian and impulse components of the output noise are:

1. Gaussian noise.

$$G_1(f) = 2\omega^2 \eta(f) \text{ volts}^2/H_z$$

In a bandwidth f_a, the noise is given by:

$$N_1 = \int_{-f_a}^{f_a} G_1(f)\, df = 16\pi^2 \eta(f) f_a^3/3 \qquad \ldots\ldots (1)$$

2. Impulse noise.

Suppose the impulse area is 2π and the impulse rate is ν per second. On the assumption that these are independent and are distributed according to a Poisson distribution, we have:

$$G_2(f) = 4\pi^2 \nu \text{ volts}^2/H_z$$

at frequencies for which the impulse duration is negligible compared with the period.

Hence in the bandwidth f_a we have:

$$N_2 = 8\pi^2 \nu f_a \qquad \ldots\ldots (2)$$

If threshold is defined to be the point where $N_2 + N_1 = \frac{1}{2}$ db more than N_1, (i.e. $N_2 = .12N_1$) we have:

$$\nu_{th} = 0.08\, \eta(f) f_a^2 \qquad \ldots\ldots (3)$$

APPENDIX E: Typical FMFB system.

IF transfer function to phase $H_1(S) = \dfrac{a\Delta^2}{(S+\Delta)(S+a\Delta)}$

Baseband filter transfer function $H_2(S) = \dfrac{S+a\Delta}{a\Delta(S+1)}$

The transfer functions of the IF phase $\theta(t)$ and the VCO phase $\phi(t)$ from the input phase $\theta_i(t)$ are (for the linear region):

$$H_{\theta i \to \phi} = \frac{\Delta(F-1)}{S^2 + (1+\Delta)S + \Delta F} \qquad \ldots\ldots (1)$$

$$H_{\theta i \to \theta} = \frac{a\Delta^2(S+1)}{(S^2 + (1+\Delta)S + \Delta F)(S + a\Delta)} \qquad \ldots\ldots (2)$$

For a unit carrier amplitude, the spectral density of $\theta_i(t)$ is $2\eta(f)$. Hence the mean square values are:

$$\langle \phi^2 \rangle = \frac{\eta(f)\Delta(F-1)^2}{F(1+\Delta)} \qquad \ldots\ldots (3)$$

$$\langle \dot{\phi}^2 \rangle = \frac{\eta(f)\Delta^2(F-1)^2}{(1+\Delta)} \qquad \ldots\ldots (4)$$

$$\langle \theta^2 \rangle = \frac{\eta(f)\, a\Delta\{1 + (a+1)\Delta + aF\Delta^2\}}{F\{F+a + (a^2+2a+F)\Delta + a(a+1)\Delta^2\}} \qquad \ldots\ldots (5)$$

$$\langle \dot{\theta}^2 \rangle = \frac{\eta(f)\, a^2\Delta^3\{1 + (F+a)\Delta + a\Delta^2\}}{\{F+a + (a^2+2a+F)\Delta + a(a+1)\Delta^2\}} \qquad \ldots\ldots (6)$$

Also the IF CNR is given by:

$$\rho_{IF} = \frac{(1+a)}{2a\Delta\eta(f)} \qquad \ldots\ldots (7)$$

To model the experimental set up the following values were chosen: $F = 10$, $a = 10$, $\Delta = 3$. Early models involving the power series approximations had $a = \infty$. In the determination of γ_o and ϕ_o, the feedback factor F and the IF bandwidth Δ were varied with 'a' being constant at 10.

APPENDIX F: Experimental model of FMFB.

The experimental set up of an FMFB system is shown in Figure F-1. The system was designed for a baseband bandwidth of 10KH$_z$, an IF bandwidth of 60KH$_z$ and a feedback factor of 10 (20 db).

The mixer stage consisted of a tunnel diode mixer which converted the incoming 290 MH$_z$ signal into a 50 MH$_z$ first IF. Integral with the mixer was a varactor diode tuned tunnel diode oscillator. The theory and construction of the mixer and oscillator is described in [23] .

Following the mixer, two stages of 50 MH$_z$ amplification were provided before conversion to a second IF of 5 MH$_z$. One stage of 5 MH$_z$ amplification was followed by a limiter stage and frequency detector. AGC was applied to the 50 MH$_z$ stages only. This was effective over an 80 db input signal range.

A direct coupled baseband amplifier and filter completed the feedback path. Direct coupling was used to improve the tuning stability.

The IF amplifier consisted of several tuned stages, and in order to maintain a predominantly single pole response, all circuits were broadband except one (the 5 MH$_z$ stage). The baseband filter was a single pole filter, although some lead compensation was used to improve the stability and transient behaviour of the loop.

In practice it would be better to confine the feedback to relatively few stages rather than apply feedback around the whole system. This would reduce the problems associated with loop stability and also obviate the necessity of using IF circuits with specially tailored responses. However, the system constructed enabled representative

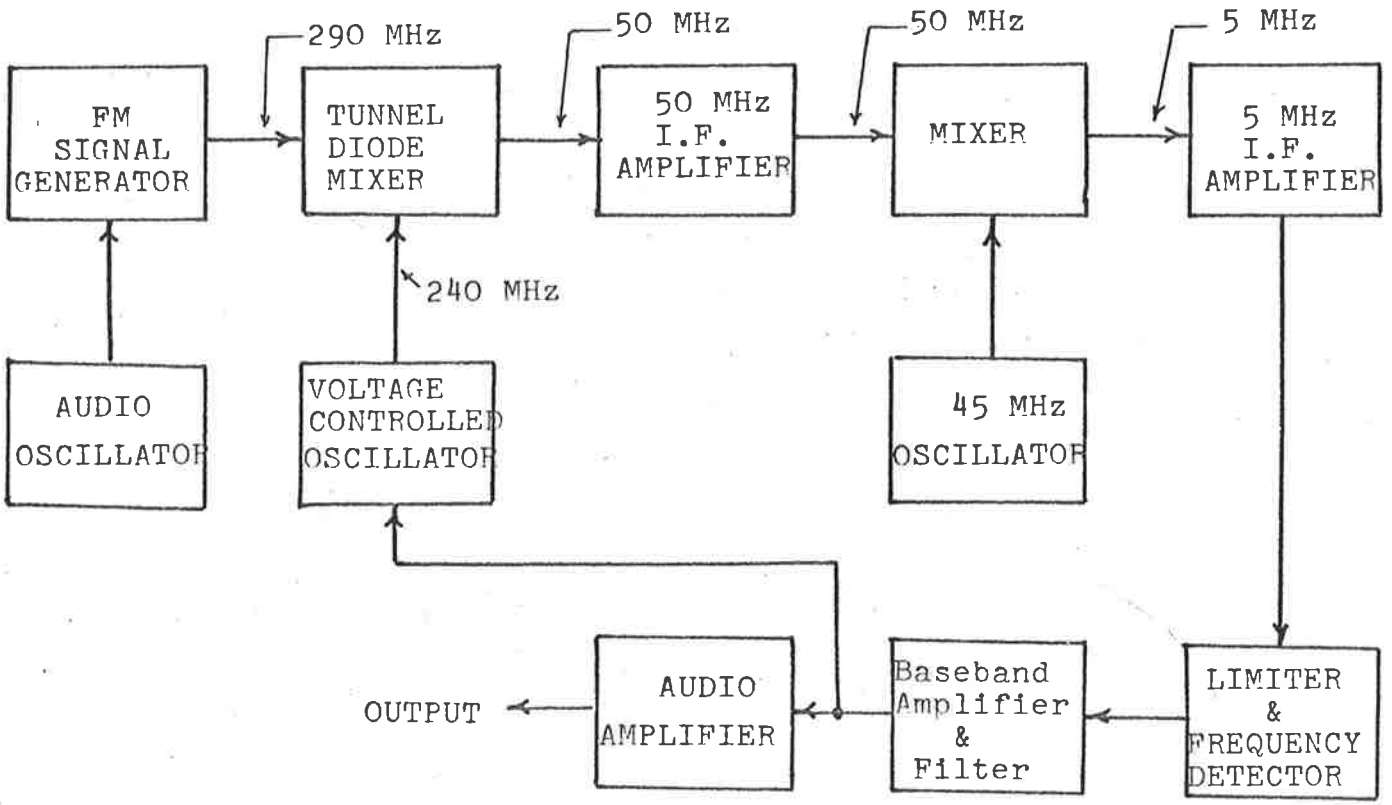

FIGURE F-1: BLOCK DIAGRAM OF EXPERIMENTAL FMFB SYSTEM.

Fla

measurements to be obtained.

A source of error which proved significant was 1/f noise in the transistor amplifier stages at baseband. Under high output SNR conditions this noise tended to mask the quadratic spectrum noise. This was largely eliminated by using a lower cut off frequency of 440 H_z in all measurements involving output noise. Another minor source of error involved feed-through of amplitude noise from the limiter.

Absolute measurements of CNR required a knowledge of the receiver noise factor. This was measured by a diode noise generator and found to be 11 db. As the image rejection of the first mixer is quite good, this noise factor may be added to the incoming noise spectral density in order to obtain the effective input noise psd.

The system was designed to have the dicriminator and feedback thresholds occur at the same carrier level, as under these conditions the system is optimum.

The output in Figure F-1 was passed through filters with steep skirts in order to measure the output noise. The effective bandwidth was 440 - 10250 H_z.

Figure F-2 shows the complete circuit diagram of the experimental FMFB system.

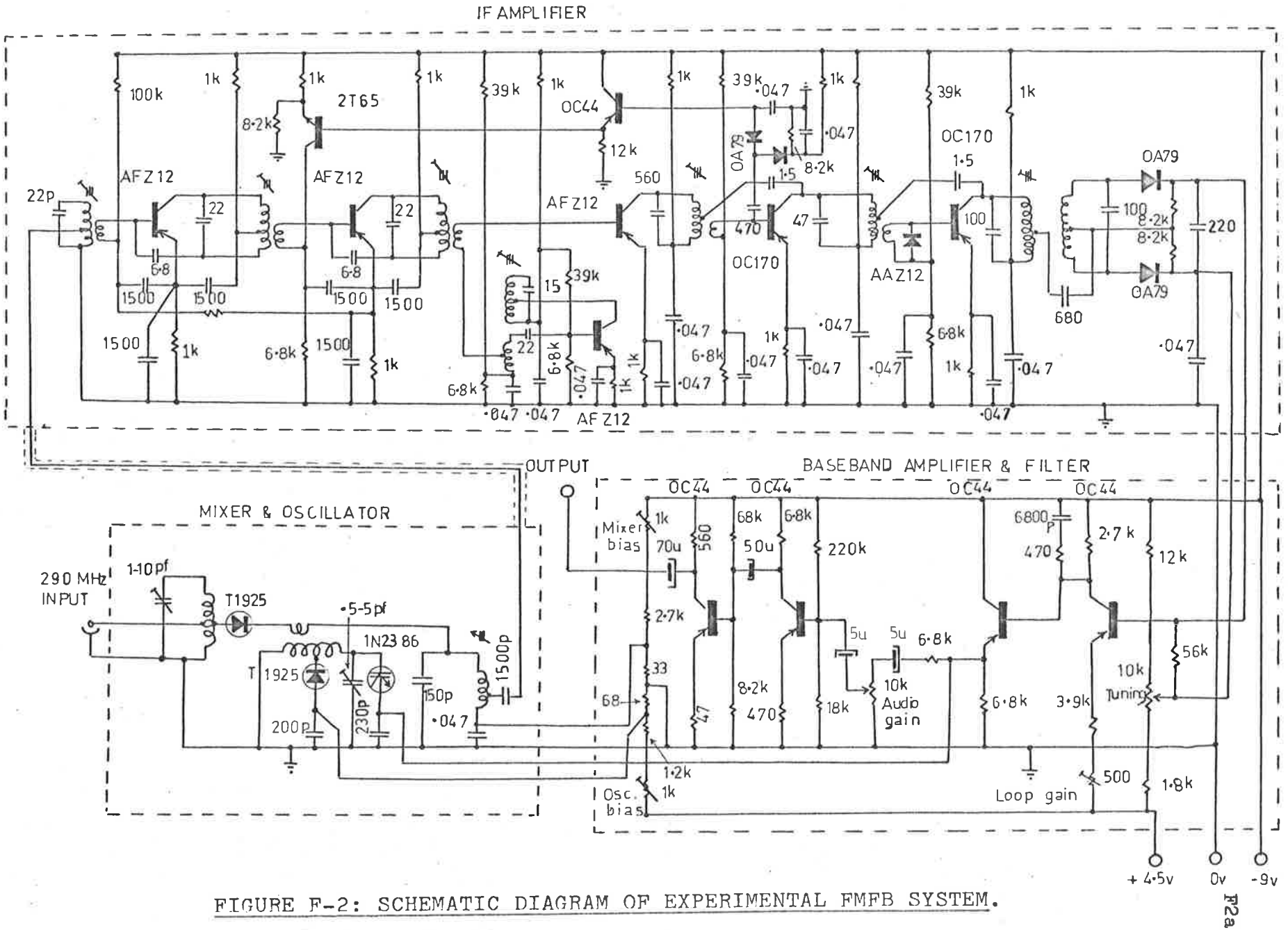

FIGURE F-2: SCHEMATIC DIAGRAM OF EXPERIMENTAL FMFB SYSTEM.

APPENDIX G: Digital simulations.

In digital simulations, the differential equations corresponding to the different transfer functions were solved numerically using a fourth order Runge-Kutta integration formula[22]. A standard program was developed which enabled solution of simultaneous high order differential equations without having to express them as a series of equivalent first order equations.

All narrow band RF voltages were represented in phasor form and the appropriate low pass transfer functions involving the phasors used to represent the effect of RF filtering.

The input and output of a bandpass filter of transfer function H(S) may be resolved as:

$$v_{in}(t) = R_e \left\{ (a_1(t) + ja_2(t))\, e^{j\omega_c t} \right\}$$
$$v_{out}(t) = R_e \left\{ (b_1(t) + j\, b_2(t)) e^{j\omega_c t} \right\} \qquad \ldots\ldots (1)$$

where ω_c is a convenient carrier frequency, but otherwise arbitrary. The resolutions are unique if $v_{in}(t)$ and $v_{out}(t)$ have no significant components at frequencies exceeding $2\omega_c$.

The transfer functions connecting a_i to b_j are given by $H_{ij}(S)$ below:

$$H_{11}(S) = H_{22}(S) = \tfrac{1}{2}\left[H(S + j\omega_c) + H(S - j\omega_c) \right]$$
$$H_{12}(S) = -H_{21}(S) = \frac{1}{2j}\left[H(S + j\omega_c) - H(S - j\omega_c) \right] \qquad \ldots\ldots (2)$$

A 36 bit shift register code was used to generate a pseudo-random binary sequence. The particular code used generated a feedback bit corresponding to the logical difference of bits 31 and 36. This gives a maximum length sequence of length $2^{36}-1$ bits.

In the digital simulations, the pseudorandom sequence generated a two level signal ± 1 at intervals corresponding to the integration process increment h. The psd of the output is:

$$G(f) = h\left\{\frac{\sin \pi fh}{\pi fh}\right\}^2 \qquad \ldots\ldots (3)$$

which is white for $fh \ll 1$.

In actual fact because the sequence is periodic, it has a line spectrum. However, since the discrete components are separated by approximately $2^{-36}/h$ H_z, the approximation to a continuous spectrum is extremely good.

The binary sequence itself is of course not a good representation of gaussian noise. If, however, it is passed through a low pass filter of cutoff frequency $\ll 1/h$ then the output is approximately gaussian. In many applications it is sufficient to allow the system itself do the filtering.

Figure G-1 shows the amplitude distribution of the output of an RC filter of time constant 100 h when excited by the pseudorandom sequence. The observations were taken over a time of 10^5h, corresponding to 10^5 bits of the sequence. A class interval width of 0.02 volts was used.

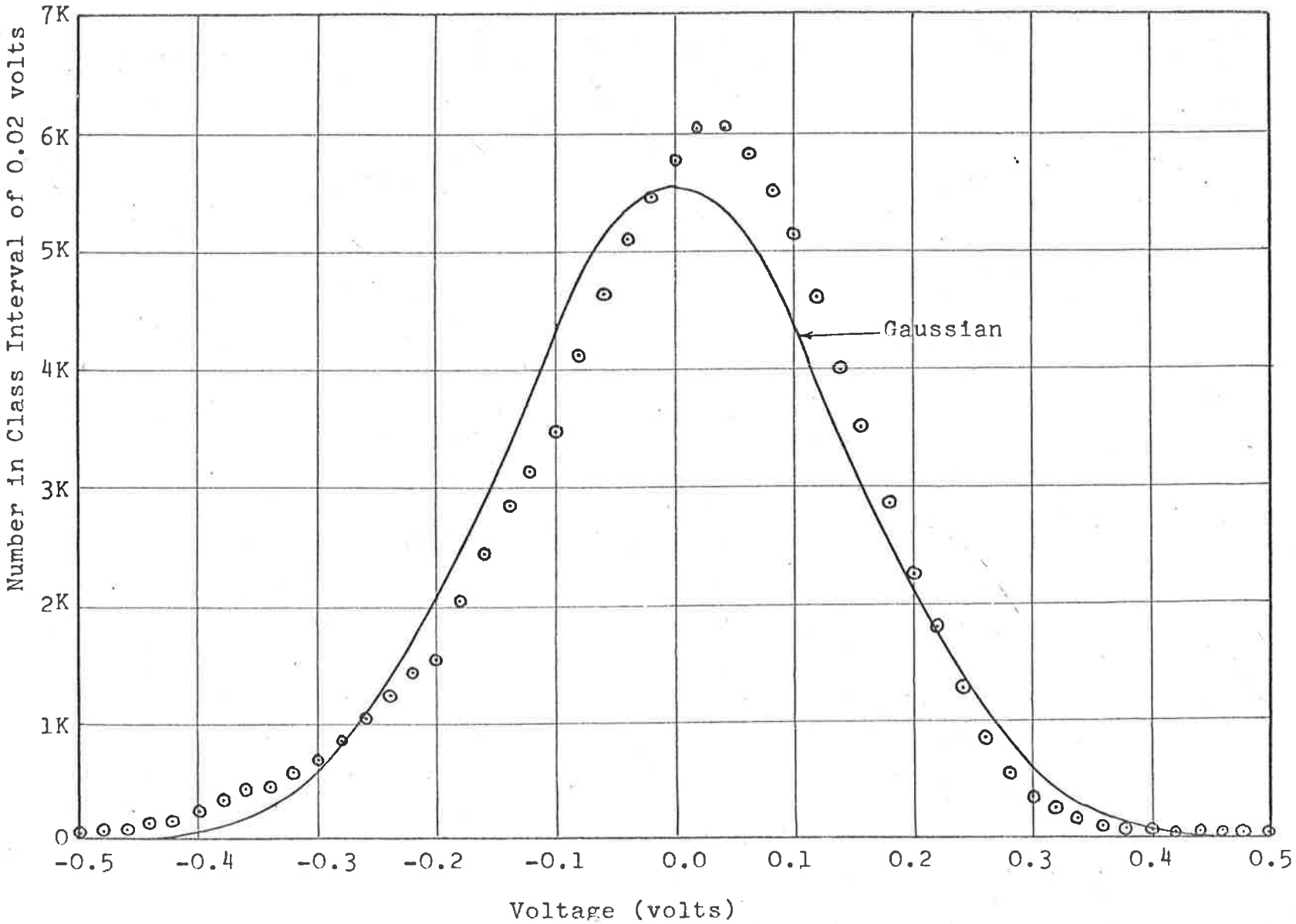

FIGURE G-1: AMPLITUDE DISTRIBUTION OF FILTERED PSEUDO-RANDOM NOISE.

The distribution is approximately gaussian although it is slightly skewed. The fit to the tails of the gaussian distribution is not good in terms of relative error. This was also observed by Smith [27].

The above indicates that a filtered pseudorandom sequence is a reasonably good approximation to gaussian noise except where the tails of the distribution are of importance. In these cases the results may be subject to considerable error. This applies in particular to the simulation of impulse phenomena in FMFB.

Referring to Figure 2.5 the systems modelled in the various simulations were:

(i) Simulation 1 modelled the typical FMFB system of Appendix E except that $a = \infty$. i.e. the IF filter had only a single pole response. This was also the model used for the earlier power series approximations of section 2.4.3.

(ii) Simulation 2 modelled the system of Appendix E with $a = 10$. This system was the one used in theoretical calculations and was the one closely approximated by the experimental system of Appendix F.

(iii)Simulation 3 modelled the same system as simulation 2, except that the equivalent $n'(t)$ representation of Figure 2.8a was used.

In all three cases, the total number of jumps observed was limited by the computer time required for simulation. Generally a number greater than 25 was obtained in order to give a reasonable approximation to the impulse rate. In view of the limitations of the pseudorandom sequence as a substitute for gaussian noise, greater refinement was not considered necessary.

APPENDIX H: Published papers.

1. B.R. Davis: "Factors affecting the threshold of feedback FM detectors"; Trans. I.E.E.E. on Space Electronics and Telemetry, Vol. SET-10: 90, Sept. 1964.

2. B.R. Davis: "Equivalent variable centre-frequency amplifiers"; The Radio and Electronic Engineer, Vol. 28:381, Dec. 1964.

Davis, B. R. (1964). Factors Affecting the Threshold of Feedback FM Detectors. *IEEE Transactions on Space Electronics and Telemetry, 10*(3), 90-94.

Davis, B. R. (1964). Equivalent variable centre-frequency amplifiers. *Radio and Electronic Engineer, 28*(6), 381-388.

6. BIBLIOGRAPHY.

1. E. Armstrong: "A method of reducing disturbances in radio signallin by a system of frequency modulation"; Proc. I.R.E. 24:689 May 1936.

2. J.G. Chaffee: "The application of negative feedback to FM systems"; Proc. I.R.E. 27:317, May 1939.

3. L.H. Enloe: "Decreasing the threshold in FM by frequency feedback"; Proc. I.R.E. 50:18, January 1962.

4. F. Stumpers: "Theory of FM noise"; Proc. I.R.E. 36:1081, September 1948.

5. S. Rice: "Noise in FM receivers"; Chapter 25, Time Series Analysis, John Wiley 1963. Ed. M. Rosenblatt.

6. D.L. Schilling and J. Billig: "A comparison of the threshold performance of a frequency demodulator using feedback and the phase locked loop"; Polytech. Inst. of Brooklyn Res. Rep. PIB MRI-1207-64, February 28th 1964.

7. B.R. Davis: "Factors affecting the threshold of feedback FM detectors"; Trans. I.E.E.E. on Space Electronics and Telemetry, Vol. SET-10 p90, September 1964.

8. R. Booton: "The analysis of non-linear control systems with random inputs"; Proc. Symp. on Nonlinear Cct. Anal., Polytech. Inst. of Brooklyn, N.Y., pp 369-391, April 1953.

9. R.E. Heitzman: "Minimum power reception using frequency feedback"; Proc. I.R.E. 50:2503, December 1962.

10. C. Ruthroff: "Project Echo: FM demodulators with negative feedback"; B.S.T.J. 50:1149, July 1961.

11. R. Sanders: "Communication efficiency of several communication systems"; Proc. I.R.E. 48:575, April 1960.

12. J.A. Develet: "A threshold criterion for phase-lock demodulation"; Proc. I.R.E. 51:349-356, February, 1956.

13. R.M. Jaffee and E. Rechtin: "Design and performance of phase lock circuits capable of near optimum performance over a wide range of input signal and noise levels"; Trans. I.R.E. on Information Theory, Vol. I T1- pp 66-76, March 1955.

14. J.J. Downing: "Modulation Systems and Noise"; Prentice Hall 1964, P 104.

15. R.M. Gagliardi: "Transmitter power reduction with frequency tracking FM receivers"; Trans. I.E.E.E. on Space Electronics and Telemetry, Vol. SET-9:18, March 1963.

16. B.R. Davis: "Equivalent variable centre-frequency amplifiers"; The Radio and Electronic Engineer Vol. 28:381, December 1964.

17. E.J. Baghdady: "Lectures on Communication System Theory"; McGraw Hill p548, 1961.

18. P. Beckman: "Prabability in Communication Engineering"; Harcourt Brace and World 1967: (a) pp 219-231; (b) p 123.

19. M.J. Malone: "A comparison of low pass filters for time multiplexed

FM systems"; W.R.E Tech. Memo EID 132.

20. E.J. Baghdady: "Signal cancellation techniques"; Electromagnetic Wave Propagation, Edited by J. Michiels, M. Desirant 1960.

21. G.L. Beers: "A frequency dividing locked in oscillator FM receiver"; Proc. I.R.E. 32:730, December, 1944.

22. A. Ralston and H. Wilf: "Mathematical methods for digital computers"; John Wiley 1960, Chapter 9.

23. B.R. Davis: "A high frequency converter using tunnel diodes"; Proc. I.R.E.E. (Aust.) 25:25, January 1964.

24. F. Roberts and J. Simmonds: "The physical realisability of electrical networks having prescribed characteristics, with particular reference to those of the probability function type"; Philosophical Magazine Vol. 35 No. 250, November 1944.

25. H. James, N. Nichols and R. Phillips: "Theory of servomechanisms"; Vol. 25 MIT Radiation Laboratory Series, McGraw Hill 1947, pp 369-370.

26. B. Smith: "The phase-lock loop with filter: frequency of skipping cycles"; Proc I.E.E.E. 54:296, February 1966.

27. B. Smith: "An asymmetrical property of binary pseudorandom noise generators"; Proc. I.E.E.E. 54:793, May 1966.

28. M. Abramowitz, I. Stegun: "Handbook of Mathematical Functions"; Dover 1965.

29. C.L. Ruthroff and W.F. Bodtmann: "Design and performance of a broadband FM demodulator with frequency compression"; Proc. I.R.E. 50:2436, December, 1962.